

Taguchi Methods in Internal Combustion Engine Optimisation

Jeremy James Green



Thesis presented in partial fulfillment of the
requirements for the degree of Master of Mechanical Engineering
at the University of Stellenbosch

Study Leader: Dr AB Taylor

December 2001

DECLARATION

I the undersigned hereby declare that the work contained in this thesis is my own original work and has not been previously in its entirety or in part been submitted at any university for a degree.

ABSTRACT

Statistical experimental design techniques are powerful tools that are often approached with suspicion and apprehension by experimenters. The trend is to avoid any statistically structured and designed experimentation program, and to rather use the traditional method of following ones “gut feel”. This approach, more often than not, will supply a satisfactory solution, but there is so much more information available for the same amount of effort.

This thesis strives to outline the method and application of the Taguchi methodology of experimental design. The Taguchi method is a practical, statistical experimental design technique that does not rely on the designer’s knowledge of the complex statistics typically needed to design experimental programs, a fact that tends to exclude design of experiments from the average engineers’ toolbox. The essence of the statistical design of experiments is this: The traditional method of varying one variable at a time and investigating its effect on an output is no longer sufficient. Instead all the input variables are varied at the same time in a structured manner. The output trends resulting from each input variable are then statistically extracted from the data in the midst of the variation.

Taguchi method achieves this by designing experiments where every level of every input variable occurs an equal number of times with every level of every other input variable. The experimental designs are represented in orthogonal arrays that are chosen and populated by the experimenter by following a simple procedure.

Four case studies are worked through in this text and, where possible, compared to the “traditional” approach to the same problem. The case studies show the additional information and time savings available with the Taguchi method, as well as clearly indicating the importance of using a stable system on which to do the experiments. The Taguchi method generated more information in fewer experiments than the traditional approaches as well as allowing analysis of problems too complex to analyse without a statistical design of the experimentation procedure.

OPSOMMING

Statistiese eksperimentele ontwerptechnieke is besonder kragtige instrumente wat baie keer met agterdog deur eksperimenteerders beheer word. Die neiging is om enige statistiese gestruktureerde and ontwerpte eksperimentele program te vermy, en om liever die tradisionele metode, wat op 'n mens se intuïsie staatmaak, te gebruik. Hierdie benadering sal baie keer 'n bevredigende oplossing gee, maar daar is veel meer inligting vir dieselfde hoeveelheid inspanning verkrygbaar, wanneer die Taguchimetode gebruik word.

Hierdie tesis streef om die metode en toepassing van die Taguchimetodologie van eksperimentele ontwerp voor te lê. Die Taguchimetode is 'n praktiese statistiese eksperimentele ontwerptechniek .wat nie op die ontwerper se kennis van komplekse statistiek om eksperimentele programme te ontwerp berus nie. Hierdie komplekse statistiek neig ook om eksperimentele ontwerp van die gemiddelde ingenieursvaardighede uit te sluit. Die kern van statistiese eksperimentele ontwerp is die volgende: Die tradisionele metode van een veranderlike op 'n slag te varieer om die effek op die uitset te ondersoek, is onvoldoende. In plaas daarvan, word al die insetveranderlikes gelyktydig gevarieer in 'n gestruktureerd manier. Die neigings van elke veranderlike is dan statisties ontleed van die data ten midde van die variasie van al die ander veranderlikes.

Die Taguchimetode bereik die ontwerpte eksperimente deur elke vlak van elke insetveranderlik in 'n gelyke aantal keer met elke vlak van elke ander insetveranderlike te varieer. Hierdie is verteenwoordig deur ortogonale reekse wat gekies en gevul is deur 'n eenvoudige wisselpatroon te volg.

Vier gevallestudies is deurgewerk en, waar moontlik, vergelyk met die tradisionele siening van dieselfde probleem. Die gevallestudies wys hoe toereikbaar die additionele inligting in die Taguchimethode toepassings is. Hulle beklemtoon ook die belangrikheid van 'n stabiele sisteem waarop die eksperimente berus. Die Taguchimetode het meer inligting verskaf met minder eksperimente as die tradisionele toenaderings, en ook toegelaat dat die analise van probleme, te kompleks om te analiseer sonder om 'n statistiese ontwerp van eksperimentele prosedure te volg, opgelos kon word.

DEDICATIONS/ACKNOWLEDGEMENTS

There are many people who have contributed to the completion of this thesis. Thank you to Dr Taylor and the team at the Centre for Automotive Engineering (CAE) for the support and assistance they provided during the experimentation. Thanks also to GUD and Nissan for funding sections of the research undertaken. Thanks to the Foundation for Research and Development (FRD) and university for the financial assistance received. DeBeers, DebTech also need to be mentioned for graciously deferring my bursary obligations, thus allowing me to complete the necessary courses and test work.

To my parents who always told me I could do anything, thank you for not letting me forget what I had said I would do. It would be obvious to say that without them this thesis would never have been written, but their help with proof reading and encouragement, ensured that it did not remain “the work in progress” that it was for too long.

Of Paul Williams, I'd like to make special mention. There I mentioned him. Thanks for all your contributions, not only academic in nature. The times we had working together will be part of my good memories when I look back at my university years. The best years of your life they say. It was great sharing them with you.

Last, and definitely not least, Thanks to my wife Kirsty. We met and got to know each other during the period that I worked on this thesis and she worked on hers. Well, it is finished! Thanks for your support, without which I have no doubt this work would never have seen completion. Thanks for the holidays and weekends sacrificed, all the proof reading and the loan of your computer. I thank God that we have come through together and I pray that He bless our time together forever.

Thank you everybody.

“To Boo”

TABLE OF CONTENTS

DECLARATION	II
ABSTRACT	III
OPSOMMING	IV
DEDICATIONS/ACKNOWLEDGEMENTS	V
TABLE OF CONTENTS	VI
LIST OF FIGURES	VIII
LIST OF TABLES	X
SYMBOL LIST	XII
EXECUTIVE SUMMARY	XIV
CHAPTER 1. INTRODUCTION	1
1.1. RESEARCH OBJECTIVES.....	2
CHAPTER 2. ENGINE THEORY	4
2.1. ENGINE PERFORMANCE.....	4
2.2. ENGINE CYCLE.....	4
2.3. INDUCTION SYSTEM.....	6
2.4. VOLUMETRIC EFFICIENCY.....	6
2.5. THEORIES OF FLOW EFFECTS.....	7
2.6. EFFECTS OF COMPONENTS ON ENGINE PERFORMANCE	16
2.7. CASE STUDIES	23
CHAPTER 3. ENGINE TESTING	25
3.1. ENGINE TEST FACILITY.....	25
3.2. ENGINE COOLING	27
3.3. FUELLING AND FUEL INJECTION.....	28
3.4. ENGINE MANAGEMENT SYSTEM	30
3.5. ENGINE TEST AUTOMATION (ETA)	31
3.6. AIR FLOW	31
3.7. ATMOSPHERIC CORRECTIONS	31
3.8. KNOCK	32
3.9. CLOSING COMMENTS	34
CHAPTER 4. EXPERIMENTAL DESIGN	35
4.1. INTRODUCTION	35
4.2. EXPERIMENTATION AND RESEARCH	36
4.3. TRADITIONAL EXPERIMENTATION	36
4.4. STATISTICAL DESIGN OF EXPERIMENTS	36
4.5. FULL FACTORIAL TO FRACTIONAL FACTORIAL	37
4.6. ALTERNATIVE DESIGNS.....	41
4.7. CLOSING COMMENTS	44
CHAPTER 5. TAGUCHI METHOD OF EXPERIMENTAL DESIGN	45
5.1. TAGUCHI METHODS: A QUALITY CONTROL TOOL.....	45
5.2. CHARACTERISTICS OF TAGUCHI METHODS.....	46
5.3. CLOSING COMMENTS	57
CHAPTER 6. TAGUCHI METHODS AS AN EXPERIMENTAL DESIGN TOOL (CASE STUDY ONE - EVALUATION)	58

6.1. EXPERIMENTAL PLANNING FOLLOWING THE TAGUCHI METHOD	58
6.2. PLANNING THE EXPERIMENT	60
6.3. DESIGNING THE EXPERIMENT.....	67
6.4. CONDUCTING THE EXPERIMENT.....	71
6.5. ANALYSING THE EXPERIMENT.....	74
CHAPTER 7. CASE STUDY ONE – TRADITIONAL METHODS VS TAGUCHI METHODS.....	82
7.1. INTRODUCTION	82
7.2. TRADITIONAL EXPERIMENTAL METHOD	82
7.3. TRADITIONAL EXPERIMENTAL ANALYSIS	83
7.4. EXPERIMENTAL EVALUATION METHOD - CONCLUSION	86
CHAPTER 8. CASE STUDY TWO - OPTIMISATION.....	87
8.1. PROJECT BACKGROUND	87
8.2. TRADITIONAL EXPERIMENTAL METHODS	87
8.3. TAGUCHI METHOD.....	87
8.4. PLANNING THE EXPERIMENT	88
8.5. DESIGNING THE EXPERIMENT	93
8.6. CONDUCTING THE EXPERIMENT	95
8.7. ANALYSING THE EXPERIMENT	96
8.8. EXPERIMENTAL METHOD EVALUATION	98
CHAPTER 9. CASE STUDY THREE - MODELLING AND SIMULATION	100
9.1. CASE STUDY BACKGROUND	100
9.2. INTRODUCTION	100
9.3. EXPERIMENT PLANNING FOLLOWING DR TAGUCHI’S METHOD.....	101
9.4. DESIGNING THE EXPERIMENT	105
9.5. CONDUCTING THE EXPERIMENT	108
9.6. ANALYSING THE EXPERIMENT	110
9.7. CONCLUSIONS.....	114
CHAPTER 10. CASE STUDY FOUR - TAGUCHI VS FULL FACTORIAL.....	116
10.1. PREPARATION	116
10.2. TAGUCHI INVESTIGATION	117
10.3. FULL FACTORIAL.....	118
10.4. COMPARISON.....	119
10.5. PREDICTION EQUATION.....	122
10.6. CONCLUSIONS.....	123
CHAPTER 11. CONCLUSIONS AND RECOMMENDATIONS.....	124
GLOSSARY.....	126
REFERENCES	128
APPENDIX A. CHANNEL LISTING FOR ETA CHANNELS (CHAPTER 3).....	131
APPENDIX B. CASE STUDY ONE TEST SUMMARY	137
APPENDIX C. CASE STUDY ONE EXHAUST TEMPERATURES.....	138
APPENDIX D. CASE STUDY ONE CO % LEVELS	139
APPENDIX E. CASE STUDY ONE TORQUE COMPARISON.....	140
APPENDIX F. CASE STUDY ONE POWER COMPARISON.....	141
APPENDIX G. CASE STUDY ONE: CARBURETTOR ADAPTER RESULTS.....	142
APPENDIX H. CASE STUDY TWO DATA VERIFICATION	145
APPENDIX I. CASE STUDY TWO: BIRDCAGE APPLICATION TABULAR RESULTS SUMMARY.....	146
APPENDIX J. BIRDCAGE GRAPH RESULTS	150
APPENDIX K. SIMULATION RESULTS FOR TEP @ 5300 RPM	154
APPENDIX L. SIMULATION RESULTS FOR LET @ 2800 RPM	155

LIST OF FIGURES

Figure 2-1. Volumetric Efficiency for Varying Inlet Tract Diameters and Lengths [After Heisler 1995].....	9
Figure 2-2. Inlet Configuration	14
Figure 2-3. Pipe Length Effect on Volumetric Efficiency. [Heisler 1995].....	17
Figure 2-4. (a) Circular and (b) Pie-Chart Representations of Valve Timing.....	19
Figure 2-5. Spiral Valve Timing Diagram.....	20
Figure 2-6. Inlet and Exhaust Valve Profiles and Angles (with altered valve timing from -180 to +420 as opposed to the expected -360 to +360).....	20
Figure 3-1. Hot Exhaust System During Testing.....	26
Figure 3-2. Engine Control Room Figure 3-3. Test Stand	26
Figure 3-4. Water Flow Circuit.....	28
Figure 3-5. Fuel System.....	29
Figure 3-6. Mass Fuel Flow Meter.....	29
Figure 3-7. Engine Control and Monitoring.....	30
Figure 4-1. CCRD Diagram	42
Figure 5-1. Quality Engineering Optimisation [Bryne and Taguchi 1986]	47
Figure 5-2. Taguchi Loss Function	48
Figure 5-3. Inspection-Driven Specifications vs. Quality-Driven Specifications.....	49
Figure 5-4. Orthogonal Array Flow Sheet	53
Figure 5-5. Linear Graphs of $L_{16}(2^{15})$ Orthogonal Array.....	56
Figure 6-1. Basic Carburettor Adapter Configuration Showing the Positions of the Two Flow Diverting Inserts.....	59
Figure 6-2. Taguchi Methodology	60
Figure 6-3. Prototype Configurations a shows the open adapter without any flow diverters in place, b shows the inclusion of the baffle plate, c shows the inclusion of the anti-swirl plate and d shows the expected air flow with both the baffle plate and the anti-swirl plates inserted with the flow approximating the pancake filter air flow pattern.....	65
Figure 6-4: Linear Graph of $L_4(2^3)$ Orthogonal Array.....	69
Figure 6-5 . Level Analysis Graphs for Case Study One. a, b and c are the power graphs for the baffle plate, the anti swirl plate and the interaction respectively. D, e, and f are the torque trends for the same.....	76
Figure 6-6. Top-End-Power Interaction Analysis	77
Figure 6-7. Mid-Range-Torque Interaction Analysis.....	78
Figure 7-1. Torque Output Comparison.....	83
Figure 7-2. Power Output Comparison	84
Figure 7-3. Top-End-Power and Mid-Range-Torque Comparison of all Tests.....	85
Figure 7-4. TEP and MRT for Prototype Carburettor Adapter Taguchi Investigation	85
Figure 8-1. Taguchi Methodology	88
Figure 8-2 MRT and TEP vs Carburettor Height for an Infinite Diameter [After Petzler 1996].....	91
Figure 8-3. TEP and MRT vs Plenum Volume [from Petzler 1996].....	92
Figure 8-4. Linear Graph of $L_9(3^4)$	93
Figure 8-5. Linear Graph of $L_{18}(2^1 \times 3^7)$	94
Figure 8-6. SFC Output Variable @ 3200 rpm	97
Figure 8-7. Power Output @ 4800 rpm (TEP)	97

<i>Figure 8-8. Power Output for Corrected Block Variance @ 4800 rpm</i>	98
<i>Figure 9-1. Alternative Linear Graph of L₁₆(4⁵)</i>	106
<i>Figure 9-2. Chosen Linear Graph of L₁₆(4⁵)</i>	107
<i>Figure 9-3. Torque @ 5300 rpm</i>	111
<i>Figure 9-4. Power @ 5300 rpm (TEP)</i>	111
<i>Figure 9-5. Torque @ 2800 rpm (LET)</i>	111
<i>Figure 9-6. Power @ 2800 rpm</i>	111
<i>Figure 9-7. Prototype Inlet Manifold</i>	115
<i>Figure 10-1. Taguchi Power Response Results @ 5300 rpm</i>	118
<i>Figure 10-2. Full Factorial Power Response Results @ 5300 rpm</i>	119
<i>Figure 10-3. Comparison of Full Factorial and Taguchi Analysis Trends</i>	120
<i>Figure 10-4. Taguchi and Full Factorial Difference</i>	121
<i>Figure 11-1. SFC @ 3200 rpm</i>	150
<i>Figure 11-2. Torque @ 3200 rpm</i>	150
<i>Figure 11-3. Power @ 3200 rpm</i>	150
<i>Figure 11-4. Average Exhaust Temp @ 3200 rpm</i>	150
<i>Figure 11-5. Exhaust Temperature Variance @ 3200 rpm</i>	151
<i>Figure 11-6. Average CO% @ 3200 rpm</i>	151
<i>Figure 11-7. CO% Variance @ 3200 rpm</i>	151
<i>Figure 11-8. SFC @ 4800 rpm</i>	151
<i>Figure 11-9. Torque @ 4800 rpm</i>	152
<i>Figure 11-10. Power @ 4800 rpm</i>	152
<i>Figure 11-11. Average Exhaust Temperature @ 4800 rpm</i>	152
<i>Figure 11-12. Exhaust Temperature Variance @ 4800 rpm</i>	152
<i>Figure 11-13. Average CO% @ 4800 rpm</i>	153
<i>Figure 11-14. CO% Variance @ 4800 rpm</i>	153

LIST OF TABLES

Table 4-1. 2^3 Full Factorial Design.....	38
Table 4-2. Saturated Two Level Design.....	39
Table 4-3. 2^{7-4}_{III} Design.....	40
Table 4-4. Latin Square Design.....	43
Table 4-5 Hyper-Greco Latin Square.....	44
Table 5-1. Examples of Noise Classification [Bryne and Taguchi 1986].....	50
Table 5-2. $L_{16}(4^5)$ Orthogonal Array.....	52
Table 5-3 Commonly Used Orthogonal Arrays.....	54
Table 5-4. Interaction Table of $L_{16}(2^{15})$ Orthogonal Array. [ASI 1987].....	54
Table 6-1. Parameter Levels.....	66
Table 6-2. $L_4(2^3)$ Orthogonal Array.....	69
Table 6-3. Signed $L_4(2^3)$ Orthogonal Array.....	70
Table 6-4. Case Study One Orthogonal Array.....	70
Table 6-5. Test Results Summary.....	72
Table 6-6. Taguchi Experiment Results Summary.....	72
Table 6-7 Before and After Repeatability Test.....	73
Table 6-8. Configuration Two Repeated.....	73
Table 6-9. Configuration Four Repeated.....	73
Table 6-10: Top-End-Power Response Table.....	74
Table 6-11: Mid-Range Torque Response Table.....	75
Table 6-12. Top-End-Power Interaction Analysis.....	77
Table 6-13. Mid-Range-Torque Interaction Analysis.....	78
Table 6-14. Significant Effects.....	79
Table 6-15. Optimum Level Settings.....	79
Table 7-1. : Fuel Consumption [kg/ hr].....	83
Table 8-1. Level Settings for Birdcage Configurations.....	92
Table 8-2. Orthogonal Array with Assigned Variables and Levels.....	95
Table 9-1. Design Performance Targets.....	100
Table 9-2. Supplied Camshafts.....	102
Table 9-3. Camshaft Profile Levels.....	103
Table 9-4. IVO Level Determination.....	103
Table 9-5. Calculation of DIFFANG.....	104
Table 9-6. DIFFANG Level Determination.....	104
Table 9-7. Length and Diameter Level Determination.....	105
Table 9-8. $L_{16}(4^5)$ Orthogonal Array.....	106
Table 9-9. Variable Parameters and Levels.....	107
Table 9-10. Modelling Matrix.....	107
Table 9-11. Simulation Results @ 5300 RPM (TEP [kW]).....	109
Table 9-12. Simulation Results @ 2800 RPM (LET [Nm]).....	109

<i>Table 9-13. Torque Response Table @ 5300 rpm</i>	<i>110</i>
<i>Table 9-14. Power Response Table @ 5300 rpm (TEP).....</i>	<i>110</i>
<i>Table 9-15. Torque Level response @ 2800 rpm (LET).....</i>	<i>110</i>
<i>Table 9-16. Power Response Table @ 2800 rpm.....</i>	<i>111</i>
<i>Table 9-17. Optimum Level Settings</i>	<i>113</i>
<i>Table 10-1. Levels of the input Variables.....</i>	<i>116</i>
<i>Table 10-2. Orthogonal Array used in the Taguchi analysis.</i>	<i>117</i>
<i>Table 10-3. Taguchi Analysis Power Response Table @ 5300 rpm.....</i>	<i>117</i>
<i>Table 10-4. Full Factorial Power Response Table @ 53200 rpm.....</i>	<i>118</i>
<i>Table 10-5. Comparison of Full Factorial and Taguchi Results.....</i>	<i>119</i>
<i>Table 10-6. Difference Between Full Factorial and Taguchi Results.....</i>	<i>121</i>
<i>Table 10-7. Final Comparison</i>	<i>123</i>

SYMBOL LIST

Abbreviations

ABDC	After Bottom Dead Centre	kPa	Kilo-Pascal
ANOM	Analysis of Means	kW	Kilo-Watts
ANOVA	Analysis of Variance	LET	Low End Torque [Nm]
AC	Alternating Current	mA	Millie-Amperes
ATDC	After Top Dead centre	MAP	Manifold Absolute Pressure [kPa, Pa]
BBDC	Before Bottom Dead Centre	MON	Motored Octane Number
BDC	Bottom dead centre	MRT	Mid Range Torque [Nm]
BTDC	Before Top Dead Centre	Nm	Newton Meter
CFD	Computational Fluid Dynamics	NO _x	Nitrous Oxide
CO	Carbon-monoxide	Pa	Pascal
CO ₂	Carbon-dioxide	PID	Proportional, Integral and Differential
CV	Constant Velocity	rev	Revolution/s
DC	Direct Current	RON	Research Octane Number
DOF's	Degrees of Freedom	Rpm	Revolution per minute
ECU	Engine Control Unit	S/N	Signal to Noise Ratio
EC38	Eddy Current 38 dynamometer	SABS	South African Bureaux of Standards
ESA	Engine Simulation Analysis	SED	Statistical Experimental Design
ETA	Engine Test Automation.	SFC	Specific Fuel Consumption [g/W or kg/kW]
EVC	Exhaust Valve Closing	SMD	Sentrum vir Meganiese Dienste (Centre for Mechanical Services at US)
EVO	Exhaust Valve Opening	SOHC	Single Over Head Cam
HC	Hydro Carbon	TDC	Top dead centre
IO	Input Output	TEP	Top End Power
IVC	Inlet Valve Closing	US	University of Stellenbosch
IVO	Inlet Valve Opening	WOT	Wide Open Throttle

Greek Letters

μ	Efficiency [%]	displacement [degrees]
π	Pi [3.14159]	
θ_t	Crank shaft angular	

Symbols

ω	Engine rotation speed [radians]	m_a	Mass of air inducted [g, kg]
ρ_i	Density in intake manifold [kg/m ³]	m_f	Mass of fuel inducted [g, kg]
A	cross sectional area of tuned pipe [m ²]	mm	Millimetre
C	Celsius [°]	N	Newton
C	Speed of sound [30 m/s at STP]	N	Engine Crankshaft speed [rpm]
c	Velocity of sound in air [m/s]	n	Resonant frequency [Hz]
e_v	Volumetric Efficiency [%]	R_s	Engine Speed [rpm]
G	Gram	T, t	Time [sec, min, hour]
k	the loss constant for the loss function	T	Torque [Nm]
L	the loss at the specifications limit for the loss function	V	resonating volume [m ³]
L	Length [m or mm]	V_d	Displaced Volume [m ³]
M	the mean target for the loss function	Y	the value of the response for the loss function
m	Meter		
<u>Subscript</u>			
I	Inlet, intake	f	Fuel
v	Volumetric (as in ρ_v)	e	Exhaust, exit
a	Air		

EXECUTIVE SUMMARY

Experimental design as a research technique is greatly under-utilised in automotive engine research in South Africa. Traditional experimentation methods are still used extensively in the examination and optimisation of investigated parameters. This traditional approach involves varying one parameter at a time in order to quantify trends and effects on a product or process in terms of one or several evaluation parameters. The experimental design approach varies all parameters simultaneously in order to quantify each individual parameter independently and is a much more powerful and effective option.

In this publication the necessary technical background is investigated for the testing and optimisation of engine induction systems. Induction mechanisms and basic internal combustion theory are discussed, and engine testing techniques are addressed from both hardware (engine test bed) and software (engine control and data capture) points of view.

Genuchi Taguchi originally developed the Taguchi methodology for experimental design as a quality control tool. It was largely applied to quality control in a production line environment, hence improving the quality of the end product. Taguchi methods are unique in that the application and data analysis can be divorced from the advanced statistics that are often necessary in the design and analysis of a complex experiment. The method uses an engineering approach to problems rather than a purely statistical one and emphasises engineering judgement on a foundation of statistics. Orthogonal arrays are used to follow a simple recipe with four main sections: experiment planning, experiment design, experimentation and finally experimental analysis. The design and application of extremely complex but efficient experiments are thereby made possible for engineers with limited statistical knowledge.

The statistics, as needed for the development of a Taguchi type experimental design application, are addressed from the relevant basic statistical concepts. The technique is moved from a quality control tool, to that of experimental design and so transferring the same time and cost benefits from quality control to experimentation and design. Other similar design techniques such as CCRD (Central Composite Rotatable Design), Plackett-Burman (Hadamard) matrices and Latin squares are also discussed in the literature investigation.

The Taguchi experimental method was applied in prototype evaluation, experimental optimisation and trend investigation, and engine modelling. Each of these applications was compared to the traditional experimental process that would otherwise have been used for such an experimental investigation.

The first application was a prototype evaluation in which the effect of the inclusion of two flow diverters in a prototype carburettor adapter was evaluated in terms of power, torque and fuel consumption. Each diverter effect was quantified, and the optimum configuration found. The interaction between the two diverters was quantified statistically. This was not possible using the traditional experimental method. The structured experiment process of the Taguchi design allowed for systematic data analysis and a

formalised result presentation. This compared favourably to the subjective analysis and results of the traditional method.

The second application was an optimisation exercise in which the induction system between the air filter and the carburettor (carburettor adapter) was investigated in terms of four parameters, namely the feed pipe length and diameter, and the carburettor adapter plenum height and diameter. The investigation was made possible only through the use of Taguchi methods. Each parameter was tested at three levels or values resulting in a full factorial design matrix of 81 experiments. Using an L18(21x37) orthogonal array 18 tests were used to quantify the main effects and any arising interactions. The optimum configuration for the investigated components was determined and the performance predicted and then tested for conformation. The large amount of data gathered from so few experiments show the power of the Taguchi methodology of experimental design.

The third application was a modelling investigation in which software was used to simulate the engine performance. Inlet manifold and camshaft dimensions were varied simultaneously. The full factorial design of this investigation involved a simulation of 1024 runs compared to the Taguchi designed experiment where 18 simulations were used to obtain equivalent information. The results from these investigations were compared to determine the accuracy lost in the reduced number of experiments. It was seen that the Taguchi matrix provided very good results when compared to the full factorial investigation at a fraction of the computer time. This indicated a saving in time and effort.

Finally the Taguchi method of experimental design was evaluated as a tool in the automotive engine research field. It served well as a theoretical tool although there were disadvantages in using it in practise. This was largely due to the large amount of experimental preparation needed and the lengthy experimentation required before results were forthcoming. When many parameters are investigated and varied simultaneously, the data analysis can become very involved and reliant on statistics to sift through the data to determine the trends. Results are only forthcoming after the investigation has been completed. A progressively growing knowledge throughout the experimentation process, as achieved with traditional methods, is thus exchanged for a more complete knowledge of the investigated product or process, but only after all data analysis has been completed.

This thesis serves both as an example of the application of Taguchi methods as a research tool, and as a guideline for further Taguchi method experimental designs.

Chapter 1. Introduction

The internal combustion engine¹ is comprised of a collection of many independent yet inter-related components, each affecting the others performance. In order to optimise this complex system of interactive, interdependent components, a complete understanding of the mechanisms affecting the system is required, as well as a knowledge of the applied optimisation methods.

An engine can be optimised, where only the best or optimum conditions are sought for its operation, or alternatively it can be investigated, where a complete understanding of the system is sought. A system can be affected by two kinds of variables (controllable variables, such as exhaust length, engine speed, fuel type and uncontrollable variables, such as atmospheric pressure, engine wear and humidity). The uncontrollable variables must be minimised and/or corrected for, i.e. by using SABS torque correction factors to compensate for atmospheric and temperature variations or by preparing the inlet air to be at a desired temperature and humidity. The measurement of a system's performance is done by measuring an output variable such as torque, power or fuel consumption [Biles and Swain 1980]. The system is investigated by varying the controllable variables (independent variables) and measuring the associated effect on the output variable (dependent variables).

The induction mechanisms of an engine are those mechanisms that affect the airflow in the induction system. The mechanisms show the interdependence between inlet and exhaust pipe configurations and the valve timing (camshaft). The interdependence implies that by changing the exhaust valve timing, a new and different exhaust will be required to give optimum performance and by changing the exhaust configuration, a new valve timing setting will be needed for optimum performance.

Traditionally one component or dimension of a component is optimised and then the next in a sequential manner. The overall optimum configuration of the engine is therefore never reached, as the components do not function in isolation. The optimisation of one component will alter the operation of the others, and indeed change the optimum operating conditions of each one. It is therefore necessary to examine the interactions that exist within the system as well as each single variable as all the engine components are dependent on each other. Alternatively the parameters can be optimised independently of the values of the other variables.

To investigate all the possible combinations would prove tedious and exhausting and in most cases is not feasible. For example, if seven variables were chosen for an experiment, and each variable was to be tested at three levels, in order to characterise each variable's effect completely it would be necessary to test all the combinations. This would necessitate the testing of 2187 (3⁷) engine configurations in a full

¹ All the experimental applications described in the case studies in this thesis were undertaken on petrol engines and thus the diesel engine is not discussed in this text. All references in this document to the internal combustion engine therefore refer specifically to the petrol engine.

factorial analysis. Using Taguchi experimental design techniques, it is possible to drastically reduce this number of experiments without foregoing any information [Barker 1986.]. Only 18 experimental configurations are needed to complete this investigation [Peace 1993]. This method of statistical experimental design essentially quantifies the trends of each variable irrespective of the trends or values of the other variables in the system, and it accomplishes it in much fewer experiments than other 'traditional' experimental design methods, i.e. fractional factorial designs.

The general background, set-up and testing of internal combustion engines can be divorced from the statistical theory of the experimental design methods used to design the experiment. Similarly the design method as prescribed by Taguchi Methods can be developed and explained without specific reference to the application. However, in order to optimise any given process or product, there must be a thorough understanding of that process or product. The engine testing methods are very important to ensure integrity of the information gathered for analysis, these are discussed in Chapters 2 and 3. Without a good understanding of the techniques and equipment used there is an increased possibility of spurious data, incorrect results and incorrect conclusions resulting from the tests. Experimental design methods are discussed in Chapter 4, and a description of the Taguchi Method of experimental design is discussed along with its development from a quality control tool to an experimental design tool in Chapters 5 and 6. An illustrative example is given in Chapter 7 and three further case studies are then undertaken in Chapters 8 through 10 to illustrate the different possible applications of Taguchi Methods and the advantages and disadvantages of the method in each of these areas. In some cases Taguchi Methods are compared to the traditional methods that would otherwise have been used.

1.1. Research Objectives

It was the objective of this thesis to investigate the use of Taguchi Methods as an experimental design tool for testing automotive engines in the automotive research industry. The success of the Taguchi method of experimental design is determined by comparing and contrasting it to the traditional method of experimental design by using both techniques in some of the case studies. Each case study was in a different aspect of the automotive engine optimisation field, illustrating the diverse application of the method.

In the first case study, a simple Taguchi matrix was used to examine the influence of two flow diverters in a carburettor adapter on engine performance. The main trends as well as the degree of interaction were investigated to determine the optimum configuration of the flow diverters. The results are compared to a traditional method of testing and evaluation. This case study illustrates the success of the Taguchi design method in a prototype evaluation.

In the second case study, a more complex and lengthy experiment was conducted where the design variables of a carburettor adapter were investigated. The trends in the effect of the length and diameter

of the feed pipe as well as the diameter and height of the plenum chamber were determined using an 18 experiment matrix. This case study clearly illustrates the advantages of the Taguchi experimental design method in reducing experimental time in a trend investigation application.

The third case study used an engine modelling software package to identify variable trends and also minimise the amount of testing required. The variables investigated were the inlet manifold diameter and length, and the valve angles and valve lift. Case study four used a more developed version of the same package as used in case study three and compared the Taguchi Method results to the equivalent results from a full factorial investigation.

Chapter 2. Engine Theory

2.1. Engine Performance

The internal combustion engine is designed to convert potential energy contained in the liquid fuel, into kinetic energy that can be used to propel a vehicle. The basic mechanism for a petrol engine is as follows: A charge of air-fuel mixture is drawn into the combustion chamber, compressed and ignited. The expansion resulting from the charge burning forces the piston downward producing kinetic energy, which is used to turn the drive shaft connected to the wheels, and propel the vehicle forward. This mechanism is discussed in more detail in Section 2.2.

There are many factors that influence the performance of an engine. The air-fuel ratio of a petrol engine needs to be close to stoichiometric (14 to 1), for complete combustion to take place and achieve maximum energy efficiency. Limiting the amount of charge drawn into the combustion chamber controls the power and torque of the engine. By reducing the amount of charge entering the cylinder, the mass of fuel is reduced and there is less energy available to do work, hence a reduction in power and torque. The charge mass is reduced by reducing the manifold pressure and thus the combustion chamber pressure. This is achieved by throttling the airflow into the combustion chamber using a butterfly valve in the air intake pipe or throttle body.

An open throttle valve (Wide Open Throttle, WOT) results in the highest pressure (close to atmospheric pressure) in the combustion chamber due to the low pressure drop across the throttle body. The higher pressure in the combustion chamber results in the greatest charge mass drawn into the combustion chamber, and thus the highest power and torque. As the throttle closes, the pressure drop across the throttle body increases, and the pressure in the combustion chamber drops. Less charge is therefore drawn into the combustion chamber and made available for combustion. For maximum power/torque output from the engine the amount of charge drawn into the engine must be maximised. This is referred to as the volumetric efficiency and is discussed further in Section 2.4.

2.2. Engine Cycle

A four-stroke engine gets its name from the fact that the entire cycle of the engine comprises of four strokes, namely, an inlet, a compression, an expansion and an exhaust stroke. Each stroke occurs over 180° of engine revolution. The cycle duration is thus 720° (noted as being from -360° to $+360^\circ$). In a

four-cylinder engine each of the cylinder cycles is offset by 180° to the others. The engine therefore is always experiencing a power² stroke.

The first stroke of the cycle is the induction stroke, where fresh charge is drawn into the cylinder. On the downward stroke of the piston air is drawn into the cylinder through the inlet valve port due to reduced pressure in the cylinder. As the piston continues downward the low pressure intensifies and more charge is drawn into the combustion chamber to equalise the pressure difference across the inlet valve. The compression stroke starts at bottom dead centre (BDC) when the piston changes direction and starts to move upward. The induction process is still in progress due to the momentum of the incoming air and the inlet valve closes after BDC³.

The compression stroke compresses the charge by utilising the energy in the flywheel supplied by the previous power stroke as well as the power strokes of the other cylinders. With the inlet valve closed the gasses in the combustion chamber are compressed as the piston moves upward. Just before the piston gets to top dead centre (TDC) the sparkplug fires and ignites the fuel-air mixture in the combustion chamber. Ignition lag and slow initial burning allow the piston to pass TDC before the majority of the charge is burnt and maximum pressure reached. As the charge burns it expands and increases in temperature. The combustion products are much less dense than the air-fuel-mixture, and this together with the rise in temperature results in the gases expanding, causing the pressure in the combustion chamber to rise dramatically to as much as 50 bar [Heisler 1995]. This increase in pressure forces the piston downward and powers the engine during the expansion stroke.

The exhaust valve opens 40 to 75 degrees before the piston gets to BDC. The initial venting of the exhaust gases when the exhaust valve opens is violent and dramatic due to the large pressure difference that is present across the exhaust valve. This pressure release is called exhaust blow down and causes pressure and inertial effects in the exhaust pipes that aid exhaust scavenging⁴ at the end of the exhaust stroke. The exhaust stroke forces the burned gases out of the cylinder as the piston moves upward.

At 10 to 30 degrees before the piston reaches TDC the inlet valve opens and fresh charge is introduced into the cylinder. The action of the inlet valve opening causes pressure and inertial effects in the inlet manifold, which effect the induction process. The incoming fresh charge helps with the exhaust scavenging by driving out the exhaust gases. The exhaust valve closes 10 to 30 degrees after TDC at which stage the induction stroke has already commenced. This results in a valve overlap of 20 to 60 degrees [Heisler 1995]. The cycle is repeated from TDC with the induction stroke.

All the valve timing angles can be changed by changing the camshaft designs and are specific to, and different for, each engine make and model. The valve timing is therefore an engine design variable that needs investigation and facilitates optimisation.

² Sometimes called an expansion Stroke.

2.3. Induction System

The components of the induction system form a complex piping system of restrictions, expansions, pipes and plenum chambers through which the air, fuel and exhaust gases (during reversion where exhaust gases flow into the inlet manifold) must flow. The gases experience phenomena including momentum affects and pressure pulsation as a result of the gas movement. These phenomena effect the engine breathing characteristics in a complex manner that involves interaction and superposition of flow effects. The ultimate result of these phenomena is a change in volumetric efficiency, which in turn affects engine performance.

The geometry of each of the components is specific to an engine's make and model. The interaction between components necessitates the investigation and optimisation of the dimensions of each component for each engine designed.

2.4. Volumetric Efficiency

Volumetric efficiency is defined as the ratio of the mass of charge inducted into the cylinder to the mass that would occupy the displaced volume at the air density in the intake manifold [Ferguson 1986]. It can be calculated by Equation 2-1

$$e_v = \frac{4\pi(\dot{m}_a + \dot{m}_f)}{\rho_i V_d \omega} = \frac{2(\dot{m}_a + \dot{m}_f)}{\rho_i V_d R_s} \quad [2-1]$$

Where	e_v	= Volumetric Efficiency [%]
	•	
	\dot{m}_a	= Mass flow of Air inducted [kg/s]
	•	
	\dot{m}_f	= Mass flow of fuel inducted [kg/s]
	ρ_i	= density in intake manifold [kg/m ³]
	V_d	= Displaced volume [m ³]
	ω	= Engine Speed [radians/s]
	R_s	= Engine Speed [rpm]

The volumetric efficiency of a naturally aspirated engine ranges from 40% to 115% depending on engine speed and throttling, amongst other things, but it is usually approximately 84 % [Ferguson 1986]. Volumetric efficiency is best examined under wide-open throttle conditions where the engine is delivering maximum output. It is also under these conditions that maximisation is required. Throttling

³ IVC occurs approximately 40° to 75° after BDC

restricts the flow of air into the combustion chamber and therefore reduces performance. Under these conditions optimisation could be performed to reduce exhaust emissions and fuel consumption as well as maximising the output power and torque.

The effect of a change in volumetric efficiency is reflected in a change in engine torque. Volumetric efficiency is very difficult to measure accurately, as it is not a direct measurement, but is calculated from measurements of fuel consumption, air consumption, and engine speed. By measuring torque however, we have a good indication of the volumetric efficiency, and torque is easily and accurately measured. In most engine tests therefore, torque is used as the comparative or evaluative variable to represent volumetric efficiency. Torque is measured by using a dynamometer, which absorbs or provides power (under motored conditions) to the engine. The dynamometer is supported on bearings but restrained from rotating by a load cell. The force in the load cell [N] multiplied by the lever arm defines as the distance from rotation axis to load cell point of attachment [m] gives the torque of the engine [Nm].

Other variables that can be used for engine performance evaluation are:

- Power [kW], which is the product of torque [N] and engine speed [rad], indicates the level of engine output and is a measure of the rate at which work can be done,
- Specific Fuel Consumption [SFC], measured as g/kWh (fuel consumption/power), indicates the engines efficiency,
- Engine Emissions such as Carbon-monoxide % [CO%], Nitrous oxides [NO_x], Carbon-dioxide [CO₂], Hydro-carbons [HC's], which all indicate combustion efficiency, and
- Exhaust temperature and oxygen measurement (lambda) for each cylinder indicates even fuel distribution and fuelling homogeneity across the cylinders.

2.5. Theories of Flow Effects

The breathing mechanisms of the engine are complex and there is a high degree of interaction between the incoming charge and the exhaust gases due to the valve overlap when both the inlet and the exhaust valves are open simultaneously. There are three main theories that attempt to describe the flow phenomena and the complex interactions of flow. The theory of induction inertial cylinder charging suggests that the inertial mass (momentum) of moving air can be used to ram extra charge into the combustion chamber.

The second theory, induction wave ram cylinder charging, suggests that the pressure pulses that move within the piping system can be used to induce lower pressures in the combustion chamber and thus aid the engine breathing. The Helmholtz resonator theory suggests that standing waves are set up within

⁴ The action of the incoming charge pushing out the exhaust gasses [Ferguson 1986]

the piping system as a result of the natural frequency of the piping geometry. These can be used to tune the geometry to provide a boost to the volumetric efficiency.

All the theories tend to provide maximum benefit to the engine at specific engine speeds, and all the mechanisms are taking place simultaneously superimposed onto each other. Therefore by utilising each of the mechanisms at different engine speeds, it may be possible to design a piping system that gives additional power boost across the entire speed range to generate a flat torque curve and give good drivability or at the same speed to provide a “power band”. The theories essentially provide different techniques for visualising what is most likely the same event/phenomenon occurring at different frequencies, places and times during the combustion process. The three main theories that describe the flow phenomena that affect induction flow are discussed in more detail below.

2.5.1. Induction Inertial Ram Cylinder Charging

This theory states that the inertia (momentum) of the incoming charge can be used to ram additional charge into the combustion chamber. The incoming velocity (kinetic energy) is translated to a higher pressure in the combustion chamber. A higher pressure means more charge and more charge translates to greater power.

The induction stroke of the internal combustion engine starts with the inlet valve open and the piston reaching TDC. As the piston moves downward after TDC, the pressure in the combustion chamber is lower than atmospheric pressure, forming a partial vacuum in the cylinder. The pressure difference across the inlet port between the combustion chamber and the charge in the inlet manifold tract forces the column of charge to accelerate into the combustion chamber. This charge acceleration results in the increase of momentum of the incoming charge.

The point where the piston is at maximum speed downwards, and the kinetic energy of the charge entering the combustion chamber is almost at its greatest, is when the piston reaches mid stroke. The piston acceleration reverses and the piston slows during the second part of the induction stroke until it stops at BDC, changes direction and starts moving upwards. The incoming column of charge in the inlet tract however, possesses kinetic energy as a result of its incoming velocity, and it continues to enter the combustion chamber. This results in an increase in pressure in the combustion chamber and the charge is rammed into it despite the decreasing volume.

As the piston moves past BDC and starts the compression stroke, the inlet valve is still open and the charge is still entering the combustion chamber due to its inertia. This further increases the pressure and results in more charge being able to occupy the space in the combustion chamber and the pressure can reach values greater than atmospheric pressure in highly optimised engines. This enables volumetric efficiency to reach values of greater than 100% [Heisler 1995]

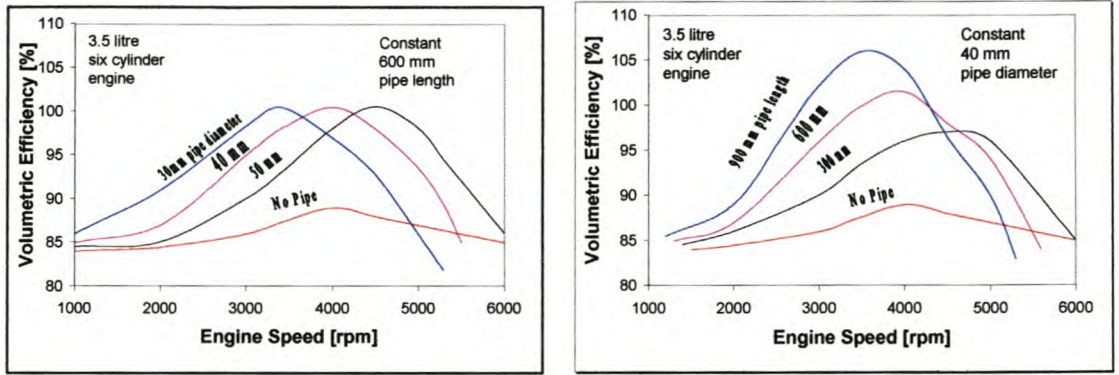


Figure 2-1. Volumetric Efficiency for Varying Inlet Tract Diameters and Lengths [After Heisler 1995]

Figure 2-1 shows some of the effects that geometry has on volumetric efficiency.

- It can be said that reducing the pipe diameter will increase the air velocity and thus increase the momentum for a constant volumetric flow rate (constant engine speed). The experimental data used in Figure 2-1 shows that for a given tract length, the ram charge pressure peak (higher volumetric efficiency) is seen to occur at lower engine speeds with smaller diameter pipes although the magnitude of the pressure peak is shown to be unaffected by the pipe diameter.
- The graphs also show that while keeping the pipe diameter constant, a longer tract will provide a greater charge column mass and thus increased momentum and a greater ram-charging effect and an associated increase in peak volumetric efficiency. Increased flow resistance due to the longer pipe however, results in the pressure peak occurring at lower engine speeds. The tail off after the pressure peak is more pronounced in the longer pipes than the short because of the increased pipe surface area, and the accompanying increase in flow resistance.

Momentum is defined as the product of the mass and the square of the velocity (Equation 2-2)

$$\text{Momentum} = \text{mass} \times \text{velocity}^2 \quad [2-2]$$

- An increase in either mass or velocity will increase the momentum effect.
- Velocity will have the greater influence in the momentum effect, as momentum is proportional to the square of velocity. However with an increase in velocity there is an associated increase in wall friction. The optimum velocity will therefore be a compromise between momentum maximisation and the minimisation of flow losses due to friction.
- The valve overlap in adjacent cylinders can interfere with the induction ram charging. For example, if cylinder two is in an inlet valve open position, there will be a low pressure in the inlet tract. If this coincides with the inlet valve closing (IVC), a high pressure event of adjacent cylinder one, then

the low pressure in inlet tract two could rob some of the pressure in inlet tract one and result in a decreased inertial ram-charging for cylinder two unless catered for by adequate pipe length.

- The ramming of the outside branches of a four cylinder engine is more pronounced at low engine speeds due to the longer inlet tract. At high engine speeds, the flow resistance results in a decrease of volumetric efficiency in cylinders one and four with respect to cylinders two and three.

A secondary effect of the inertial ram charging comes into play when the inlet valve is closed. The momentum of the charge moving into the combustion chamber is halted against the closed valve and the momentum causes a stagnant pressure build up behind the inlet valve in the inlet tract. This stagnant pressure propagates towards the open end of the inlet tract as the charge energy is converted from kinetic energy to pressure energy. (This can be seen in Bernoulli's equation).

The entire inlet tract will reach a stage when it will be at a stagnation pressure that is greater than the atmospheric pressure at the open end. The pressure difference results in the air at the open end of the tract moving out into the atmosphere and the pressure in the tract starts to drop progressively from the open end. The energy of the charge is then converted from pressure energy back into kinetic energy out of the tract. The pressure drop starts at the open end and propagates toward the closed inlet valve as the energy conversion takes place.

When the low pressure progresses to the closed inlet valve, the tract will once again reach stagnation pressure, however, this time it will be lower than the atmospheric pressure at the open end of the tract. This pressure difference then results in air entering the tract and forming a high-pressure region. The air then gains momentum as it moves into the inlet tract and the high pressure front will move down the inlet tract towards the inlet valve. When the tract again reaches stagnation pressure higher than the atmospheric pressure at the open end of the pipe, the cycle repeats. This cycle will continue for as long as the inlet valve is closed.

If the inlet valve opens when the inlet tract is at a high stagnation pressure, (or when the high-pressure inertial front reaches the inlet port) the high pressure will cause a greater pressure differential between the inlet tract and the combustion chamber. This will result in better cylinder filling and better volumetric efficiency. The exhaust gas extraction will also be aided as a result of the high pressure in the inlet tract as the increased energy of the incoming air tends to force the exhaust gases into the exhaust tract during valve overlap. This too results in improved volumetric efficiency.

If the inlet valve opens when the combustion chamber pressure is higher than the pressure in the inlet tract then reversion occurs. When the inlet valve opens the combustion products flow from the combustion chamber into the inlet tract until the pressure across the inlet valve is equalised. When the piston starts moving downwards, the pressure in the combustion chamber will again be lower than the pressure in the inlet tract and the air will flow into the combustion chamber. The combustion products

in the inlet tract will flow back into the combustion chamber before the fresh charge does. This reduces the amount of fresh charge that can enter the combustion chamber and therefore reduces the volumetric efficiency.

Optimal utilisation of the inertial ram cylinder charging effect can be achieved by tuning (optimising) the inlet pipe length such that the high pressure front is at the inlet valve at the time of opening. The tuning will be specific to one engine speed however as the valve timing is dependent on the engine speed whereas the pressure pulse velocities are dependent on the air temperature which essentially will remain constant during operation.

2.5.2. Induction Wave Ram Cylinder Charging

The wave effect refers to pressure waves or pulses that are present in the inlet tract of the manifold as a result of the instantaneous pressure differences that occur when a valve opens. The pressure pulses travel at the speed of sound through the gases in the induction and exhaust pipes and are both above and below atmospheric pressure. The pressure pulses are superimposed on the pressure fronts discussed in the previous section.

A simple way to visualise the pressure wave moving through the inlet tract is by using a coil spring that has been slightly stretched. By introducing a pulse at one end (a slight jerk) the compressed part of the spring will travel down the length of the spring and be **reflected** at the other side without significant movement of the entire spring. The pulse travels back and forth with less energy in each reflection.

When the inlet valve opens, the low pressure in the cylinder (as a result of the outgoing exhaust gas momentum) causes a negative pressure pulse/wave to travel from the inlet port, through the column of charge, towards the open end of the tract. When the wave reaches the open end it is **rarefacted** as a positive pressure wave. This happens because the negative pressure wave reaching the open end causes a pressure depression and the air then rushes into the tract to fill the depression. The inertia of the incoming air causes a positive pressure wave that travels from the open end back towards the inlet valve. When the inlet valve closes the pulses continue to reflect back and forth with decreasing magnitude until they decay away.

When the pressure wave reaches the back of the open inlet valve port it is rarefacted back towards the open end as a negative pressure pulse due to the valve being open. It also aids in cylinder filling by pushing air into the combustion chamber. These positive and negative pressure pulses travel back and forth with decaying amplitudes in the inlet tracts until the inlet valve closes [Heisler 1995].

This positive pressure pulse can be used to ram extra charge into the cylinder if the pipe is tuned such that the positive pressure wave reaches the inlet valve just before closing. The positive pressure wave will enter the combustion chamber and be contained there by the valve closing thus resulting in a higher

pressure in the combustion chamber. The increased density of the charge during ramming will result in a higher volumetric efficiency.

Pipe length tuning is determined from Equations 2-3 to 2-5. [Heisler 1995]

$$\text{Speed of Sound} = \frac{\text{Distance the pulse or wave travelled [m]}}{\text{time taken [s]}} \quad [2-3]$$

$$\text{rearranging gives: } \text{time} = \frac{\text{Inlet tract length} \times 2}{\text{speed of sound}} \quad [2-4]$$

$$t = \frac{2L}{1000C} \quad [2-5]$$

$$\text{giving } L = \frac{1000C * t}{2} \quad [2-6]$$

Where: t = time for pulse to travel twice the tract length [s]

L = Length of tract from open end to inlet valve port [mm]

C = speed of sound through air [± 330 m/s]

Also: Crankshaft displacement = time of travel x angular speed [2-7]

$$\begin{aligned} \text{Substituting we get } \therefore \theta &= t \times \frac{360}{60} N = \frac{2L}{1000C} \times \frac{360}{60} N \\ &= \frac{2L}{1000C} \times 6N = \frac{0.012LN}{C} (\text{deg}) \end{aligned} \quad [2-8]$$

Where θ = crank shaft angular displacement [degrees]

N = engine crankshaft speed [rpm]

For example: For an induction period of 240 degrees (θ) and at an engine speed of 3000 rpm the length of the pipe would have to be,

$$L = \frac{240 * 330}{0.012 \times 3000} = 2.200 \text{ m} \quad [2-9]$$

for the induction wave ram cylinder charging to be tuned to the first positive pulse returning to the inlet valve. To be tuned for the second positive pulse return the inlet pipe would need to be 1.1m long, and to be tuned for the third and fourth pulse returns, pipe lengths of 0.733m and 0.55m would be needed respectively.

The pressure pulse is, however, not always returned rarefacted. The cycling of the compression and expansion waves will be interrupted when the inlet valve closes and a secondary effect comes into play. When an expansion or compression wave/pulse reaches a closed end of a pipe, it is **reflected** not

rarefacted. A compression pulse will be returned as a compression pulse but with lower amplitude and visa versa for the expansion wave.

The inlet tract length can therefore also be tuned for the secondary effect to ensure that a compression wave gets to the inlet valve as it is opening. This will aid exhaust gas scavenging as well as cylinder filling and improve volumetric efficiency and engine performance [Heisler 1995].

2.5.3. Helmholtz Resonator Cylinder Charging

The Helmholtz resonator theory is used in low speed tuning applications where the tuned pipe length using the induction wave ram charging theory (Section 2.5.2) would result in the individual tract lengths being too long. This is found in heavy-duty diesel engines where the maximum engine speed is only in the region of 2000 rpm. The theory is also known as the organ pipe theory, as it uses the resonant frequency of a spherical chamber with a pipe projecting from it to determine the optimum dimensions. It is important to note that while the previous theory focused on the pipe dimensions to tune the system, in this instance it is the plenum dimensions (chamber dimensions) that are critical in determining the resonant frequency of the system. The resonant frequency of the chamber and pipe is given by [Heisler 1995] as:

$$n = \frac{C}{2\pi} \sqrt{\frac{A}{LV}} \quad [2-10]$$

where

- n = resonant frequency [Hz]
- C = velocity of sound in air [m/s]
- A = cross sectional area of tuned pipe [m²]
- L = Length of the tuned pipe [m]
- V = resonating volume [m³]

The natural resonant frequency of vibration of a chamber and tuning pipe are used to excite the air inside the chamber. The inlet valve opening (once every two engine revolutions) produces a negative pressure wave that disturbs the air in the resonator chamber and pipes. The engine speed and system dimensions can be tuned so that the pressure-wave pulse frequency corresponds to the natural frequency of the system.

The air in the chamber will be excited into a state of resonance with the inlet valve motion producing a series of pressure waves. These can be timed correctly, exposing the cylinder to blasts of compressed air at the end of the induction stroke, just before the inlet valve closes (IVC), where the piston movement is

no longer assisting with cylinder filling. The resonance volume can be chosen to resonate at the speed where the boost in torque is needed or desired.

Figure 2-2 shows a system where the inlet pipes are 550 mm long with a diameter of 4 cm. The characteristic tuned speed for this configuration is twice the resonant frequency, i.e. 2510 rpm.

$$\begin{aligned}
 n &= \frac{330}{2\pi} \sqrt{\frac{\pi 0.02^2}{0.55 \times 0.01 \times 0.01 \times 0.04}} \\
 &= 1255.2 \text{ Hz} \\
 &= 2510.5 \text{ rpm}
 \end{aligned}
 \tag{2-11}$$

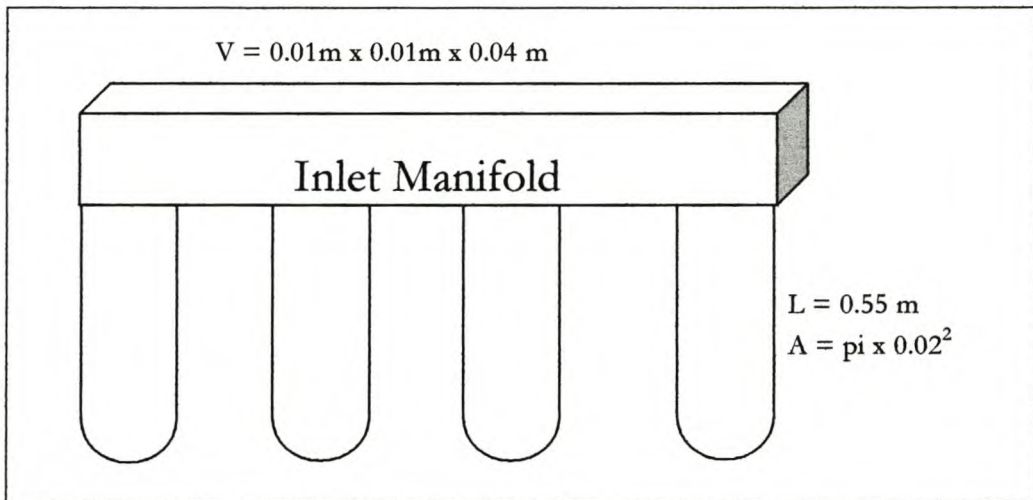


Figure 2-2. Inlet Configuration

This theory is not easily applied to systems where adjacent cylinders with overlapping induction periods share a tuning pipe, as the pulses will interfere with each other both constructively and destructively. The tuning benefits are very specific to one engine speed. The advantage gained from tuning reduces sharply as the engine operation varies away from the tuned speed. To combat this phenomenon, multi-stage systems are used. Valves controlled by engine speed are used to divert flow between different pipes or to combine resonance volumes that change the system configuration to be tuned for a different engine speed as the engine operation changes. In this way, wide flat torque curves are attainable due to the good volumetric efficiency across all speeds.

2.5.4. Exhaust Blow-Down Influencing Induction

During the valve overlap where both the inlet valve and the exhaust valves are open, there is a considerable amount of interaction between the charge induction and exhaust gas removal. Both the ram inertial effect and the ram induction effect are present in the exhaust system and both are accentuated due to the high temperatures and pressures that are present in the exhaust system. The average speed of exhaust gases in the exhaust tract is 174 m/s to 250 m/s, compared to the ± 80 m/s of

the inlet gases. The speed of sound is higher in the exhaust gases (518 m/s vs 330 m/s) due to the high temperature environment (400°C) [Heisler 1995]. The pressure difference over the exhaust valve when it opens is very high, resulting in exhaust blow down at the point where the exhaust valve opens. Just before the exhaust valve opens the pressure in the combustion chamber can be as high as 550kPa [Taylor 1998].

This high-pressure difference causes a compression wave to travel down the exhaust tract and it is rarefacted at the open end (either the atmosphere or an expansion box) and returns as an expansion wave lower than atmospheric pressure. This expansion wave is then rarefacted as a compression wave to travel back to the open end of the exhaust. This cycle continues for as long as the exhaust valve is open.

The exhaust lengths are tuned in a similar manner to inlet tracts, so that the rarefacted expansion pulse gets to the exhaust valve just before the exhaust valve closes. The residual exhaust gases are therefore better scavenged and the incoming charge is drawn into the cylinder, as the inlet valve will still be open at this stage.

The negative pressure expansion wave will also be propagated through the combustion chamber and into the inlet manifold. The combustion chamber is at its smallest at this stage (the piston is at the top of its travel) and it acts as a pipe and no longer as a chamber. This pulse then joins the existing pressure waves, being reflected back and forth through the tract until they die out due to friction.

The exhaust expansion wave has a relatively high amplitude due to the energy inherent in the exhaust blow-down process. It is therefore possible that the pressure wave from the exhaust pipes contributes more to the improvement of the volumetric efficiency than the inlet manifold pressure waves. The tuning of the inlet tract lengths should therefore take into account the exhaust blow-down pulses. This tuning can possibly be used together with scavenging and ramming to give up to 130% volumetric efficiency [Vizard 1993].

Tuning is very speed dependent and at engine speeds outside the tuning range, negative effects may result due to the expansion waves being out of phase. With careful tuning all the above effects can be used to produce a flat torque curve across the range of engine speeds, each mechanism will contribute to volumetric efficiency at a different engine speed.

It is also important to note that the pulses originating from adjacent cylinders will affect the breathing of each cylinder. Only with the aid of powerful computer simulations can all these phenomena be simultaneously investigated to try and determine the influence of each factor. Even then, it is difficult to distinguish which effects are responsible for the observed trends [Heisler 1995]. Therefore advanced investigation technologies are needed to optimise engines such as those used in case studies three and four.

2.6. Effects of Components on Engine Performance

There are many components making up the induction system of an internal combustion engine. The effect of each on the performance of an engine has been studied in detail by many researchers all over the world. Most components affect the breathing of the engine (volumetric efficiency) and in that way influence the performance. Bad breathing will result in poor volumetric efficiency and therefore reduced performance. Some of the variables that affect the engine performance are:

2.6.1. Compression Ratio

The compression ratio is defined as the ratio of maximum to minimum volume in the combustion chamber. By raising the compression ratio and reducing the clearance volume of the cylinder, the volumetric efficiency decreases. Although the Otto cycle suggests an increase in efficiency with respect to compression ratio [Ferguson 1986] it is only possibly due to the omission of the internal friction and the assumption of constant volume heat addition. Less fresh charge is drawn into the cylinder and at the same time there is a lowering of the cylinder's residual gases with a reduction of compression ratio [Heisler 1995]. Friction and heat losses also increase with an increased compression ratio [Ferguson 1986] further detracting from the engine efficiency.

2.6.2. Ram Pipe Dimensions and Plenum Chambers

The interaction of the pulses and momentum effects between cylinders has an effect on the breathing of other cylinders. By tuning the inlet manifold pipe lengths and plenum chambers to make use of these interactions, higher volumetric efficiency can be attained.

Changes in pipe length and diameter with a constant bore and stroke and equal conditions of inlet and exhaust pressures, inlet temperature, fuelling and optimum spark timing, result in the following trends.

2.6.2.1. Length

The effect of the length of the pipe is dependent on the speed at which the air travels through the pipe. The speed is limited to the choking that occurs at the inlet valve of the engine and the mach index quantifies this speed [Taylor 1977]. The mach index characterises the average gas speed through the inlet valve that would be required to realise complete filling of the cylinder at a specific engine speed. At low speeds (low mach index) the flow losses are low and therefore volumetric efficiency increase. At high values of mach index (Z) the flow velocities result in increased friction losses and decreased volumetric efficiency [Ferguson 1986]. The mach index, Z , is defined by Equation 2-12.

$$Z = \frac{\pi^2 b^2 \overline{U}_p}{4 \overline{A}_i c_i} \quad [2-12]$$

Where

Z = Mach Index

b = Cylinder Bore

\overline{A}_i = Mean Inlet Area

\overline{U}_p = Mean Piston velocity

c_i = speed of sound in the inlet conditions

Ferguson [1986] describes a complex experiment where length, diameter and inlet valve timing are varied under constant conditions. Generally speaking the results show that extending the length of the inlet pipe will result in improved breathing (volumetric efficiency) at low values of the mach index Z (0.4), and reduced breathing for high values of Z (0.8). A possible reason for the increased efficiency at low Z is the increased use of the ramming effects present in the induction system of the engine without the increased friction associated with higher air velocities. Also the lower resonant frequency of long pipes is better suited to the low engine speeds and therefore a low mach index.

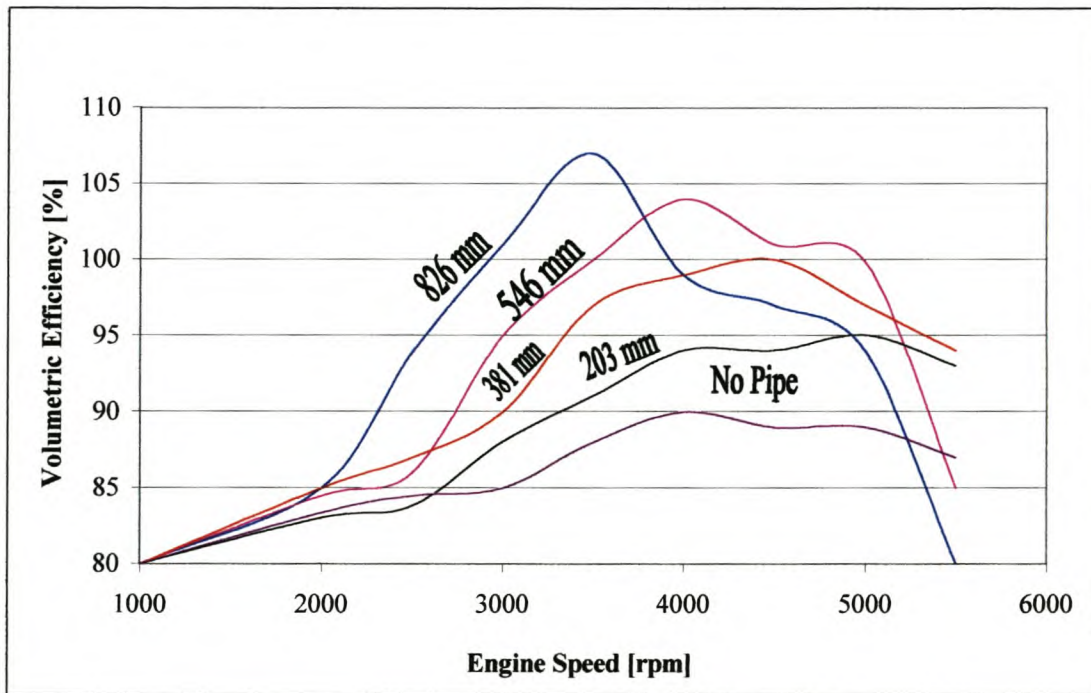


Figure 2-3. Pipe Length Effect on Volumetric Efficiency. [Heisler 1995]

The effect of inlet pipe length is shown in Figure 2-3 for another application, where increased pipe length improved peak efficiency and moved the peak to a lower engine speed (lower mach index). It can also be seen that the peak volumetric efficiency is above 100%, which is achieved by good use of the pulse and kinetic properties of the gas, both inlet and exhaust.

For high-speed engines therefore the shorter pipes are better because this avoids the dramatic drop in volumetric efficiency at high engine speeds.

2.6.2.2. Diameter

Ferguson [1986] showed that an increase in pipe diameter moved the peak volumetric efficiency to a higher engine speed and volumetric efficiency is linked to optimum flow rate. The diameter influences pipe flow rate in two ways. The flow area is changed, resulting in different flow velocities for constant flow rates, and the surface area, and therefore flow losses due to friction, is influenced by a change in diameter.

A reduced pipe diameter will result in increased flow rate for constant volume flow and a larger pipe diameter will result in a larger surface area in contact with the flow and therefore higher flow resistance due to friction [Heisler 1995]. The flow velocity will however be reduced and friction losses will also decrease. The reduced velocity in the larger diameter could result in poorer utilisation of the inertial ramming phenomenon and thus poorer volumetric efficiency.

For large diameters, the low flow velocity at low engine speeds may result in many of the fuel droplets not being able to stay in suspension and the heavier liquid particles may precipitate onto the walls. This will result in uneven fuelling with fuel starvation in the gas and periodic enrichment in certain cylinders as the liquid fuel enters the cylinder. Although this phenomenon occurs under normal operating conditions, it is accentuated under low flow velocity conditions.

2.6.3. Air Filter

In South Africa the conditions under which engines operate are harsher than in most developed countries. The high dust content of the air makes it necessary to use a remote air filter with better filtering characteristics than the pancake air filter used in Europe. The pancake air filter is normally located directly above the carburettor throat and the airflows radially through the filter.

2.6.4. Carburettor Adapter

A carburettor adapter is necessary to link the remote air filter to the carburettor. The main function of the carburettor adapter is to optimise the airflow pattern into the carburettor throat. Radial airflow with no swirl or vorticity as it enters the carburettor throat is ideal. The adapter is also designed to make best use of the pressure and inertial waves that occur in the inlet tracts. Optimal design results in a smooth, low loss flow, with even fuel distribution between the cylinders.

2.6.5. Carburettor

The carburettor is the means by which fuel is added to the incoming air. It also provides the correct air-fuel mixture by atomising the required liquid fuel into droplets that will evaporate quickly. The incoming air is accelerated through a venturi and the resultant pressure drop ($P_2 < P_1$) forces fuel through the metering orifice. The amount of fuel drawn into the air stream is dependent on the pressure at the fuel nozzle, which is in turn dependant on the amount of throttling of the inlet air, as well as the pressure distribution within the venturi. If there is uneven flow through the venturi, like swirl and tumble, then there will be additional pressure effects that will result in incorrect and uneven fuelling.

The throttle controls the airflow through the venturi. The pressure drop across the butterfly valve used for the throttle is increased as the valve is closed and the available area for airflow reduced. The reduction in area results in lower volumetric flow rate, which produces higher pressures in the venturi and hence lower fuel addition. [Heisler 1995]

2.6.6. Valves

There are many aspects to the valves in an internal combustion engine that effect the way the engine breathes. The valve lift, size, shape and positioning as well as the opening and closing positions are vital aspects when examining factors that effect the engine induction process.

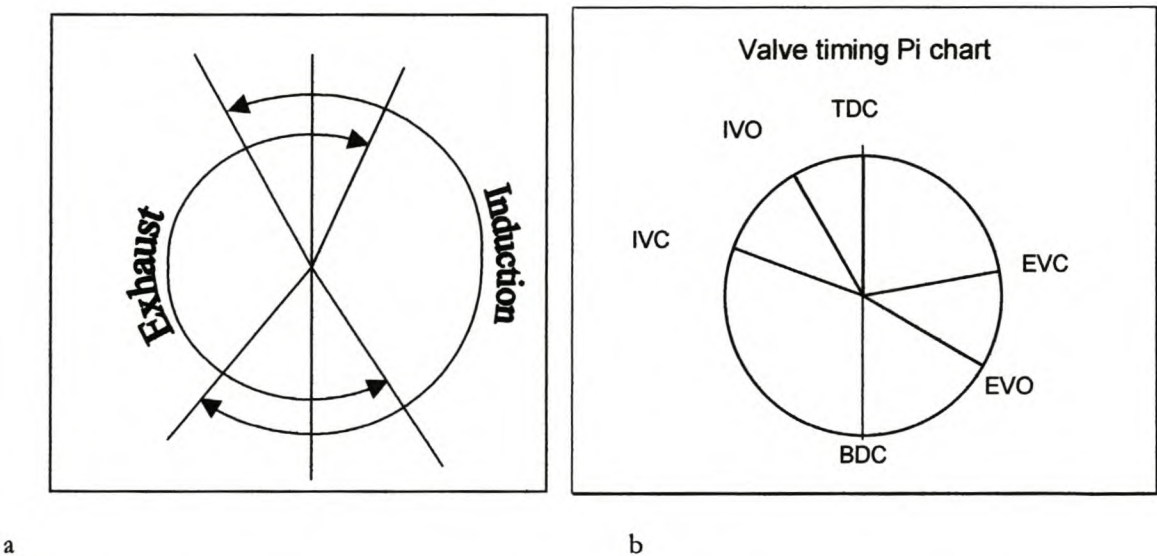


Figure 2-4. (a) Circular and (b) Pie-Chart Representations of Valve Timing

Valve timing can be represented graphically in a number of different ways. A circular timing diagram (Figure 2-4 (a)) shows the induction and exhaust duration's clearly. A pi diagram (Figure 2-4 (b)) shows

the periods of overlap and duration while a spiral valve timing diagram (Figure 2-5) shows the order of valve movements.

A spiral valve-timing diagram (Figure 2-5) gives an overall picture of the four phases of the engine following on one from the other (induction, compression, expansion and exhaust). A linear representation of the valve profiles (showing lift vs. cam angle) superimposed on each other gives a better representation of the valve opening and closing progressions and the magnitude of valve overlap (Figure 2-6).

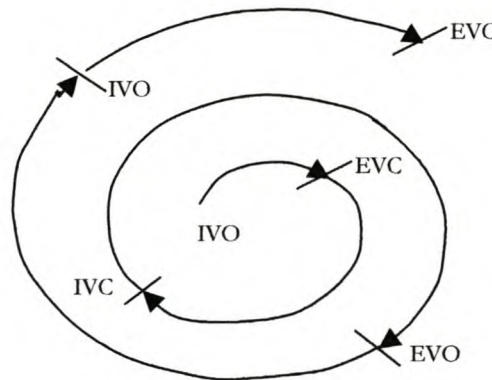


Figure 2-5. Spiral Valve Timing Diagram

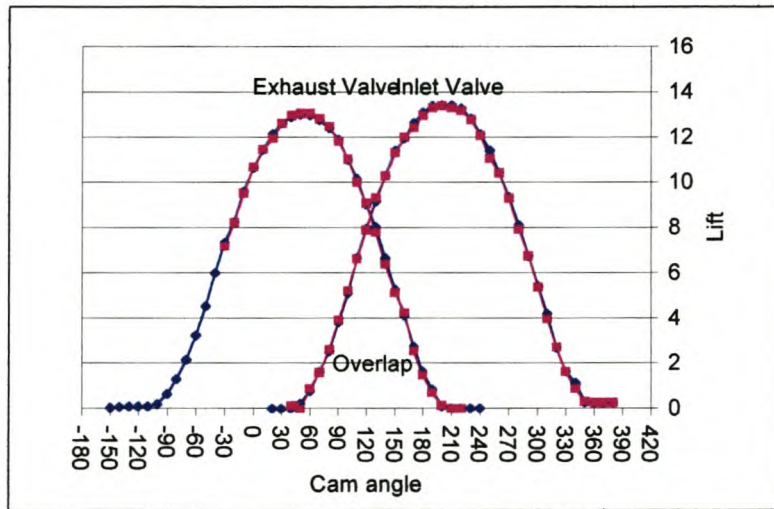


Figure 2-6. Inlet and Exhaust Valve Profiles and Angles (with altered valve timing from -180 to +420 as opposed to the expected -360 to +360)

2.6.6.1. Valve Lift

Valve lift describes the distance that a valve will move between the open and closed positions. The valve will remain in the centre of the valve port when it is open leaving a circular band through which the air must flow. This affects the ease with which the engine breathes. A higher lift will give a larger area for the air to pass through and therefore lower flow losses and improved breathing. The Speed of the valve getting to its maximum lift position determines the time taken for the flow through the valve to attain its maximum value.

2.6.6.2. Valve Size

The average gas speed through the valve should be kept subsonic (mach index $Z < 0.6$) to avoid flow choking. Therefore the inlet valves are sized according to the maximum piston speed of the engine. The speed of sound is much higher in the exhaust gases than in the intake gases (due to the temperature and density differences) and therefore the exhaust valve only needs a smaller diameter and lift to avoid the flow choke. Generally the inlet valves are limited in size by geometric restraints and are sized as large as possible. Using two inlet valves circumvents the problem to some extent by increasing the flow area. Typical valve size ratio's of exhaust to inlet valve areas are 70% to 80% [Ferguson 1986].

2.6.6.3. Inlet Valve Opening (IVO)

The inlet valve opens before TDC of the exhaust stroke. The outgoing exhaust gases still have enough momentum to leave a vacuum and draw in the fresh charge, which in turn will sweep out the last exhaust gases with its momentum. The IVO is tuned to maximise the fresh charge induced.

If the valve is opened too early the exhaust gas will be at a higher pressure than the inlet manifold and the exhaust gases will flow into the inlet manifold, reversing the flow. This is particularly possible under part load/part throttle conditions where the inlet manifold pressure is low. The exhaust gases in the inlet manifold will displace the incoming charge, diluting it and heating it up. This will cause a decrease in density and fuelling, resulting in lower volumetric efficiency and loss of engine performance. Emissions are increased due to the inefficient burning (HC and CO increases). If the inlet valve opens late, then there will be a loss of potential induction time and the volumetric efficiency of the engine will decrease.

2.6.6.4. Inlet Valve Closing (IVC)

The inlet valve is open for the entire induction stroke and closes after BDC. The exact instant of inlet valve closure is very important in determining the volumetric efficiency. The air flows into the cylinder as a result of a pressure difference across the valve. The pressure difference is the result of the piston moving downwards, as well as pressure pulses in the inlet tracts. Flow will continue in the positive direction (into the cylinder) until the pressure in the cylinder exceeds the pressure in the inlet manifold. At this point reversion will take place and air will flow back into the inlet manifold resulting in a decrease of volumetric efficiency.

If the valve is closed before reversion occurs then there will potentially be a lower charge that could have entered the cylinder. If the valve closes after reversion then there is a loss of charge due to the reverse flow. Optimum volumetric efficiency will occur if the valve closes at the precise point of reverse flow initiation.

Reversion occurs after BDC. As the piston starts the compression stroke, the low pressure that was drawing the charge into the combustion chamber will become a high pressure at the piston face. As the piston moves upward the high-pressure front also moves upward away from the piston face. At the valve however there is still a positive pressure difference and air is flowing into the cylinder. When the high pressure, caused by the upward movement of the piston and compression of the gases, reaches the inlet valve, flow will stagnate and then reverse as the pressure in the combustion chamber exceeds the pressure in the inlet manifold.

The speed of the engine will determine the instant at which reversion occurs. Thus volumetric efficiency is a function of engine speed as seen in Figure 2-3. At slow speeds flow reversal will occur and charge will be lost while at high speeds potential charge is lost due to the valve closing while gas is still flowing into the chamber.

The IVC position is used to tune the spread of the maximum torque and performance of the engine across the engine speed range. For a low inlet valve lag (valve opens early) there will be a loss at high speed of the inertial ramming effect while a big lag will result in a drop off of performance at low speeds, due both to the low velocities, and reversion. The tuning is therefore a function of the engine's intended use.

2.6.6.5. Exhaust Valve Opening (EVO)

The instant of EVO influences the expulsion of the exhaust gases from the combustion chamber and tuning is used to maximise exhaust gas expulsion. The valve opens before BDC when the gas is still at a pressure higher than the pressure in the exhaust system. This causes exhaust blow-down to occur and a pressure wave is sent into the exhaust tract. The inertia of the gas helps in its extraction. The piston essentially only sweeps out the residual gases. Therefore negative work during this stroke is kept to a minimum.

The effects the exhaust valves opening early, is a loss of pressure energy and therefore a loss of power. The high-pressure gas that is released will contain energy that could still be used in the propulsion of the engine. The exhaust valve is best opened when the piston is near BDC, an ineffectual crank position. The effect of late opening is that the piston has to do more work to sweep out the residual gases at the end of the stroke as a result of the less efficient exhaust blow down.

2.6.6.6. Exhaust Valve Closing (EVC)

The exhaust valve is open for the entire exhaust stroke and for the first part of the induction stroke. The outward flowing gases in the cylinder possess kinetic energy and leave a partial vacuum in the cylinder due to their inertia. Fresh charge is sucked into the partial cylinder vacuum with the inlet valve partially open. At this stage, the piston cannot yet form a vacuum to draw in fresh charge as it is in an

ineffective crank position and the downward movement is slow, although at maximum acceleration downwards.

The timing of the exhaust valve closing is best determined by the tuning of the exhaust inertial and pressure ramming phenomenon as well as the overlap time to ensure that fresh charge does not make its way into the exhaust system before the valve closes. If the valve closes too early there will still be exhaust gases in the combustion chamber. This will reduce the volumetric efficiency of the engine, as the residual exhaust gases will take up space that the fresh charge could take. The residual gases will also increase the temperature of the incoming charge resulting in a lower charge density and therefore lower volumetric efficiency. If the valve closes late then fresh charge will flow into the exhaust tract without combusting and result in fuel loss (decrease in overall engine efficiency), increased emissions and a backfire if the unburned fuel ignites in the hot environment of the exhaust tract [Ferguson 1986].

2.6.6.7. Valve Overlap

The overlap of the inlet and exhaust valves is a result of the inlet valve closing after the exhaust valve opens. This results in the combustion chamber acting as a pipe for the pressure pulses to travel through, thus best utilising the momentum of the airflow to increase volumetric efficiency. Exhaust gases flowing into the inlet port during overlap result in a decrease in volumetric efficiency, because before any charged air can enter the combustion chamber, the exhaust gas must first travel back into the combustion chamber. Only then does the cylinder fill with fresh charge.

Greater overlap results in more emissions at low speeds and partial throttle. At high engine speeds and wide open throttle however, the larger overlap results in better engine breathing. The overlap is therefore a function of the engines intended use and the region where it is likely to spend most of its working life.

For example a racing engine, designed for a high, narrow speed range and close gear ratios will not be concerned about low speed performance and probably not about emissions. A large overlap will therefore be suitable for this engine. A local delivery van where most of the driving is low speed, stop start driving, will not use high engine speeds and emissions will be important. A small overlap will then be more suitable.

2.7. Case Studies

The theories discussed in this section are applied in four case studies using Taguchi methods to design the experimentation matrices. In the first case study, a carburettor adapter is investigated. The flow is manipulated using flow diverters to try and produce smooth radial flow in the carburettor throat to provide equal fuelling to all four cylinders and to maximise engine performance in terms of top-end-power and mid-range-torque.

In the second case study the dimensions of a carburettor adapter (height and diameter) and the dimensions of the feed pipe (length and diameter) were investigated. The aim was to provide smooth and even flow into the carburettor to get even cylinder fuelling and overall engine performance enhancement in terms of top end power, mid range torque and fuel consumption.

The third case study investigates variables of engine design in a modelling simulation. Taguchi Methods are used to minimise the amount of testing required in order to identify the optimum operating conditions. Camshaft variables (inlet and exhaust valve opening and closing angles as well as valve lift) and inlet pipe variables (length and diameter) are investigated to maximise engine performance in terms of top-end-power and mid-range-torque.

Case study four does not directly apply any engine testing theory. It uses the same simulation package as Case Study Three and compares the results from a Taguchi experimental method with a full factorial equivalent. The benefits in terms of timesavings are well illustrated.

Chapter 3. Engine Testing

In order to design and develop quality automotive engines, a vast amount of testing and experimentation needs to take place. Engines are put onto dynamometers and run under varying controlled conditions to simulate the conditions under which the engine will be used. In this way, the engine operation can be optimised in a controlled environment to provide the highest quality product.

During experimentation many factors need to be monitored in order to maintain constant operating conditions whilst optimising the input variables. For the experiments conducted for this thesis, atmospheric conditions (wet and dry bulb temperature and pressure) were recorded to enable for the correction of engine performance due to atmospheric variations using SABS torque correction factors. Variables such as engine speed and throttle position were monitored for each test point to ensure that the operation points were identical and repeatable for the testing of various engine components. Torque, power, fuel consumption, emissions and exhaust temperatures were monitored as output variables to evaluate engine performance. Oil temperature and pressure, and water temperatures for both the dynamometer and the engine were monitored and used as a safety warning of an engine malfunction. The onset of knock was also monitored using a knock sensor in order to prevent serious engine damage.

3.1. Engine Test Facility

The Centre for Automotive Engineering (CAE) test laboratories at the University of Stellenbosch was used for all the test work. The testing facility consists of seven engine test cells, housing nine engine test stands ranging from 160 kW eddy current units to an advanced DC dynamometer used for dynamic driving simulations. A standard eddy current dynamometer was used in the test work for this thesis. The engine exhaust gases were removed from the test cell by directing the exhaust system into the extraction system as shown in Figure 3-1.

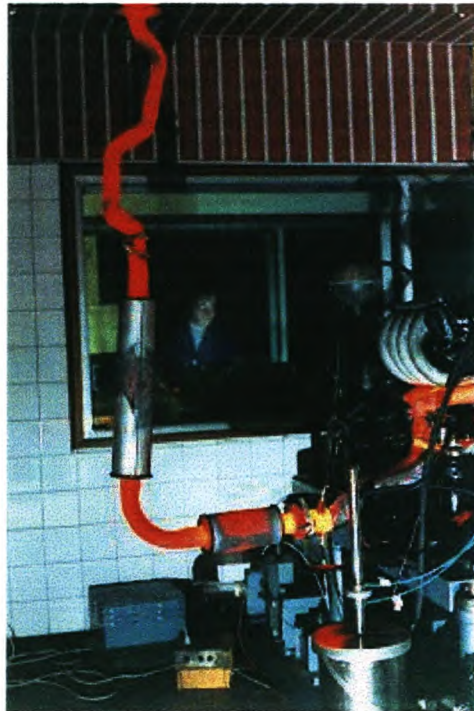


Figure 3-1. Hot Exhaust System During Testing

The same extraction system provided air cooling for the engine at a ventilation rate of approximately 1.5 m³/s through each test cell. The operator in the control room was isolated from the engine and dynamometer by double soundproof doors and double panes of hardened shatter proof glass for safety and soundproofing. All engine control was done from the control room via computer control of the engine control unit (ECU) (Figure 3-2).

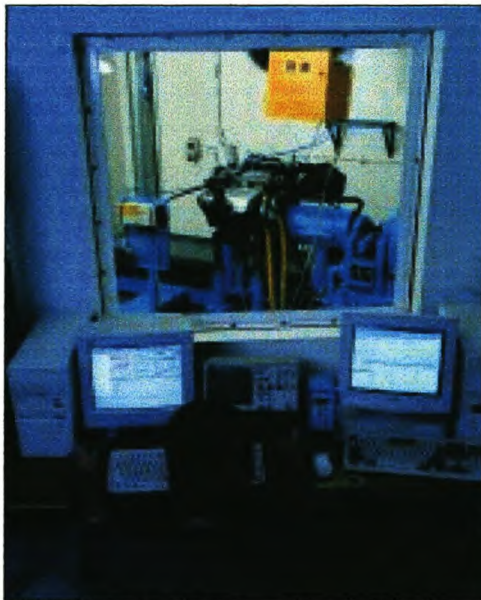


Figure 3-2. Engine Control Room

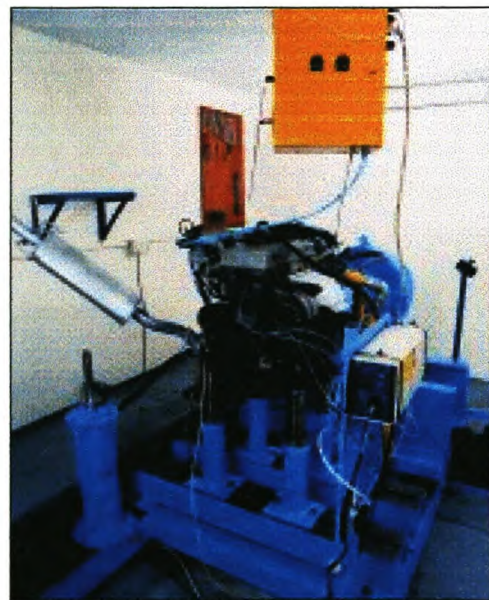


Figure 3-3. Test Stand

Data logging was made possible through the use of an Action Instruments I/O PAKPLUS industrial quality input/output processor. Sixteen possible channels were configured using plug-in digital and analogue modules that communicated with the computer via an RS-232 system.

The engine test stand (Figure 3-3) was fabricated from heavy rolled steel sections to provide stability and strength. The main structure was mounted on rubber feet for vibration absorption. The extensive adjustment allowable on the bed enabled the shaft from the engine to the dynamometer to be aligned accurately. A two litre, SOHC, eight-valve engine from a one ton commercial vehicle was used for all the testing. No gearbox was used in the testing so the engine was coupled directly to the test bed via a shaft and two constant velocity (CV) joints.

A standard Froude eddy-current (EC38) dynamometer was mounted on the test bed. The dynamometer consisted of two stationary coils and a rotating rotor situated between the coils. It worked on the principle of opposing magnetic fields. The stationary coils were mounted on trunion bearings that allowed the casing to swivel in the same axis as the incoming shaft. The magnetic field generated by the electromagnetic coils induced eddy currents in the rotating spokes of the rotor. These eddy currents then in turn produced an opposing magnetic field and thus power was absorbed. Heat from the rotor was transferred away through a small air gap between the rotor and the water-cooled loss plates to the cooling water in the outer jacket of the dynamometer.

PID control of the supply voltage to the coil was used to achieve speed control. Varying the voltage supplied to the electromagnetic excitation coils controlled the strength of opposing magnetic fields, and thus the power absorption capacity. The amount of power absorbed was measured by means of a load cell restricting the casing's rotation. The force was then used to calculate the torque. This, together with the speed of the shaft was used to determine the power absorbed by the dynamometer.

3.2. Engine Cooling

Due to the absence of a radiator on the engine, the engine water was cooled using a shell and tube heat exchanger and an external supply of cool water. The standard water system for the engine was used, including the water pump and thermostat for temperature control. The radiator was replaced with a water to water heat exchanger to facilitate heat extraction from the system. The engine-water heat exchanger and dynamometer heat exchanger were both supplied with a constant supply of cooling water at 1.8 bar.

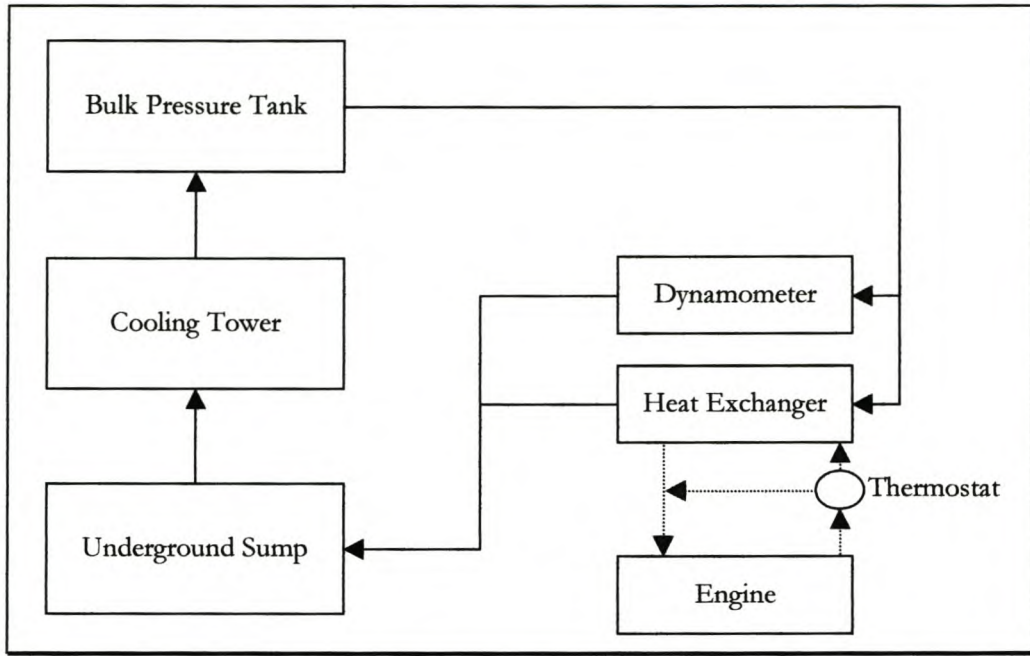


Figure 3-4. Water Flow Circuit

The cooling water system consisted of an overhead tank providing the pressure, a cooling tower to regulate the temperature, and an under-floor sump for the used water as shown in Figure 3-4. The water was circulated through these components in a closed system to control the flow rate and the temperature. The water supply line was fitted with a flow switch to prevent the engine from starting with an insufficient flow of coolant water, thus protecting both the dynamometer and the engine from overheating.

3.3. Fuelling and Fuel Injection

Both carburettor and fuel injection systems were used in the testing. The two configurations are shown in Figure 3-5. This necessitated the use of two fuel pumps. A low-pressure pump was used to supply the carburettor with fuel, and a high pressure pump was used to supply fuel at a pressure of 3 bar for the fuel injection configuration. For both systems, the fuel supply was via a fuel mass flow meter from the bulk tank. By changing the piping into the fuel mass flow meter and changing the pump that received power from the ignition switch, the two fuel systems were interchangeable.

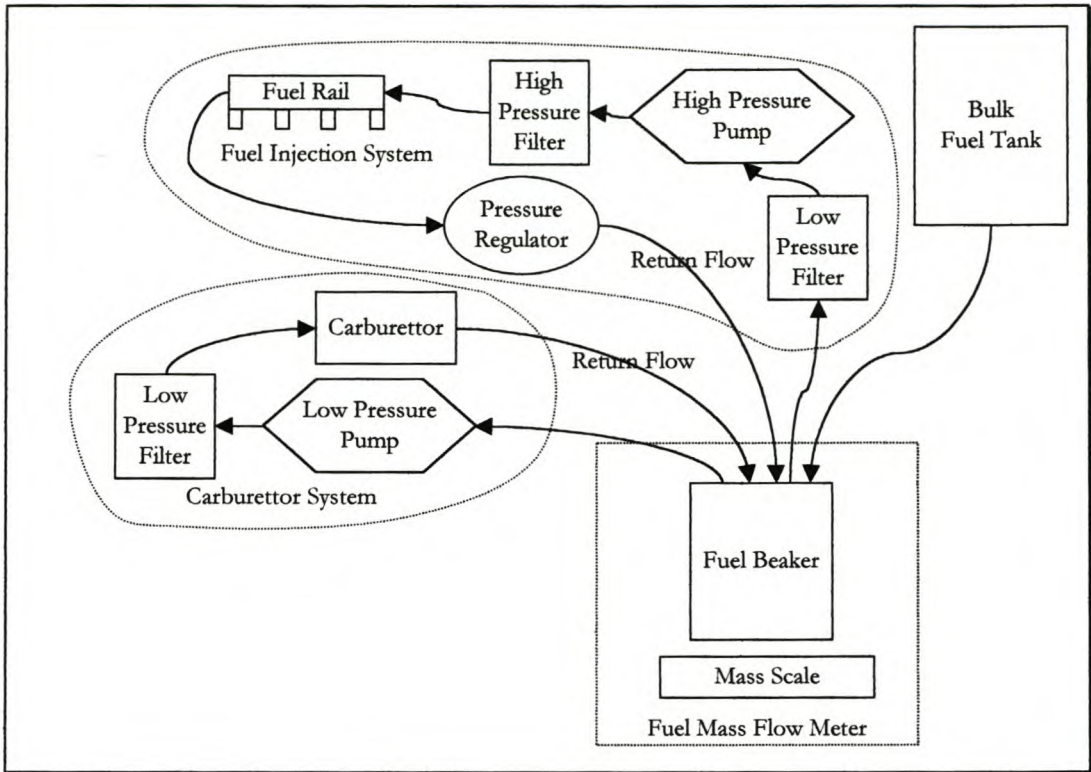


Figure 3-5. Fuel System

The fuel mass flow meter (Figure 3-6) consisted of a beaker and a scale and a filler pipe and pump from the bulk fuel tank. The beaker was filled when the low level limit switch in the meter was activated. When the level in the beaker activated the high level switch the filling pump was switched off and the fuel mass flow was measured by recording the varying mass of the fuel in the beaker.

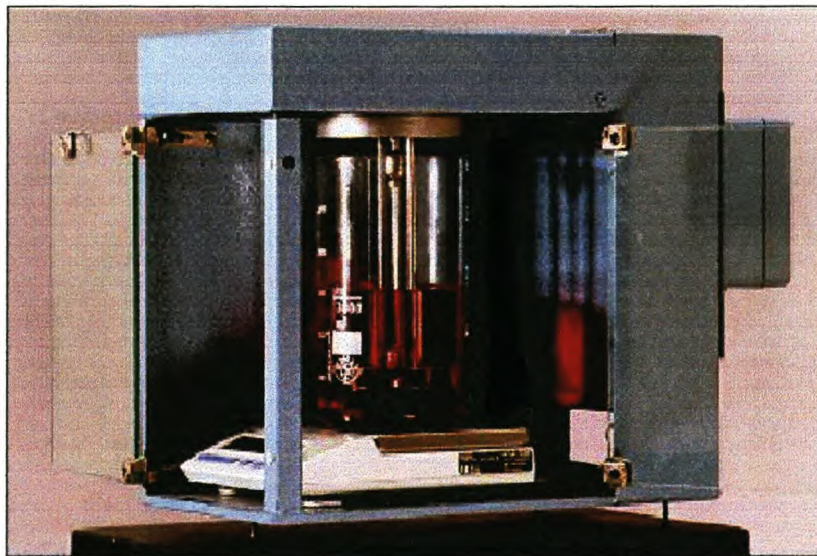


Figure 3-6. Mass Fuel Flow Meter

In the carburettor configuration, the fuel was pumped directly from the mass flow meter through a low pressure filter (to protect the fuel pump from damage), to the carburettor using a 12 volt low pressure

fuel pump. In the fuel injection configuration, a high pressure pump was used to draw the fuel through a low pressure filter (to protect the pump from damage) and then push it through a high pressure filter (to protect the injectors from fouling), before going to the fuel rail and injectors. A pressure regulator and gauge were connected on the down stream side of the fuel rail. The gauge was used to set the pressure regulator at 3 bar and, by means of a return pipe to the mass flow meter beaker, the fuel pressure was maintained at 3 bar. The Centre for Mechanical Services (Sentrum vir Meganiese Dienste, SMD) at the University of Stellenbosch manufactured the fuel rail.

3.4. Engine Management System

The fuel injectors were controlled using a DUPEC engine control unit (ECU). Manifold absolute pressure (MAP) and engine speed were monitored by the ECU and used by DUPEC to control fuel injection and ignition timing. Changing the data maps stored within DUPEC enabled the injection timing and ignition timing to be changed while the engine was running. The vacuum advance used to alter the ignition timing was disconnected as all the tests were done at wide open throttle (WOT).

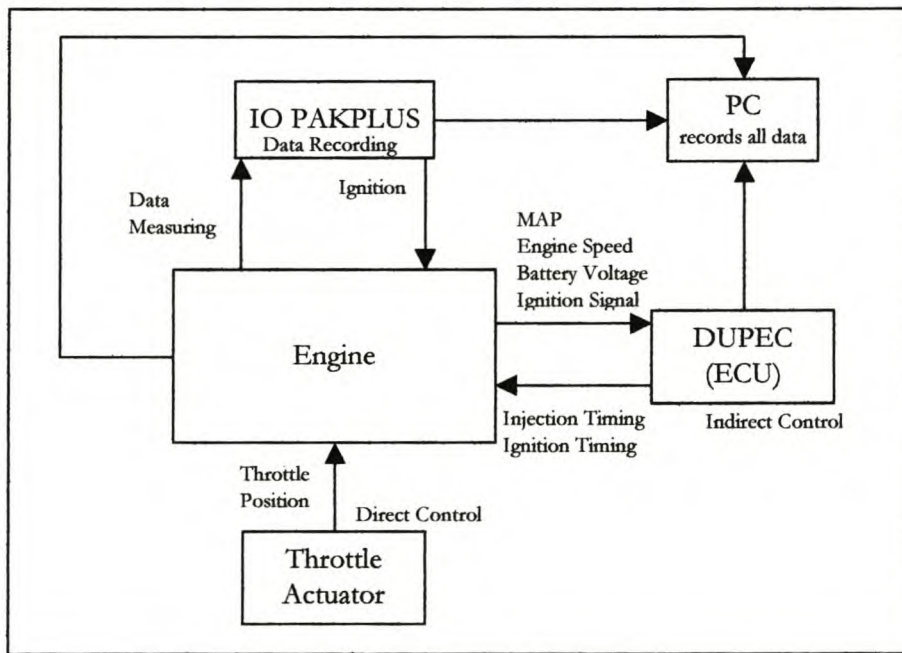


Figure 3-7. Engine Control and Monitoring

Other factors that were monitored and corrected for were battery voltage, ignition voltage, air temperature and water temperature. Low voltages were corrected for by lengthening the injection time, as the injectors were slower to react to the signal when the voltage was low. Water temperature was set to a default value of 70° C and the air temperature was set to a default value of 25° C for the controller, thus removing two degrees of freedom in the control system. All the tests were carried out under comparable controlled conditions so these two measurements were deemed unnecessary.

3.5. Engine Test Automation (ETA)

ETA software developed in the Centre for Automotive Engineering (CAE) of the University of Stellenbosch (US) was used for the user interface with the engine and data logging. The sixteen input-output (IO) channels were configured according to the module and measurement type for that channel, and a possible additional 48 calculated or user defined channels were available. These additional channels were used for calculated channels such as, power, specific fuel consumption (SFC), and average temperatures. Additional communication port channels, such as mass fuel consumption, and operator entered values for data that could not be electronically captured, (i.e. wet bulb and dry bulb temperatures and emissions data) could also be programmed into the additional channels

Each of the channels used had configurable alarms for high, high-high, low and low-low values. For critical channels, the triggering of an alarm would result in the engine being stopped by cutting the ignition signal to the engine. i.e. a low-low alarm on oil pressure would result in the engine ignition being cut to prevent damage. All alarms were written to an error file in real time when they occurred. This enabled the operator to determine the reason for possible engine failure or data irregularities after the test had been completed.

A list of channels and alarms is given in Appendix A along with an explanation of each channel used during testing.

3.6. Air flow

The airflow in the engine was measured using a Ricardo air flow meter. The flow meter worked on the principle that there is a pressure drop across a pipe length when there is laminar flow in the pipe. By measuring the pipe dimensions and the pressure drop across it, one is able to calculate the air flow volume through the pipe. The flow metre consisted of an air filter and then a section of many thin pipes in parallel that forced the air flow to become laminar through them. The pressure drop across a section of the pipes was measured and used to calculate the air flow rate, taking into account the measured air temperature and pressure (density) during the test. This, together with the fuel mass flow rate was used to calculate an air fuel ratio.

3.7. Atmospheric Corrections

Due to the fact that all the tests could not be completed under the same atmospheric conditions and the fact that differing air density and humidity influence volumetric efficiency, torque corrections needed to be done on all data to enable them to be compared. SABS standards prescribe the calculation that is needed to correct for the discrepancies due to differing atmospheric pressure and humidity (reference SABS standards).

3.8. Knock

Knock is a complex unpredictable phenomenon that is, more often than not, damaging to internal combustion engines. It is the phenomenon whereby fuel is ignited before it is consumed by the flame front originating at the spark plug. It is also known as auto-ignition, pre-ignition and detonation, all corresponding to different aspects or causes of the same fundamental event. Knock is identified by the sound made when high velocity pressure waves reflect off the cylinder walls causing an audible pinging sound. The oscillation of the pressure wave back and forth in the cylinder causes the cylinder walls to become excited and thus the pitch of the wave is dependant on the oscillation frequency i.e. the velocity of the wave and the cylinder dimensions (distance the wave has to travel). Velocities of these waves have been measured at 1200 m/s [Fitton 1993], which translates to approximately 500 cycles per second. Knock sensitivity is measured as an anti-knock index or road octane number and it is a function of the fuel used in the engine. This is defined as the average of the RON (research octane number) and MON (motored octane number) numbers [Heisler 1995].

3.8.1. Mechanisms of Knock

During the normal combustion process the flame front moves from the centrally located spark plug outward towards the end gas regions. The temperature in the combustion chamber rises due to the increased pressure as a result of the combustion process. The unburned gases are also heated by the radiation from the burnt gases and, initially from the warm cylinder walls. If the pressure and temperature rises surpass a critical level, spontaneous ignition of the unburned gases occurs. High-pressure waves are generated when the fuel bulk ignites prior to the flame front consuming the charge. This occurs in areas of high temperature and pressure, typically the end gas regions near the rings of the piston. The pressure of the resulting wave is dependent on the pressure of the charge when auto-ignition occurred.

Pre-ignition is the term given to the knock phenomenon when detonation occurs before the spark has been delivered to the charge. This occurs as a result of local overheating of the fuel mixture, due to a hotspot in the combustion chamber. A portion of the gasket or carbon build-up that exceeds 800°C may provide such a hot spot [Heisler 1995]. Under these circumstances the engine will experience runaway where the engine will no longer require a spark to function and the effect will become self propagating and develop into severe knock where drastic damage is done to the engine.

Excessive spark advance will result in knock due to the higher temperatures and pressures resulting from an advanced spark. The advanced ignition of the charge will cause combustion to start before the piston can start its downward movement, expanding the combustion chamber volume and absorbing the combustion energy. This could lead to knock run-away and severe knock damage to the engine.

3.8.2. Consequences

Auto detonation does not necessarily result in any damage to engine. It is characterised by a light pinging noise coming from the combustion chamber. Severe knock however, scours away at the stagnant gases in the boundary layer at the cylinder walls. This causes the heat rejection through the wall to be increased, and the average cylinder temperature rises. The protective lubricating oil film on the cylinder wall is also scoured away resulting in increased friction and engine wear. The bearings, rings and pistons experience increased vibratory loads and also increased peak pressures (400 kPa) as a result of the knock. The high cyclic pressure loading causes micro cracks to form and the material to flake. Thin walls of sections of the piston also risk damage due to pressure differences that result across the material [Fitton 1993].

3.8.3. Contributing Factors

Factors contributing to high temperatures an increased likelihood of knock are lean fuel mixtures and over advanced ignition timing. Insufficient cooling around the combustion chamber and carbonisation on the chamber walls could result in hot spots. A long flame path in the combustion chamber where the end gases are exposed to high temperatures and pressures for an extended time period also increases the likelihood of knock occurring. High compression ratio's used in conjunction with low octane fuels promote knock occurrence.

A knock resistant fuel will result in more severe knock, if pre-ignition is allowed to occur, due to the higher amount of energy that will be present in the end gas at auto-ignition. If the auto-ignition point moves to before TDC, then negative work will be done in compressing the burnt gases and a decrease in power, torque and speed will result. If the advancement continues, auto detonation could occur before the inlet valve has closed and then the flame front will propagate into the inlet manifold. Exhaust temperatures will decrease due to the increased energy lost to the coolant, as well as decreased CO% emissions. In a multi-cylinder engine where knock occurs in one of the cylinders the other non-knocking cylinders will pull the knocking cylinder along, resulting in excessive and accentuated knock damage.

3.8.4. Knock Prevention

The effect and occurrence of knock can be minimised in a number of ways. Increased turbulence in the combustion chamber results in the end gases being burnt quicker due to the increased flame front speed. By reducing the flame path the end gases are not exposed to the elevated pressures and temperatures for as long. By quenching the end mixture it is burnt quicker and knock is prevented.

Piezometric knock sensors that detect the incipient oscillations of knock are used in modern cars where the ignition timing and fuel injection duration are constantly monitored, changed and optimised by the

engine management system during operation. This “on the edge” engine management system constantly controls the engine so that it operates at the knock limit, thus achieving high performance and efficiency.

3.9. Closing Comments

In the four case studies described in this thesis, there were additional testing apparatus and tools used. These are discussed as necessary in the relevant chapters. In case study two (birdcage), a four gas analyser was used and the custom equipment needed for its’ use is described in the relevant chapter. In case studies three and four, a software program, Engine Simulation Analysis (ESA), was used to generate the data that was used. It was developed at CAE and is discussed again in Chapter 3.

Chapter 4. Experimental Design

It is not the purpose of this text to completely describe the method and proofs behind the techniques illustrated. Indeed there has been much written on the subject of experimental design (Beveridge et al 1970, Biles and Swain 1980, Box 1978, Daniel 1976, Fletcher 1980, Khuri and Cornell 1996, Lunneborg 1994, Box et al 1988, Daniel 1962, Davies and Hay 1950, Draper and Hunter 1966, Hunter and Naylor 1971, Marquardt 1963, Plakett and Burmann 1946, Statsoft 1998). This text provides an outline and guide to the techniques needed in order to perform a successful experimental design using Taguchi Methods as was used in this thesis. Other experimental methods are discussed briefly to provide a comparison with Taguchi Methods and to highlight the advantages and disadvantages.

4.1. Introduction

Why Experiment? Primarily, the goal of experimentation is either to **optimise** an output of a system (product or process), or to better **understand** a system (product or process). The aim is to identify and quantify the effect that a controlled input variable has on a measured output variable. The input variable can then be set to a predetermined value to obtain the optimum output.

Traditional thinking maintains that all variables should be kept constant, while one variable at a time is varied and its effect determined and optimised. Modern thinking, however, has turned to varying everything at the same time in a structured statistical experimental design constructed using advanced mathematical and statistical techniques. The effect of a variable within the variation of the other variables is determined as well as identifying and quantifying interactive effects between variables. The information is more comprehensive and is attained with less experimentation resulting in saved time, money and effort. This is the basis of Taguchi Methods.

All experimentation requires the specification of a range for each control variable (input variable) and a number of levels (values) within that range at which the response will be evaluated. The more levels chosen, the more information can be gleaned from the investigation of the process, product or system, but the design also increases in complexity and size.

Optimisation can be described as a science to determine the “best” solution to a mathematically defined problem either constrained or unconstrained. Problems can be constrained by specifying relationships between variables, variable limits or response limits. Analytical optimisation techniques utilise mathematical theory to identify maxima and minima. Numerical methods of optimisation usually involve iterative techniques that refine the answer with each iteration, getting closer to the optimum each time. Golden section search, steepest gradient method, discretisation and CFD are all examples of iterative analytical optimisation techniques.

A disadvantage of optimisation techniques is that they generally do not supply any other information about the process other than the optimum settings. The possibility always exists that the process will not identify the global optimum but simply a localised one.

4.2. Experimentation and Research

Research can take one of two forms. Correlation research aims to identify relationships (correlation's) between variables without changing them. For example identifying the relationships between blood pressure and cholesterol level. In experimentation research however, the variables are manipulated (independent variables) and the response of the affected variables (dependent variables), is monitored to determine a relationship [Statsoft 1998]. For example, changing fuels in a car and monitoring the altered performance.

4.3. Traditional Experimentation

Experimental design is often a process that is ignored in favour of a traditional simplistic comparative testing structure. Traditional consecutive experiments are conducted in which single variables are changed, compared and a response trend measured and identified. The result is that the independent variable is said to have a positive, negative or no effect on the chosen output variable.

Tests are specified and structured largely on intuition and experience, with no set design as to which variable to investigate first, what levels to test them at and at what levels other variable should be set at during the investigation. This method of testing is inefficient and yields a minimum amount of information about the process or system being investigated. Only the main effects of the chosen investigated variables are determined and only for the tested combination of other variables. No insight is given to the interactive and second order effects that could be present in the system.

4.4. Statistical Design of Experiments

Japanese industry was first to realise the potential in statistical experimental design (SED). An English agriculturist, R. Fisher was a pioneer in the exploration of such designs in 1928, experimenting on crops in Britain by varying ground condition and fertilisers. His techniques however, were not well received in western circles, and it was the Japanese who embraced the techniques and used them to develop themselves to become arguably, the world leaders in quality [Logothetis 1992].

The amount of information that can be gathered during the experimentation process using experimental design techniques is much greater than the traditional comparative technique, and the “guess work” is largely removed from the process. Trends over a range of levels, independent of the values of other

variables, can be determined, and in some designs, high order interactions and quadratic effects can also be quantified.

The statistical design of experiments has many advantages over traditional methods.

1. They provide more information per experiment performed.
2. There is an organised structured method of data collection.
3. They identify and quantify interactions between variables.
4. They give an easy to read graphical representation of the results (A picture is worth a thousand words).
5. They enable the prediction of results at levels not tested in the experimental configurations.

The single major disadvantage of statistically designed experiments is that all experiments must be completed and analysed before results are forthcoming. This means that the experiment must be well planned and executed to prevent any external variation interfering with the experimentation process. The traditional method however, allows for continual learning throughout the experimentation process.

There are generally five steps to experimental design process [Biles and Swain 1980] :

1. Formulate the problem.
2. Design the experiment.
3. Perform the experiment.
4. Tabulate and analyse the data.
5. Draw conclusions and make recommendations.

Irrespective of the type of application, the process will follow the above 5 phases. Many approaches exist for SED, a number of which are discussed below.

4.5. Full Factorial to Fractional Factorial

A full factorial design is one in which every variable is tested in combination with every level of every other variable. All possible combinations of variables are thus investigated and it is as comprehensive an investigation as is possible. The design comprises a complete matrix of all the variables at all their levels. The number of experiments required for a full factorial is k^n where n is the number of variables and k is the number of levels per variable. Therefore for a five variable experiment at two levels there would be 2^5 (32) experimental configurations. Similarly for six variables at two levels, 2^6 (64) configurations and

for five variables at three levels there would be 3^5 (243) experiments. The number of experiments needed increases exponentially with either an increase in the number of variables or the number of levels at which they will be investigated.

A simple illustration for three variables at two levels each is shown in Table 4-1. Three different representations of the experiment are shown. The coded values (shown first) of +1 (or +) and -1 (or -) represent the high level and the low level for the variables respectively. The actual values are then inserted in the matrix and are shown on the right. The three control variables are temperature (10°C and 20°C), pressure (3 and 6 bar) and catalyst type (A or B).

Table 4-1. 2^3 Full Factorial Design

Parameter	Coded Values			Coded Values			Actual Values		
	Temperature	Pressure	Catalyst	Temp	Pres	Cat	Temperature	Pressure	Catalyst
Experiment 1	-1	-1	-1	-	-	-	10	3	A
Experiment 2	-1	-1	1	-	-	+	10	3	B
Experiment 3	-1	1	-1	-	+	-	10	6	A
Experiment 4	-1	1	1	-	+	+	10	6	B
Experiment 5	1	-1	-1	+	-	-	20	3	A
Experiment 6	1	-1	1	+	-	+	20	3	B
Experiment 7	1	1	-1	+	+	-	20	6	A
Experiment 8	1	1	1	+	+	+	20	6	B

This type of design gives absolute resolution. This means that all the main effects as well as all possible interaction effects can be uniquely determined without aliasing. The response equation is shown below (equation 4-1) where y represents the system response (measured variable) A , B , and C are the varied variables (temperature, pressure and catalyst) and b_i the defining constants of the system.

$$y = b_0 + b_1A + b_2B + b_3C + b_4AB + b_5AC + b_6BC + b_7ABC \quad [4-1]$$

As can be seen from this example a two level design will give an indication of any linear effects in the variables only. To investigate non-linear (quadratic) effects a further level must be added to the design. The 3^k design, which has three levels per variable, is used to investigate the non-linear effects and to identify maxima or minima within the range of the investigation.

Table 4-2 illustrates the 2^3 full factorial design expanded to include all the possible interactions in columns 4 through 7. This is the saturated⁵ two level design represented by the $L_8(2^7)$ orthogonal array. It is possible to produce a fractional factorial design from a full factorial design by replacing the higher order interactions with additional variables [Davies and Hay 1950]. i.e. the ABC interaction can be replaced with an additional variable D , without adding to the number of experiments (Table 4-2). Three level interactions are rare and therefore this can be done without the risk of losing information. In mathematical terms this is equivalent to leaving out the third order term in a Taylor series.

⁵ Saturated design implies that only the main effects can be investigated.

Table 4-2. Saturated Two Level Design

$L_8(2^7)$

No	1	2	3	4	5	6	7
1	1	1	1	1	1	1	1
2	1	1	-1	1	-1	-1	-1
3	1	-1	1	-1	1	-1	-1
4	1	-1	-1	-1	-1	1	1
5	-1	1	1	-1	-1	1	-1
6	-1	1	-1	-1	1	-1	1
7	-1	-1	1	1	-1	-1	1
8	-1	-1	-1	1	1	1	-1

	a	b	c	ab	ac	bc	abc
Actual Effect of additional Variable D	a+bcd	b+acd	c+abd	ab+cd	ac+bd	bc+ad	d+abc

In Boolean algebra the level of the interaction term for AB is the product of the variables A and B . Similarly for $ABC = A \times B \times C$. By replacing ABC with D we say $D=ABC$, and the interaction ABC is confounded with the main effect D (column 7 Table 4-2). The effect of variable D will actually represent the summed effects of the variable D and the interaction ABC [Box and Hunter 1961]. By multiplying both sides by D we get $D^2=ABCD$. Irrespective of the value of D , D^2 will always be equal to 1, or the singularity I , ($-1 \times -1 = 1$, $1 \times 1 = 1$) which expands to give $A^2=B^2=C^2=D^2=I$. The defining identity or generator for the experimental design is therefore $I=ABCD$ (the defining identity is always equal to one). For the previous example (Table 4-1) the defining identity was $I=ABC$.

This type of design is also referred to as a 2^{4-1} design which has a number of other implications. As well as having the D main effect confounded with the ABC interaction effect, other effects are also confounded⁶. The defining identity illustrates the other confounded effects [Box and Hunter 1961]. The associated effects are called aliases⁷. By multiplying $I=ABCD$ by A on both side we get $A=A^2BCD$ and using the coded form of the experiment we know $A^2=B^2=C^2=D^2=I=1$, so we get $A=BCD$. This means that the main effect A is confounded with the three way interaction BCD . By multiplying both side by B we see $AB=CD$. These aliases show that the second order interactive effects are confounded and the effect AB actually represents the sum of the AB effect and the CD effect interaction.

All the aliases from the defining relation $I=ABCD$ are listed below and are shown in Table 4-2:

$$A=BCD; B=ACD; C=ABD; D=ABC; AB=CD; AC=BD; AD=BC \tag{4-2}$$

⁶ A confounding of two effects means that the trend identified cannot be attributed to one of the two effects but is a result of both effects.

⁷ An aliased effects is the same as a confounded effect.

This fractional factorial design is said to have a resolution of 4 which means that no main effect is confounded with any other main effect or two way interaction, but main effects are confounded with three way interactions and two way interactions are confounded. The design in Table 4-1 is a design of absolute resolution where there is no aliasing of any of the variables.

Fractional factorialisation can be taken further if the second order terms can be ignored (all second order and higher interactions are assumed to be negligible). The extra variables are then substituted for the interaction terms. This results in a 7 variable experiment with a resolution 3 and defining identity, $I=abcdef$, shown in Table 4-3.

Instead of the 2^7 (128) experiments needed for the full factorial, we have a 1/16 fractional factorial with 8 experiments evaluating the main effects only. It is also called a saturated design and it is also called an $L_8(2^7)$ orthogonal array.

Table 4-3. 2^{7-4}_{III} Design

$$L_8(2^7) = 2^{7-4}_{III}$$

Parameter	1	2	3	4	5	6	7
Experiment 1	1	1	1	1	1	1	1
Experiment 2	1	1	-1	1	-1	-1	-1
Experiment 3	1	-1	1	-1	1	-1	-1
Experiment 4	1	-1	-1	-1	-1	1	1
Experiment 5	-1	1	1	-1	-1	1	-1
Experiment 6	-1	1	-1	-1	1	-1	1
Experiment 7	-1	-1	1	1	-1	-1	1
Experiment 8	-1	-1	-1	1	1	1	-1

Full Factorial	a	b	c	ab	ac	bc	abc
Saturated	a	b	c	d	e	f	g
Assigning				d=ab	e=ac	f=bc	g=abc
I=				I=abd	I=ace	I=bcf	I=abcg
Two at a time				I=bcde=acdf=cdg=abef=beg=afg			
Three at a time				I=def=adeg=bdfg=cefg			
Four at a time				I=abcdefg			
Complete defining relation				I = bcde = acdf = cdg = abef = beg = afg = def = adeg = bdfg = cefg = abcdefg			
Actual	=a+	=b+	=c+	=d+	=e+	=f+	=g+
	bd+	ad+	ae+	ab+	ac+	bc+	cd+
	ce+	cf+	bf+	ef+	df+	de+	be+
	fg	eg	dg	cg	bg	ag	af

Table 4-3 shows the process of determining the defining identity. The added variables are assigned to the columns in place of the interactive effects. Each confounded effect is calculated into an identity. The identities are then multiplied together in all possible ways to give all possible interactions and all the

possible products form the defining identity. It is apparent that this design is highly aliased with many confounded effects. The final row shows the actual effects represented by each main effects investigated (excluding 3rd order and higher terms). The complete defining relation will give the aliasing for any single variable. This is found by multiply through by the sought variable. For variable *a* we get

$$a=bd=ce=abcf=bcg=abcde=cdf=acdg=bef=abeg=fg=adef=deg=abdfg=acefg=bcdefg \quad [4-3]$$

ignoring all the 3rd order and higher terms results in

$$a= bd=ce=fg \quad [4-4]$$

Variable *a* is therefore confounded with interactions *bd*, *ce* and *fg*. It is only when these interactions are negligible that the main effect alone can be evaluated.

Resolution 5 designs, where all three main affects, and all the second order interactions, can be investigated without confounding, are also easily designed [Whitell , Morbey 1961] but require more experiments than lower resolution experiments. Plackett and Burman designs use arrays that are identical or equivalent to the orthogonal arrays as recommended by Taguchi [Logothetis 1992]. Plakett and Burman however simply give the defining identity as the definition for the array [Plakett and Burman 1946], while Taguchi specifies the entire orthogonal array making it much easier to use and apply[Lochner 1990, Shainin 1998].

4.6. Alternative Designs

There are a number of different designs available for different purposes with different characteristics all developed by different people. A few of the alternatives are discussed below.

4.6.1. Central Composite Rotatable Design (CCRD)

The CCRD generates a response surface⁸ for the variables investigated locating maxima and minima. Response modelling generates a multi dimensional surface identifying the relationship between the input and response variables. The relationship is quantified in terms of a mathematical equation giving the response variable as a function of the input variables. The method requires testing of the input variables at five points within the variable range to generate an accurate function and this can only be done on continuous variables. The graphical representation of the response variable can only be done with respect to two input variables at a time. The generated equation however, is a function of all the input variables investigated. It was introduced as an alternative to the 3^k design [Box and Wilson 1951] and consists of:

⁸ A response surface is a surface 2 dimensional representation of the mathematical relationship of two of the variables in the experimental evaluation to the response variable.

1. A complete 2^k factorial design (coded +1,-1) consisting of n_c points making the 'cube' portion of the design.
2. n_0 centre points
3. n_s axial points a distance α from the origin (centre points) forming the 'star' portion of the design.

The CCRD investigates linear, quadratic and first order interaction effects of the variables. The total number of experiments needed is 2^k+2k+n_0 which is considerably fewer than the alternative 3^k for the full factorial design. Each variable is evaluated at 5 levels, which gives sufficient data to determine the accurate curvature of the trends and identify maxima and minima.

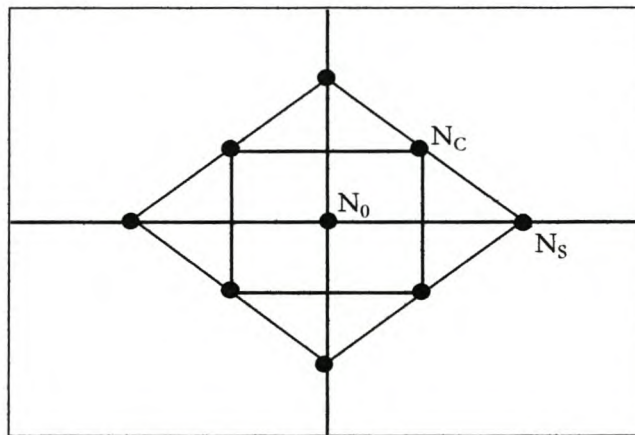


Figure 4-1. CCRD Diagram

A major restriction of the CCRD is that the variables must be continuous in the range of the experiment. The design must be orthogonal⁹ (the coded sum of products within each row must be 0). The distance α is calculated from the number of each type of point in order to maintain orthogonality and rotatability. Advantages of the CCRD are:

1. A quadratic equation for the modelled response gives a good estimate of curvature.
2. Fewer experiments are required than the 3^k design.
3. Repeat experiments at the centre points allow the variability of the system to be quantified.
4. Repeat experiments allow the determination of response and statistical error as a function of both systematic and random errors.
5. It is a resolution 5 design with unconfounded second order interactions.

⁹ Every level of every variable occurs an equal number of times with every level of every other variable.

4.6.2. Haddamard

The Hadamard matrix (or Plakett-Burman matrix) [Plakett and Burman 1946] is used primarily for screening many variables in order to determine the significant few with respect to the chosen response variable. The design is usually of resolution 3 with as few runs as possible. The design is saturated in that all the interactions are confounded with main effects and there is no degree of freedom left to estimate the error term in an ANOVA¹⁰. The Plakett-Burman designs are made up of 2^k experimental runs whereas the number of runs for a Hadamard matrix is a multiple of four. In both cases only linear effects are investigated as there are only two levels per variable.

4.6.3. Latin Square Design

The Latin Square design is a specific design where the number of variables equals the number of levels of each variable and no interactions are investigated [StatSoft 1998]. For example, to examine the effect of 4 fuel additives on reduction in oxides of nitrogen with 4 cars and 4 drivers, then a full $4 \times 4 \times 4$ factorial design would be used, resulting in 64 experimental runs. However, without an interest in any (minor) interactions between the fuel additives and drivers, fuel additives and cars, or cars and drivers, only in estimating the main effects, without any bias of confounding. Labelling the additives with the letters A, B, C, and D, the Latin square design that would enable the determination of unconfounded main effects estimates could be summarised as follows.

Table 4-4. Latin Square Design

	Cars			
Driver	1	2	3	4
1	A	B	D	C
2	D	C	A	B
3	B	D	C	A
4	C	A	B	D

Each of the entries in the table represents one experiment configuration. This is only one of the three possible arrangements in effect estimates. These "arrangements" are also called *Latin squares*. The example above constitutes a 4×4 Latin square; and rather than requiring the 64 runs of the complete factorial, you can complete the study in only 16 runs.

A nice feature of Latin Squares is that they can be superimposed to form *Greco-Latin square* designs. For example, If three additives were used, A, B and C, and three tyres were also used, D, E, and F for the

¹⁰ Analysis of Variance calculation.

test as well as three cars and three drivers, the following two 3 x 3 Latin squares could be superimposed to form a Hyper-Greco-Latin square design (Table 4-5):

Table 4-5 Hyper-Greco Latin Square

	Cars		
Drivers	1	2	3
1	A	B	C
2	B	C	A
3	C	A	B

+

	Cars		
Drivers	1	2	3
1	D	E	F
2	F	D	E
3	E	F	D

=

	Cars		
Drivers	1	2	3
1	AD	BE	CF
2	BFJ	CD	AE
3	CE	AF	BD

In the design it is possible to evaluate the main effects of the 4 variables at 3 levels in 9 experiments rather than the 81 (3⁴) needed for the full factorial design.

4.7. Closing Comments

The experimental design methods discussed here are not fundamentally different from Taguchi Methods, all are forms of a fractional factorial experimental design, it is primarily in the use of the methods that Taguchi Methods differ. A comprehensive statistical knowledge and understanding is not needed in order to apply Taguchi Methods successfully. Taguchi Methods are discussed and described in Chapter 5 and applied in a number of case studies in Chapters 6 through 9.

Chapter 5. Taguchi Method of Experimental Design.

The techniques developed by Dr Genuchi Taguchi¹¹ during the 1950s and 1960s, were born out of work done by an English agriculturist, Mr Fisher. Mr Fisher was a pioneer in the exploration of experimental design in 1928, experimenting on crops in Britain to improve output by varying ground condition and fertilisers. His techniques however, were not well received in Western circles. It was the Japanese who embraced the techniques and developed them in the area of quality control, to become arguably the world leaders in quality [Logothetis 1992].

Taguchi methods have become more and more popular in recent years. The documented examples of sizeable improvements due to the implementation of these methods [Gardener 1992, Hunter *et.al.* 1990, Kailash 1988, Shetty and Kinsella 1992, Yan et al 1993, Rosiaux 1987, Quinlan 1985, Orr and Foslom 1987] have bolstered the image of Taguchi Methods in the Western world. The American telecommunication giant, AT&T, is using these methods in the manufacture of very large-scale integrated circuits. Ford Motor Company has also gained significant quality improvements by applying Taguchi Methods [Statsoft 1998]. However, as the details of Taguchi Methods became more widely known, critical appraisals [Box et al 1988] of the methods showed that they were very similar to already well known methods of experimental design presented in a more user friendly package.

Taguchi robust design methods are set apart from traditional quality control and industrial experimentation in various respects. Of particular importance are:

1. The concept of *quality loss functions*,
2. The use of *signal-to-noise (S/N)* ratios, and
3. The use of *orthogonal arrays*.

These basic aspects of robust design methods are discussed in the rest of this Chapter. Several books have recently been published on these methods [Bendel et al 1989, Peace 1993, Ross 1988] and are highly recommended by the author in order to gain a more complete understanding of the methods.

5.1. Taguchi methods: A Quality Control Tool

Taguchi Methods are largely used under the banner of statistical process control (SPC). Taguchi's work started in the quality control spheres and was based on principles developed by W.E. Demming and R.A. Fisher [Logothetis 1992]. Demming approached quality and its improvement from a managerial and philosophical perspective and Taguchi developed the application methods and tools for quality control

¹¹ Director of the Japanese Academy of Quality and four time recipient of the Demming prize

based on his philosophies. Demming aimed to move quality control from control charts and process control into the engineering arena [Barker, 1986]. His most significant philosophy was to,

“Cease dependence on inspection to achieve quality”.

The Taguchi philosophy stemmed from the change in focus of the quality control philosophy. It shifted from viewing quality as the achievement of specifications within tolerance limits, to the continued improvement of critical variables to the goal value, representing 100% customer satisfaction. Variance away from the goal value represents loss to society and therefore cost. Taguchi defined quality as follows:

“The quality of a product is the loss imparted by the product to society from the time it is shipped, other than loss caused by its intrinsic functions.”

Taguchi shifted quality control from the production stage to the design stage and concentrated on designing a robust product. A robust product is insensitive to downstream variation in either production or user environment.

Taguchi Methods offers more than techniques for experimental design and analysis. It is a complete and integrated system to develop specifications, engineer the design, and manufacture the product to these specifications [Barker 1986]. This comprehensive approach addresses quality in the design, manufacture, and use of the product [Lochner and Matar 1990]. The key is to optimise the functional variables and minimises the effect of noise on the system through the control of the levels of the product and process variables [Bryne and Taguchi 1986]. The Taguchi Method calls upon engineering knowledge and experience and utilises experimental design methods to sharpen decisions and arrive at an optimal configuration with the least number of resources [Barker 1986]. The result is a visual plot of the data in the analysis to determine the significant variables in the experiment as opposed to an ANOVA, which is used in statistical analysis of data. For applications where statistics is not a strong field in the team this method is preferred, [Bryne and Taguchi 1986] although where possible, a statistical evaluation is a good supplementary tool.

5.2. Characteristics of Taguchi Methods

Linking quality control to optimisation may seem an obscure link. Taguchi’s philosophy of quality control was to design and build quality into the product from conception, through design and manufacture and into its use. This essentially is optimising the product with regard to quality starting during the concept phase. There are three steps involved in quality engineering optimisation according to the guru Taguchi [Bryne and Taguchi 1986] (Figure 5-1).

- 1) System Design. This requires innovation and a knowledge of science and engineering in order to select the main variables to be considered in the optimisation process, and preliminary values for these variables.
- 2) Variable Design. This step of the process focuses on the testing of the chosen variables across a range as determined in the system design step. The optimum levels for the variables are chosen for robustness and performance.
- 3) Tolerance Design. This step is taken only if the results from the variable design are unsatisfactory. Case study two (Chapter 8) illustrates a situation where the data variation was too great to identify the optimum levels of the variables and further steps are needed in the optimisation process. Improved test and analysis procedures and equipment are therefore needed in order to reduce the data variation due to system noise and identify the true trends. Removing the noise variable in other ways would then reduce the variation. Tolerance design generally involves tightening the tolerances and variations on the variables causing the loss (i.e. spending money on improved materials, machining, test methods or equipment).

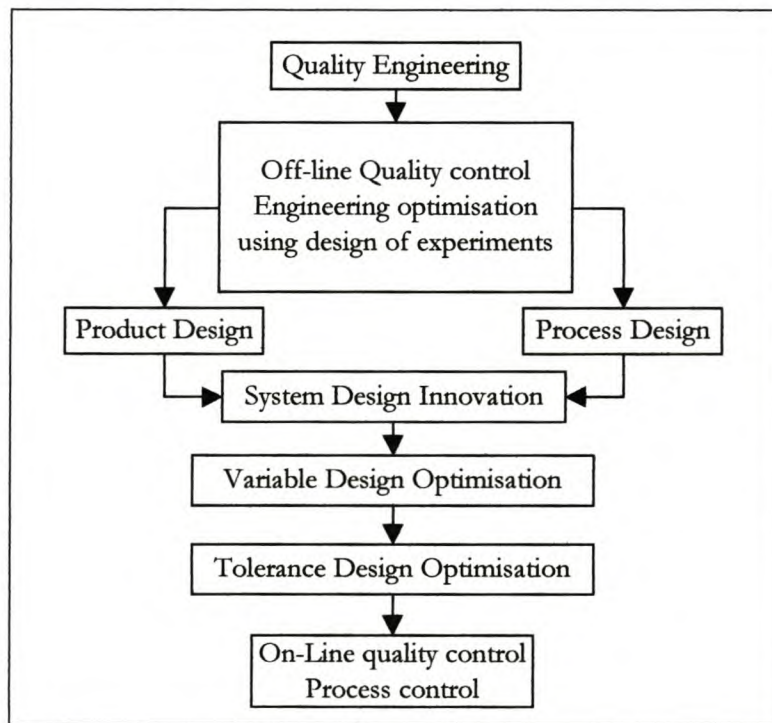


Figure 5-1. Quality Engineering Optimisation [Bryne and Taguchi 1986]

Traditionally the second step is ignored and skipped over. It is however, in this step that Taguchi methods show their worth and strength.

The focus of the majority of Taguchi type experiments is on main effect investigation and generally the interactive effects are assumed negligible. In these cases the importance of a confirmatory experiment should not be underestimated. If there are indeed interactions that need to be investigated the

confirmatory experiment will show this by being incorrect, and indicate that there are confounding or unidentified effects disturbing the data and the experiment needs to be re-developed.

5.2.1. The Loss Function

Taguchi's definition of loss (Section 5.2) includes dysfunction, malfunction or simply customer dissatisfaction that can develop into a bad reputation and loss of market share as well as warranty costs [Bryne and Taguchi 1986]. The average product performance must match or exceed the customer requirements. Taguchi's definition states that a product causes loss when it deviates from the target value, not only if it falls outside target specifications as is the traditional method of measuring specification conformance. This loss is defined to be proportional to the square of the deviation from the target. To minimise the loss one must minimise the variation of the product. The Taguchi Method views variability, from both within and without the system, as being the enemy of quality [Barker 1986].

Mathematically the loss function [equation 5.1] is derived from the first term of a Taylor expansion that links the financial loss to the functional specification as a quadratic relationship [Barker 1986]. There are many forms of the loss function but the most commonly known and used is

$$L = k(y - m)^2 \quad [5-1]$$

Where :

- L = is the loss at the specifications limit
- y = is the value of the response
- m = is the mean target
- k = is the loss constant

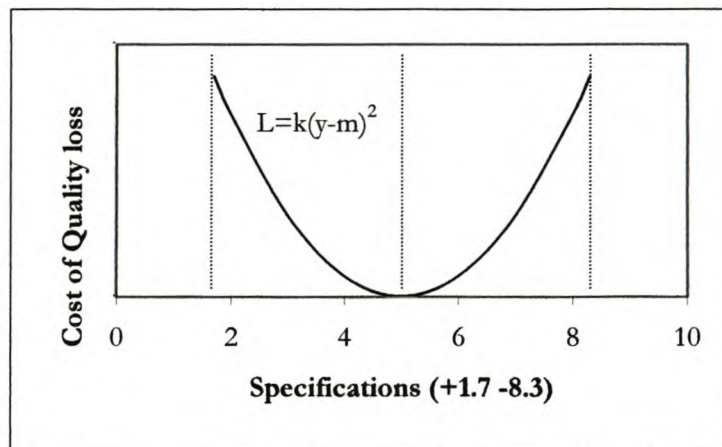


Figure 5-2. Taguchi Loss Function

Figure 5-2 shows an example of the loss function graphically within the quality specifications of +1.7 – 8.3 and the target value of 5. The cost of the loss is shown to grow exponentially as the distance from the target value increases. Loss occurs not only when the product is out of specification but also when it

deviates from the target value. Therefore by continually striving to reduce the variation in the products output variables, the loss is continually reduced [Bryne and Taguchi 1986].

The result of such a policy of loss measurement is an improvement in quality and a decrease in the overall variation of the specifications from the target value. Figure 5-3 shows the distribution of product values meeting specifications for an inspection driven quality philosophy versus a quality driven philosophy. It is clear that the quality driven philosophy of meeting specifications yields better long-term results than the inspection philosophy. Although both philosophies have the same number of products meeting specifications, the deviation of the quality driven product from the target value of 5 will be lower, with more products produced closer to 5, than the inspection driven policy.

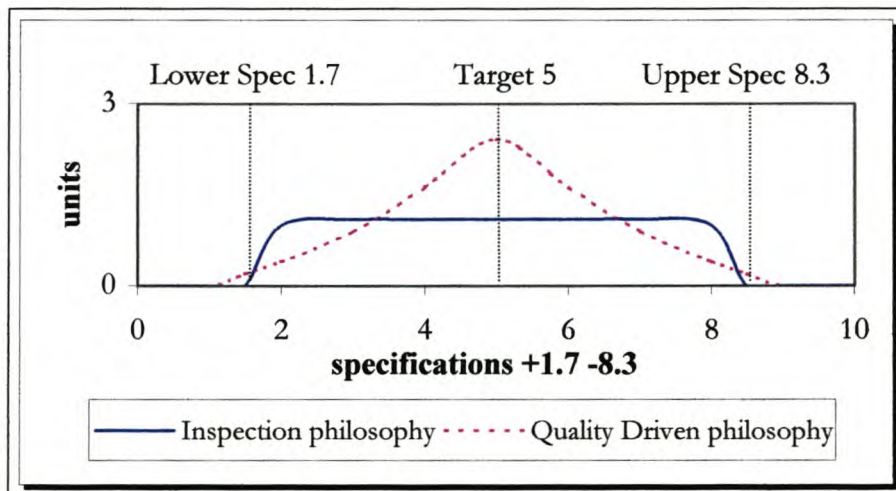


Figure 5-3. Inspection-Driven Specifications vs. Quality-Driven Specifications

5.2.2. Variation

The deviation from a target value is attributed to noise, either inner noise¹² or outer noise¹³, depending on the origin of the variation. The variables causing variation can be divided into two classifications. Controllable design variables which can be set to required values and uncontrollable noise variables whose values cannot be controlled. Generally speaking the aim of an experimental design is to optimise the controllable variables to give the best output that is least sensitive to the variation of the uncontrollable variables.

Controllable variables can therefore be divided into those variables that affect the average level of the response of interest (signal variables) and those variables that affect the variation of the response of interest (control variables). The signal variable would therefore be used to get the “best output” and the control variable would be used to minimise the variation around the “best output”. In this thesis emphasis is placed on using the signal variables to optimise the system whereas in pure quality control,

¹² Inner Noise: The variation that occurs due to production variables, tolerances and things that the manufacturer can attempt to control (voltages, speed, sizes, tolerances, ...).

control factors would also be optimised and often be considered the more important of the two types of variables.

5.2.3. Noise

Where does the noise come from? Noise is defined as either inner noise or outer noise. Some texts refer to the inner noise as controllable variables [Bryne and Taguchi 1986] and outer noise variables simply as noise, thus differentiating the design variables that can be easily controlled from the noise variables that are difficult, expensive or impossible to control. The noise variables are divided into three types shown in Table 5-1.

Table 5-1. Examples of Noise Classification [Bryne and Taguchi 1986]

	<u>Product Design</u>	<u>Process Design</u>
Outer Noise	Consumer usage conditions Low Temperature High Temperature Temperature change Shock Vibration Humidity	Ambient Temperature Humidity Seasons Incoming Material Variation Operators Voltage Changes Batch to batch variation
Inner Noise	Deterioration of Parts Deterioration of Material Oxidisation (rust)	Machinery ageing Tool Wear Deterioration
Between Product Noise	Piece to Piece variation where they are supposed to be the same	Process to Process variation where they are supposed to be the same.

The aim is to select values for the controllable variables such that the product or process is least sensitive to variation in the noise variable.

5.2.4. Signal to Noise Ratio

One of the essential elements in Taguchi's design for robustness is the signal to noise ratio (S/N). By using the signal to noise ratio, the level as well as the variation of the output variable can be evaluated and controlled. The product can then be produced at optimum levels with minimal variation. In its simplest form the S/N ratio is the ratio of the mean value to the standard deviation. The formula offers a built in trade off between the mean response and the variation of the response, although it is generally more responsive to the mean value. There are many different formulas for the signal to noise ratio but there are three generic forms that can be used for a wide range of applications [Barker 1986].

Type N: Nominal is best (dimensions, output voltages, reduction ratios, etc.) [Peace 1993] where a specific value is the aim for the output variable. The S/N ratio is defined as

¹³ Outer Noise: The variation imposed by external circumstances, such as the market place and the environment.

$$S / N_N = 10 \log_{10} \left(\frac{(S_m - V_e) / n}{V_e} \right) \quad [5-2]$$

Where

$$S_m = \frac{(\sum y_i)^2}{n} \quad [5-3]$$

$$V_e = \frac{\sum y_i^2 - (\sum y_i)^2 / n}{n - 1} \quad [5-4]$$

and y_i is the i^{th} observation (data point) and

n is the number of observations

Type S: Smaller is better (noise, emissions, contamination, etc.), where the target or aim is to get the smallest response from the output variable (minimise).

$$S / N_S = -10 \log_{10} \left(\frac{1}{n} (\sum y_i^2) \right) \quad [5-5]$$

Type B: Bigger is better (strength, power, torque), where the target or aim is to maximise the output variable.

$$S / N_B = -10 \log_{10} \left(\frac{1}{n} (\sum \frac{1}{y_i^2}) \right) \quad [5-6]$$

The S/N ratios have been constructed such that irrespective of the goal of the experimentation (maximising or minimising the output variable) the objective will be to maximise the value of the S/N ratio used in the investigation. That way the response value will be optimised and the variation minimised.

5.2.5. Orthogonal Arrays

The fundamental building block of Taguchi Methods is the orthogonal array. Orthogonal arrays have been used for many years, but their application in Taguchi methods has some special characteristics. Initially they look to be nothing more than fractional factorials, however the primary goal in the optimisation process is to minimise the design's sensitivity to noise and thus produce a robust design.

The naming convention for the arrays is $L_a(b^c)$

Where a = number of experimental runs

b = number of levels of each variable

c = number of variables in the array

Table 5-2. $L_{16}(4^5)$ Orthogonal Array

$L_{16}(4^5)$
Experiments

Test	Var 1	Var 2	Var 3	Var 4	Var 5
1	1	1	1	1	1
2	1	2	2	2	2
3	1	3	3	3	3
4	1	4	4	4	4
5	2	1	2	3	4
6	2	2	1	4	3
7	2	3	4	1	2
8	2	4	3	2	1
9	3	1	3	4	2
10	3	2	4	3	1
11	3	3	1	2	4
12	3	4	2	1	3
13	4	1	4	2	3
14	4	2	3	1	4
15	4	3	2	4	1
16	4	4	1	3	2

The orthogonal array represented in Table 5-2 shows the naming convention and structure of the array. Each of the 5 variables in the design has 4 levels. The numbers 1 through 4 represents the levels, and the labels Var1 through Var5 represent the variables. The orthogonal array design has 16 experiments that approximate the trends of 5^4 (625) variable combinations. Similarly with a $L_{27}(3^6)$ orthogonal array the 3^6 (729) variable combinations are investigated in 27 experiments. The saving in experimental time and the wealth of information gathered from the designs is self-evident. A notable characteristic of an orthogonal array is the pair-wise balancing property: That is,

“every level of every factor occurs an equal number of times with every level of every other factor”,

thus forming a well balanced experimental design. In essence the orthogonal array is an easy to read definition of the fractional factorial design for a chosen experimental design and for a 3 level experiment it can be likened to a 3(k-p) experimental design (Box and Hunter 1978, Daniel 1962).

5.2.6. Choosing an Orthogonal Array

Rosiaux [1987] used a simple flow diagram to illustrate the theoretical pathway to optimum orthogonal array choice and experimental design. Figure 5-4 shows this pathway. The investigation starts with identifying all the possible causes for the variation. If the number of causes (variables) is too great to fit into a standard orthogonal array then choose the most important variables. Decide if it is to be a two or

three level design or whether a modified design will need to be used, and whether interactions will be included in the investigation or not.

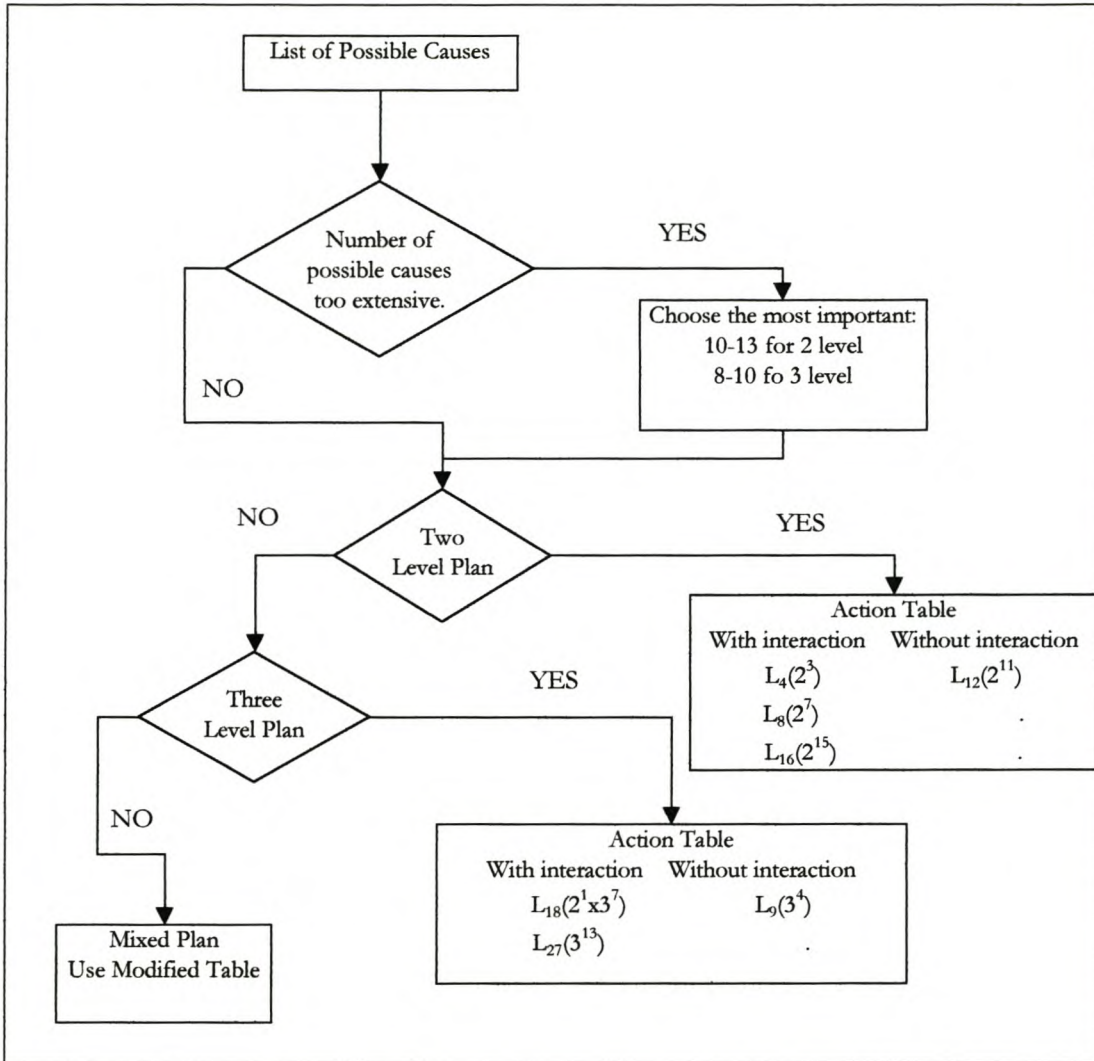


Figure 5-4. Orthogonal Array Flow Sheet

The standard orthogonal array can be modified to suite the experimental design. I.e. Rosiaux [1987] used three two level columns in a $L_{16}(2^{15})$ orthogonal array to represent four levels of a single factor. In the design an interaction table was used to choose the correct columns to use for the four level factor to avoid confounding with other variables that were deemed important. ASI [1987] published a collection of orthogonal arrays and the associated interaction tables. Table 5-3 shows some commonly used orthogonal arrays and some of their characteristics.

Table 5-3 Commonly Used Orthogonal Arrays

Orthogonal Array	Number of Factors	Number of levels per factor	Number of trials required by orthogonal array	Number of trials in a traditional full factorial experiment	Degrees Of Freedom
$L_4(2^3)$	3	2	4	8	$3 \times (2-1) = 3$
$L_8(2^7)$	7	2	8	128	$7 \times (2-1) = 7$
$L_9(3^4)$	4	3	9	81	$4 \times (3-1) = 8$
$L_{12}(2^{11})$	11	2	12	2048	$11 \times (2-1) = 11$
$L_{16}(2^{15})$	15	2	16	32768	$15 \times (2-1) = 15$
$L_{16}(4^5)$	5	4	16	1024	$5 \times (4-1) = 15$
$L_{18}(2^1 \times 3^7)$	1	2	18	4374	$1 \times (2-1) + 7 \times (3-1) = 15$
	7	3			

5.2.7. Interaction Tables (Triangular Interaction Matrices)

Due to the fractional nature of the orthogonal array, it is also very aliased, i.e. the main effects are confounded with higher order effects. Each orthogonal array has an interaction table associated with it in order to identify which columns represent the interactions between other columns (factors) and which interactions are confounded. It is important when assigning variable to columns to consult the interaction table to eliminate the effect of any major interactions that will confuse the main effect trends.

Table 5-4. Interaction Table of $L_{16}(2^{15})$ Orthogonal Array. [ASI 1987]

	Column														
	1	2	3	4	5	6	7	8	9	10	11	12	13	14	15
(1)	3	2	5	4	7	6	9	8	11	10	13	12	15	14	
(2)		1	6	7	4	5	10	11	8	9	14	15	12	13	
(3)			7	6	5	4	11	10	9	8	15	14	13	12	
(4)				1	2	3	12	13	14	15	8	9	10	11	
(5)					3	2	13	12	15	14	9	8	11	10	
(6)						1	14	15	12	13	10	11	8	9	
(7)							15	14	13	12	11	10	9	8	
(8)								1	2	3	4	5	6	7	
(9)									3	2	5	4	7	6	
(10)										1	6	7	4	5	
(11)											7	6	5	4	
(12)												1	2	3	
(13)													3	2	
(14)														1	
(15)															1

Table 5-4 is an example of an interaction table for the $L_{16}(2^{15})$ orthogonal array. If factor A were assigned to column 1 and factor B were assigned to column 4, then their interactive effect $A \times B$, is located in column 5 as indicated by the circled number.

There are some orthogonal arrays that do not have interaction tables. The L_{12} , L_{18} , L_{36} and L_{54} arrays are among a group of arrays that do not contain any confounded interactive effects and allow the experimenter to focus on main effects only. The interactive effects are evenly spread across all the columns and their arrays are among the most popular for this reason.

5.2.8. The Linear Graph

A linear graph is a graphic representation of the orthogonal array and the corresponding interaction tables. Most orthogonal arrays have a number of linear graphs associated with them representing different structures of main effects and the associated interactions. The linear graph is made up of dots representing main variable effects and the lines joining the dots represent an interaction between the main variables. This simplifies the design process greatly and removes the need of the designer to determine which columns the interactive and main effects need to go into. The linear graph is used as a tool for assigning the main effects and interactions to the correct columns to avoid confounding effects.

The linear graph in Figure 5-5 is of the $L_{16}(2^{15})$ orthogonal array and shows the number of variations that can be constructed from the same orthogonal array. The numbers represent the columns to which the respective main effects or interactions are assigned for that configuration.

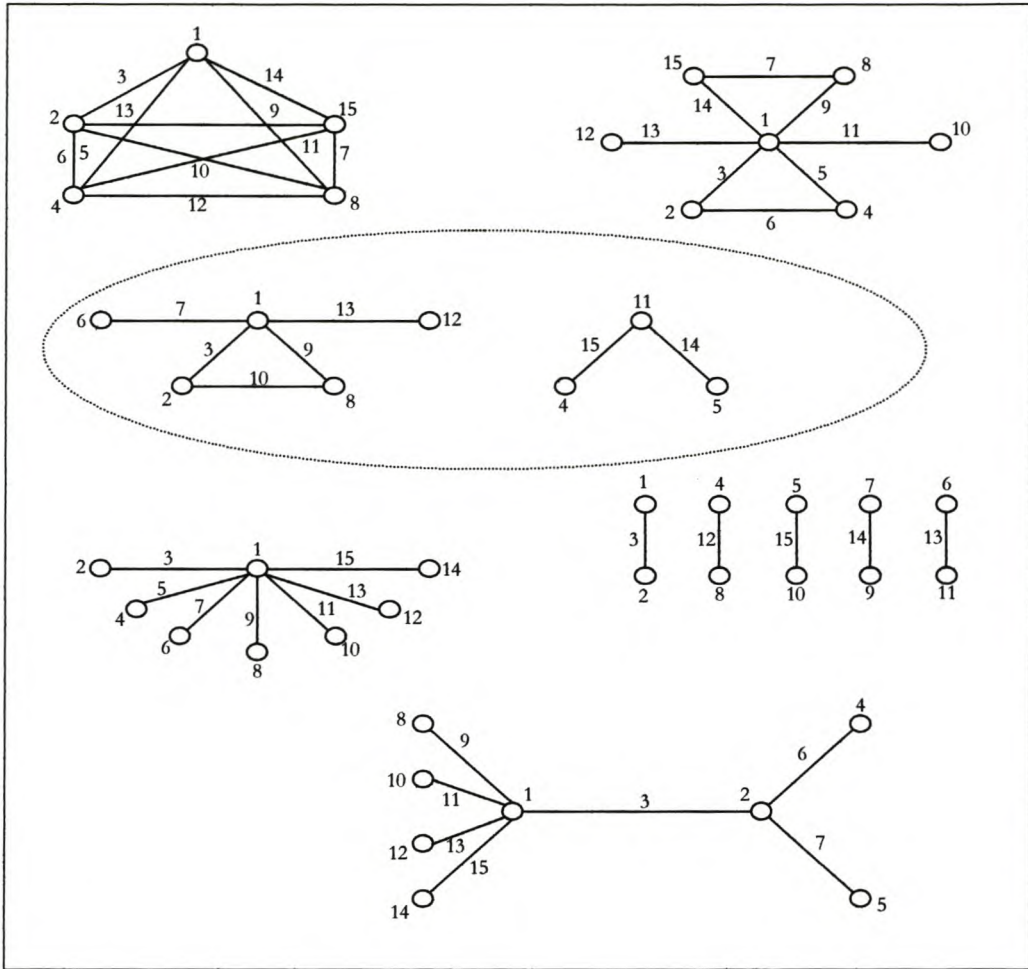


Figure 5-5. Linear Graphs of $L_{16}(2^{15})$ Orthogonal Array

Any literature on Taguchi Methods will have a selection of linear graphs in the text or the appendices.

5.2.9. Analysis

Analysis of the Taguchi experiment is not a particularly complex procedure. For the regular analysis, average response tables, average response graphs and an ANOVA can be used. For the S/N ratio analysis, S/N response tables, S/N response graphs, and a S/N ANOVA can be used.

The optimum levels for all the control variable are chosen and the predicted results for the optimum configuration are calculated. The optimum configuration must always be tested for the experiment to be completed. If the predicted result is incorrect it indicates that there is either an interaction that is significant and must be investigated or that there is another main effect that was not considered in the initial design. In either case the experiment needs to be designed and re-executed. Precise details of this procedure are given in Chapter 6 along with the first Case Study as a worked example.

5.2.10. Multiple Response Optimisation

There are instances where the optimisation procedure needs to be applied to two or more response variables [Draper and Hunter 1966], i.e. an engine would need to be optimised for torque, power and fuel consumption. The standard method of single response variable optimisation could be used and each of the investigations would yield an optimum configuration for each response variable.

The possibility that all the levels will agree for all the different response variables is very remote. In this instance it is common place for the optimisation trade-off to be left to engineering intuition and judgement for the final selection of variable levels.

The guess work can however be removed by using a multiple regression technique [Equation 5.7]. The equation makes it possible to solve for the multiple response investigation with the transformation to Y_T in terms of the control variables A_n [Logothetis et al 1987, Logothetis 1988].

$$Y_T = a + \beta_1 \times A_1 + \beta_2 \times A_2 + \beta_3 \times A_3 + \dots + \beta_n \times A_n \quad [5-7]$$

Where β_i are the regression coefficients and a the regression constant..

Using a linear programming approach the formula can be optimised under restrictions of the target values for the response variable models.

$$R_i = r + r_{i1} \times A_1 + r_{i2} \times A_2 + r_{i3} \times A_3 + \dots + r_{in} \times A_n \quad [5-8]$$

Where R_i is the i^{th} response in terms of the control variables A_n .

Although this method makes the choice of the optimum configuration very easy, it is very difficult to determine the multiple response equation and most multiple response problems are solved intuitively rather than numerically.

5.3. Closing Comments

The methods described in this chapter are very powerful when used efficiently and correctly. Chapter 6 illustrates the application of the method with the assistance of the first case study.

Chapter 6. Taguchi Methods as an Experimental Design Tool (Case Study One - Evaluation)

The aim of Taguchi Methods is to bring products to market quicker, with reduced costs and reduced development time. The driving force for this time reduction is reduced experimentation time. This chapter uses a case study to illustrate the method used in applying Taguchi methods.

6.1. Experimental Planning Following the Taguchi Method

The Taguchi Method is a broad experimental approach with many different application possibilities and configurations [Peace 1993]. This Chapter focuses on the development of the method as it will be used in the four case studies undertaken in this thesis. The first case study has been included in this chapter as an example illustrating each of the steps in the technique. Only the aspects pertaining to this type of application have been expanded upon. The basic structure has been adapted from Peace [1993] who gave comprehensive instructions on how to use the Taguchi Method of experimental design. The method is very flexible and it depends largely on the person driving the project as to where the emphasis is placed. If, for example, a statistician were to lead the team and formulate the procedure, there would be more attention placed on the statistical aspects, whereas a manager leading the team would perhaps concentrate more on the project definition and planning as being important to the success of the investigation. Both of these approaches are satisfactory as long as sufficient attention is placed on all of the other phases of the application.

The first case study involves the evaluation of a carburettor adapter prototype. The results obtained in this chapter using Taguchi Methods are compared in Chapter 7 to the traditional method of examining the test data.

6.1.1. The Carburettor Adapter

Due to specific requirements of the Southern Africa climatic conditions of increased airborne dust, a normal (Japanese standard) pancake air filter mounted directly onto the carburettor, is not suitable. A remote air filter is more effective for dust removal and therefore used in local vehicles. A carburettor adapter is therefore required to link the carburettor to the remote air filter housing.

The carburettor adapter can influence the engine performance in a number of ways. It can limit the efficiency of the engine by restricting the air flow into the combustion chamber (by restricting its flow into the carburettor). The carburettor adapter can also change the air pressure in the carburettor and

thus interfere with the fuelling and the distribution of fuel to the four cylinders. The dimensions and design are therefore important features for induction optimisation.

6.1.2. Project Background

A research program, in conjunction with a local air filter manufacturer, was established by CAE in an attempt to investigate the design procedure and to determine the specific factors of the carburettor adapter that influence the volumetric efficiency of the engine. This program used Taguchi Design of Experiments.

The effect of the adapter diameter, height and cross-over pipe dimensions, on the engine performance were investigated by Hart [1996] and Petzer [1996]. This work was initially undertaken on the carburettored prototype engine, although a fuel injection system was later added. This ensured that the fuel distribution was equal across all the cylinders and only the air flow would be affected by the carburettor. Any improvements in performance seen were as a direct result of improved breathing characteristics and not as a result of altered fuelling. From this work a prototype adapter was designed and manufactured using a rapid prototyping procedure developed at Stellenbosch University. The prototype was fitted with two inserts in an attempt to improve flow characteristics into the carburettor, shown in Figure 6-1.

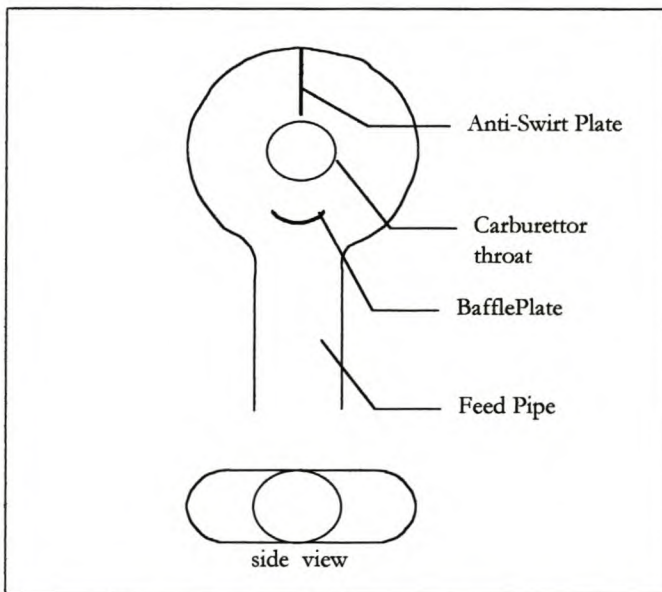


Figure 6-1. Basic Carburettor Adapter Configuration Showing the Positions of the Two Flow Diverting Inserts

The goal was to simulate the air flow in a pancake air filter which is connected directly above the carburettor, and results in better engine performance characteristics. The optimal air flow is purely radial, without any swirl as the air flows into the carburettor throat. A baffle plate was inserted to encourage the air to approach the carburettor throat from all directions as radial flow, and an anti-swirl

plate was inserted to combat the development of swirl at the carburettor throat. Case study one is an evaluation of the effects of the inserts in the prototype carburettor adapter.

6.2. Planning the Experiment

Many of the steps necessary in the quality control application of the method are not applicable to this type of application (investigation of noise factors). Also, due to the simplicity of the experiment and the uncomplicated matrix required, many of the steps seem obvious. They are, however, included as an academic exercise to illustrate the process that is followed during the experimental design and analysis. The Taguchi Methodology is illustrated in Figure 6-2. Each step is described in general and then applied to the case study.

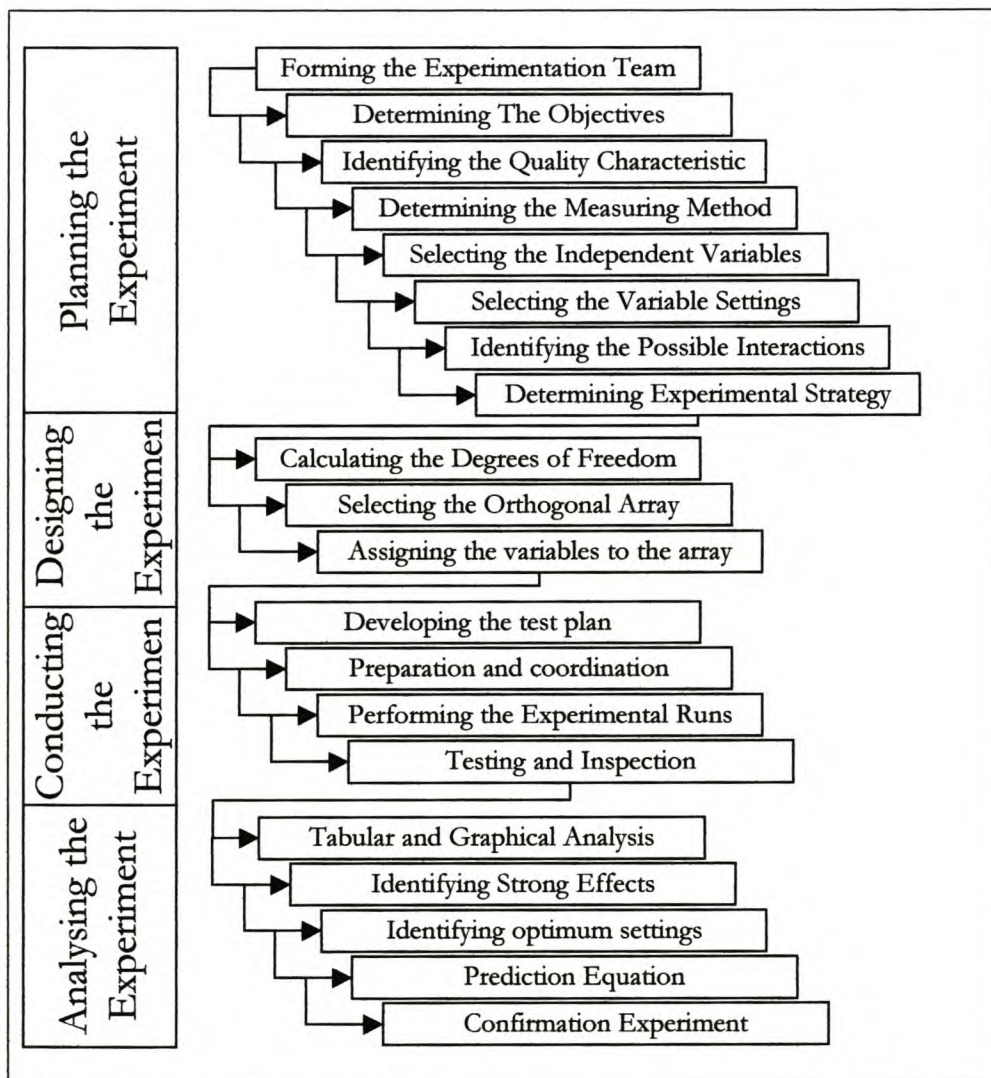


Figure 6-2. Taguchi Methodology

6.2.1. Forming the Experimentation Team

Defining the team working on the project is essential in ensuring that the skills required and the expectations and objectives for the project are met successfully and are included from the beginning. All the people involved on the project need to be on the team so that the goals and methods are supported and understood by all involved. It is important that the team be specified at the beginning of the project so that there is no confusion or lack of clarity about each members responsibility, role and position.

Case Study One:

For the Carburettor adapter investigation the project team consisted of the following people.

Team leader:	Jeremy Green
Management Support:	Dr Andrew Taylor
Technical Support:	John Fitton
	Benn Vincent
	Nico Empedocles

6.2.2. Determining the Objectives

Objectives must be defined, and understood, by all involved in the project so that there is no possibility of misunderstanding with respect to the project goals. It is important that the attainment of knowledge be included in the list of objectives, as this gives room for creativity and learning, as well as getting the job done. The goals do however, need to be clearly defined and attainable, as well as being measurable in terms of success or failure. The project can then be evaluated in terms of success or failure upon its conclusion. The problem must be well and clearly understood with a definite formulation that is written down and communicated to all involved in the project. Many tools exist for this phase of the project in attaining a clear and definite understanding of both the problem and the process, some are listed below.

- The brainstorming technique is emphasised and used more in examples or applications where the project definition and understanding is unclear at the beginning of the project. It allows for innovative and creative thinking in the definition of the quantity variables and objectives. By gathering information from many different sources there is a better all round understanding gained about the entire problem as opposed to just trying to focus on the solution, as would traditionally be the approach.
- The Pareto Chart helps identify the specific focus of the problem and the vital few things that need to be focused on rather than the trivial many.
- The process flow diagram (flow chart) helps to understand the sequence of events, interactions and interrelations between steps.
- The cause and effect diagram flows from the identification of the quality variable and assists in grouping the major and minor causes of variation.
- A Fault Tree Analysis determines the possible problems in the system and how they can be avoided. Originally a safety feature.

A FMEA (Failure Mode and Effect Analysis) assists in obtaining a greater understanding and identifying of all the possible problems in the investigation.

These tools provide opportunities for innovative and creative ideas for problem solution. They assist in the understanding of the problem and the direction the solution need to take, helping to provide focus on the few vital problems rather than the trivial many. Interdependence of the steps and factors in the investigation are identified. Safety and reliability problems can also be highlighted.

Some basic guidelines exist for the definition of the project objective.

- clearly define the objectives in terms that everyone on the team can understand;
- ensure that all team members agree on and can support the objectives selected by the team;
- attain mutual agreement on the criteria for measuring the ability to achieve the objectives;
- put into place communication safeguards to ensure that all affected personnel become aware of any changes in the objective or quality variables (output variable to be used in the optimisation process).
- provide the opportunity to respond to any changes so as to assure continued agreement and support by all team members.

Case Study One:

In this case study the project goals were predefined by the client and non negotiable.

- To determine the optimum configuration of the inserts in the prototype carburettor adapter,
- To examine the trends of two different inserts, and determine if an interaction exists between them, and if one does exist, to quantify it.

6.2.3. Identifying the Quality Characteristic (Output Variable)

There are many terms for the variable that is to be optimised: optimisation parameter, quality variable, optimisation characteristic and goal factor, all referring to the output variable that is measured and used to determine the success or failure of the experiment. The variable chosen is dependent on the objectives of the project, and largely determines the configuration of the experimental plan. In many applications there will be two variables that must be simultaneously optimised or mapped.

The output variable must be measurable, so that progress and success or failure can be measurable. The measurement instrumentation must be brought into account when determining the output variable. “Can the measurement be made accurately and affordably and timeously?” it is an important question that must be answered and can at times be the sole reason for an investigation’s failure

There are three categories of output variables:

- Measurable variables: These can be measured on a continuous scale with the aim or goal a minimum, maximum or target value.
- Attribute variables: The end result is classed into a group rather than measured. (i.e. eggs are divided into grades, A, B or C).
- Dynamic variables: This is a functional representation of the process being studied. The process is characterised by a linear relationship between an input signal and the output signal.

A continuous variable is the best type of optimisation variable to use, as it provides for good additivity, (i.e. torque and power). A classified attribute has the advantage of easy sampling and understanding (i.e. colour, make or model, material type).

Case Study One:

The output variables in the case of the carburettor adapter investigation were top-end-power¹⁴, which is representative of the engines peak power, and the mid-range-torque¹⁵, which gives an indication of the peak torque of the engine. Both top-end-power and mid-range-torque were identified as the variables to be optimised, and both are dependent on volumetric efficiency but occur at different engine operating conditions.

6.2.4. Determining the Measuring Methods

If the output variable is the speed of gas through a thin pipe, the measurement method for measuring the speed must be known or determined. Measurement methods are very important in determining the output variable as the difficulty or ease with which the measurement can be made will affect the experiments accuracy and cost. A difficult measurement to take will invariably result in more external noise and variance than one that is taken easily and increase the possibility of an unsuccessful experimental investigation.

Case Study One:

The methods used to monitor the output of the engine used in the investigation are discussed in Chapter 3. The engine was not in its standard configuration, but had a University of Stellenbosch developed Stainless Steel inlet manifold fitted to a University of Stellenbosch developed prototype cylinder head. The ETA engine data capture system was used for the testing of the engine, which was attached to a water dynamometer to absorb the generated power. A Bosch CO metre was used for the exhaust gas analysis during the testing of the prototype carburettor adapter.

¹⁴ average power between 3000 rpm and 4000 rpm

¹⁵ average torque between 2000 rpm and 3000 rpm

6.2.5. Selecting The Input Variables

Following the selection of the output variable, the variables that effect it need to be identified (independent variables). The decision tools outlined in Section 6.2.2 can be used to explore all the possibilities and then the variables can be screened to determine the final variables to be investigated.

The variables fall into two groups [Logothetis 1992]:

1. Controllable variables, whose values may be set or easily adjusted by the experimenter.
2. Uncontrollable (noise) variables, which are often related to the environment and the overall performance. The final design should be insensitive to variation of the uncontrollable factors.

The controllable factors are then further divided into those that affect the level of the response and those that affect the variability of the response.

The uncontrollable variables can be classified further into three noise categories [Peace 1993]:

1. Outer Noise: This is the variance caused by external factors. Usually the environment in which the product is used results in this type of noise.
2. Inner Noise: This is the result of the ingredients making up the final product.
3. Between Product Noise: The variations are as a result of the different units being made at different times, in different batches and account for piece to piece variation.

By designing to experiment to reduce the noise factors a robust final product or process is achieved.

Case Study One:

In the carburettor adapter investigation only the controllable factors were used. There were no noise factors included in the design. Efforts were taken to minimise the external noise from influencing the data.

1. SABS torque correction factors were used to correct for any changes atmospheric conditions.
2. The engine was operated at a stable operating condition and an average of the output variable was used over the stable operating period.
3. An engine speed control loop was used to maintain engine speed at the desired value.

The factors that were to be investigated were the inclusion/exclusion of a baffle plate and the inclusion/exclusion of an anti-swirl plate as laid out in the experimental objectives.

The **baffle plate** was intended to force the air round the sides of the carburettor adapter, forcing an evenly distributed radial flow pattern of air into the carburettor throat (Figure 6-3 (b)). This closely approximated the more efficient configuration of the pancake filter.

The **Anti-swirl plate** was intended to stop the air from rotating in the carburettor adapter chamber and forming a vortex and swirling into the carburettor entrance. The plate limits the travel of the air to 180° round the entrance to the carburettor. The plate also stopped the development of a venturi and circumferential flow round the carburettor throat (Figure 6-3 (c))

The input variables for the experiment are:

1. the baffle plate , and
2. the anti-swirl plate.

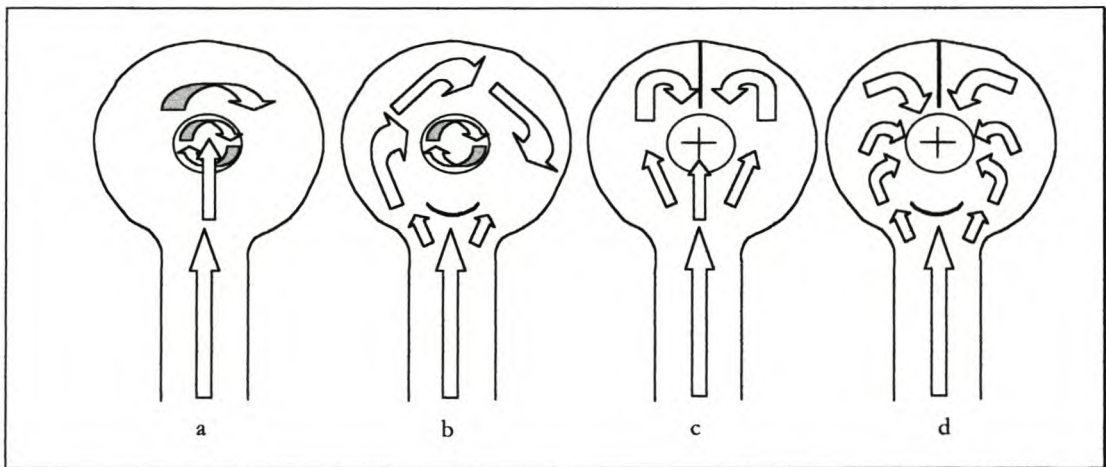


Figure 6-3. Prototype Configurations *a* shows the open adapter without any flow diverters in place, *b* shows the inclusion of the baffle plate, *c* shows the inclusion of the anti-swirl plate and *d* shows the expected air flow with both the baffle plate and the anti-swirl plates inserted with the flow approximating the pancake filter air flow pattern.

6.2.6. Selecting the Variable Levels

Selecting the variable levels is very important in defining the scope of the investigation's applicability. The range of the variables will determine the range over which the results are valid. Interpolation is regarded as acceptable but to extrapolate beyond the boundaries of the experiment is not advised. The outer levels of the investigation should therefore be chosen so that the entire extent of the variables' are covered within the experimental structure. Choosing three levels or more will result in non-linear effects in the variable influence being quantified whereas two levels will only show any linear dependence and are often used to only identify significant factors in process investigations.

Case Study One:

For the Carburettor adapter investigation the levels are obvious and there is no choice to be made. The two levels for each of the parameters are the exclusion (out) and the inclusion (in) of the respective flow diverters. The parameters and their settings are shown in Table 6-1 for Case Study One.

Table 6-1. Parameter Levels

Variable	Level 1	Level 2
Baffle Plate	In	Out
Anti swirl plate	In	Out

6.2.7. Identifying Possible Interactions

Any significant interactions need to be identified and included in the investigation. This step can easily be absorbed into step 6.2.5, identifying the input variables.

Case Study One:

In the carburettor adapter investigation there was only one possible interaction that could be investigated and it was stated as one of the project objectives. The interaction between the baffle plate and the anti-swirl plate was investigated and quantified.

6.2.8. Determine Experimental Strategy

The experimental strategy was to determine the influence of the carburettor adapter inserts on the engine by measuring torque and power as an indication of volumetric efficiency. The torque was measured at an engine speed of 3200 rpm, as a representation of mid-range-torque (MRT), and the power was measured at 4800 rpm as a representation of top-end-power (TEP). An eddy current dynamometer was used to test the engine on an engine test bed at CAE. The carburettor adapter was designed with removable inserts to allow rapid change of the experimental configuration.

It is obvious that the stages in the planning phase are all very interrelated, and the boundaries between the stages can at times be very vague. It may indeed be necessary to have feed back loops at any time with the planning phase. The iterative procedure will eventually result in a well planned experiment. It is important to remember however that nothing is ever cast in stone, and feedback and modification from the next phase may necessitate changes to the plans, to ensure that experimental investigation is a success.

6.3. Designing the Experiment

6.3.1. Calculating the Degrees of Freedom

Degrees of freedom (DOF) need to be calculated for the experiment in order to choose the appropriate linear graph and orthogonal array. The first step is to calculate the degrees of freedom for each input variable that is included in the investigation.

DOF's for each input variable:

$$n \text{ levels} = n - 1 \text{ DOF's} \quad [6-1]$$

The number of DOF's for all the input variables is simply the sum of each individual input variable's DOF. Typically all the input variables will have the same number of levels, and therefore the same number of DOF's. The total DOF's is therefore a function of the number of input variables (c) and the number of levels in the input variables (n).

$$(n \text{ levels} - 1) * c \text{ input variables} = (n - 1) \times c \text{ DOF's} \quad [6-2]$$

DOF for an interaction to be investigated is the product of the DOF of each variable in the interaction

$$\text{DOF variable A} * \text{DOF variable B} = \text{DOF of interaction} \quad [6-3]$$

It can be seen that the more levels the input variables have, the more DOF are needed for the interaction to be investigated in the experimental matrix.

For the total DOF's we must sum the DOF's for the main effect and interactions.

$$\begin{aligned} \text{variables} & : c \times (n - 1) + \\ \text{interactions} & : A(n - 1) \times B(n - 1) = \\ & \text{DOF} \end{aligned} \quad [6-4]$$

Case Study One:

For the example of the carburettor adapter there are two levels in each control variable, therefore the DOF's for each variable are,

$$\begin{aligned} n \text{ levels} & = n - 1 \text{ DOF's} \\ 2 \text{ levels} & = 2 - 1 = 1 \text{ DOF} \end{aligned} \quad [6-5]$$

There are two control variables therefore the number of DOF will be the sum of the individual DOF's, i.e.

$$\begin{aligned}
 1 + 1 &= 2 \quad \text{DOF's} \\
 &\text{or} \\
 2 \times 1 &= 2 \quad \text{DOF's}
 \end{aligned}
 \tag{6-6}$$

DOF's for the interaction to be investigated:

There are only two main effects (parameters) and therefore there can only be one interaction.

$$\begin{aligned}
 \text{DOF factor A} * \text{DOF factor B} &= \text{DOF of interaction} \\
 (2 - 1) * (2 - 1) &= 1 \quad \text{DOF}
 \end{aligned}
 \tag{6-7}$$

In total then we must sum the two types of DOF's.

$$\begin{aligned}
 \text{Factors} &: & 2 \times (2 - 1) &= 2 \\
 \text{Interactions} &: & + (2 - 1) \times (2 - 1) &= 1 \\
 && \underline{\hspace{1.5cm}} & \\
 && 3 & \text{DOF's}
 \end{aligned}
 \tag{6-8}$$

In total then there are 3 DOF's needed to investigate the two main effects (input variables) and the single interaction between them.

6.3.2. Selecting the Orthogonal Array

The Taguchi experimental matrix is chosen using the calculation of the number of degrees of freedom for the experiment and matching that with the most appropriate orthogonal array. The linear graph of the chosen orthogonal array is compared to that of the desired experimental investigation.

Case Study One:

The orthogonal array chosen must have at least as many DOF's as there are in the experiment. In this case there are three DOF's in the experiment so the orthogonal array must have at least three DOF's. The number of degrees of freedom of the $L_4(2^3)$ orthogonal array is calculated as the sum of the DOF in each column.

$$3 \times (2 - 1) = 3 \quad \text{DOF}
 \tag{6-9}$$

This suits the case study exactly. The orthogonal array for the experimental configurations is shown in Table 6-2.

Table 6-2. $L_4(2^3)$ Orthogonal Array.

$L_4(2^3)$
Matrix

Level	Var1	Var2	Var3
1	1	1	1
2	2	2	2

Experiments

Test	Var1	Var2	Var3
1	1	1	1
2	1	2	2
3	2	1	2
4	2	2	1

6.3.3. Linear Graphs

A linear graph is a graphical representation of the experiment to be conducted. The graph consists of dots for the main effects to be investigated and lines joining the dots represent the interaction between the joined dots that is to be investigated. Each orthogonal array has a number of Linear Graphs associated with it.

Case Study One:

The linear graph of the experiment is shown in Figure 6-4.

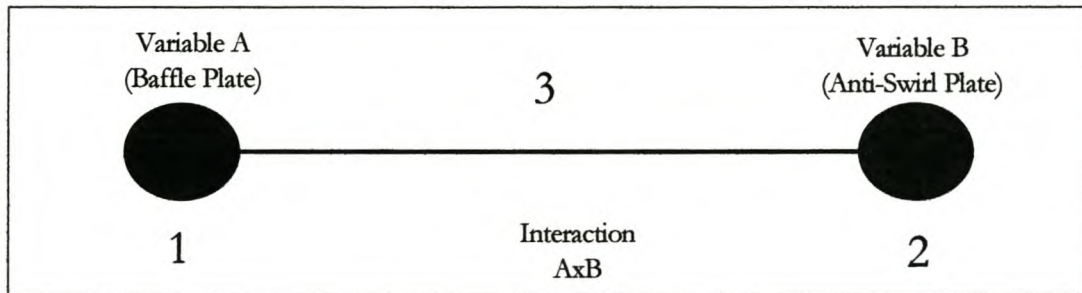


Figure 6-4: Linear Graph of $L_4(2^3)$ Orthogonal Array

The orthogonal array, $L_4(2^3)$ was found to be most suitable and enabled two variables and their interaction to be investigated in four experiments.

6.3.4. Assigning Variables to the Array

In order to avoid confounding between the main effects that are being investigated and the interactions that are also being investigated, it is important that the correct columns are used for the correct variables and interactions. In more complex investigations than the one shown here the assignment of the main effects and the interactions is very important such that there is no significant aliasing of effects. Recognising interaction columns [Logothetis 1992] can become tricky, especially for multi-level control

variable investigations. For two level investigations the interaction column is simply the product of the signed orthogonal array for the two factors involved. For larger 2 level investigations interaction tables can be used to simplify the process of assigning the variables to columns.

Case Study One:

Using Table 6-2 and substituting the 2's with -1's we get Table 6-3. Column one and two represent the baffle plate and the anti-swirl plates respectively with plus one representing its inclusion and minus one representing the plate's exclusion.

Table 6-3. Signed $L_4(2^3)$ Orthogonal Array

$L_4(2^3)$
Matrix

Level	Var1	Var2	Var3
1	+1	+1	+1
2	-1	-1	-1

Experiments

Test	Var1	Var2	Var3
1	+1	+1	+1
2	+1	-1	-1
3	-1	+1	-1
4	-1	-1	+1

The third column is the interaction column and is the product of the first two columns. Taguchi devised an easy way to recognise two way interactions between columns using triangular interaction matrices. This design, due to its simplicity, does not have a triangular interaction matrix. This was discussed in more detail in Chapter 5.2.7. Substituting the plate positions for the levels, Table 6-4 is produced and the experimental matrix complete.

Table 6-4. Case Study One Orthogonal Array

$L_4(2^3)$
Matrix

Level	Baffle Plate	Anti-Swirl Plate	Interaction
1	in	in	+1
2	out	out	-1

Experiments

Test	Baffle Plate	Anti-Swirl Plate	Interaction
1	in	in	+1
2	in	out	-1
3	out	in	-1
4	out	out	+1

6.4. Conducting the Experiment

Planning is essential for a successful experiment and therefore it is necessary to complete preparations thoroughly before commencing with the experimentation.

6.4.1. Developing the Test Plan

The test plan should be completed before experimentation commences to avoid any changes needing to be made during testing that could result in external noise from distorting the data.

Case Study One:

The test plan was to initially get a base line of best possible performance with the best possible air flow without restrictions. This was done with no carburettor adapter as the air flow would be unimpeded and performance the best. The baseline of the present carburettor adapter was then measured in order to have a comparison against which to measure the performance of the prototype carburettor adapter. Repeat tests before and after the experimental design were planned as well as a number of repeats within the matrix to determine confidence in the test results. All the tests were performed with the standard feed pipe and the standard air filter. The tests comprised of a range of speeds from which the TEP and MRT values were extracted for analysis.

6.4.2. Preparation and Co-ordination

Thorough preparation of persons and equipment needed for the experimental runs ensures smooth experimentation and reduces the chances of noise distorting the response data.

Case Study One:

The university, using CAD/CAM system and equipment, made the prototype adapter prior to the testing. A wax model was manufactured in a CNC machine and then covered with carbon fibre cloth and resin. The model was then heated so that the wax melted leaving the carbon fibre shell. This shell was then slightly modified to be able to accommodate the two flow diverters.

In the carburettor adapter investigation there were a number of preparations that needed to be made to ensure that the experimentation ran smoothly once it commenced.

- Test sheets were required for recording data that was not electronically recorded.
- Sufficient fuel was required for all the tests to ensure that there would be no variation in the fuel used for the tests (constant fuel conditions).
- Sufficient hard drive space was required to store all the electronic data from the tests.
- Sufficient CO meter filter paper was required for replacement of the fouled filter paper as per the operating instructions.

- Sufficient time was required to complete the tests before support services would be unavailable for use (reduced water pressure, test cell ventilation, safety regulations). All the testing thus had to be planned for and completed during office hours.

Rarely will the experimentation go exactly according to plan but by thorough planning there will be a minimum of interruptions and ensure the best chances of experimental consistency and success.

6.4.3. Performing the Experimental Runs

Only once all preparations are complete should experimentation commence. The entire experimental structure should be completed with as few breaks in testing as possible to avoid unnecessary external noise generated by changing environmental conditions. For experiments where there are many configurations, and the testing takes a long time, it is possible to block the configurations. Blocking of the experiments was done by performing the experiments in orthogonal sets. The inter block variance can then be investigated and quantified after experimentation.

Case Study One:

Testing was undertaken according to the experimental plan. It was apparent from the first test that was undertaken that the engine was over fuelled. Exhaust temperatures were very low and the CO%'s were very high. Based on this the fuel jets were changed for smaller ones and the test rerun. This test was then repeated at the end of the experimental procedure to determine the repeatability of the test runs and to determine if there was any drift in the results. Throughout the test programme selected experiments were repeated to constantly monitor the experiment repeatability and to build confidence in the results. As there were only four experiments in the matrix it was not possible to block them. Results are given in Appendices B through F and summarised in Table 6-5.

Table 6-5. Test Results Summary

Test Number	Test 1	Test 2	Test 3	Test 4	Test 5	Test 6	Test 7	Test 8	Test 9	Test 10
Top End Power [kW]	68.8	67.0	65.0	65.4	64.6	66.9	66.7	58.7	60.9	67.1
Mid Range Torque [Nm]	171.0	166.3	157.6	155.6	155.9	157.7	159.5	142.5	145.8	166.4

Not all the experiments that were done were needed for the Taguchi Matrix. Averages of repeated runs were taken to form the Taguchi response matrix shown in Table 6-6.

Table 6-6. Taguchi Experiment Results Summary

Run Number	Baffle(A)	Anti-Swirl(B)	AXB	Test No	Power	Torque
1	in	in	1	6	66.90	157.70
2	in	out	2	4,5	64.95	155.75
3	out	in	2	7	66.70	159.50
4	out	out	1	8,9	59.80	144.15

6.4.4. Testing and Inspection

This involves checking the data and equipment to ensure that there is no external variance present that makes the test null and void. Reproducibility test should be analysed and the data checked for any outliers that are obviously incorrect and need to be retested. Any data manipulation needed to generate the final results should also be cross checked to ensure that there are no calculation errors that could result in incorrect trends being identified.

Case Study One:

The data and test procedure were tested for reproducibility by repeating the test points at the beginning and the end with identical configurations. The before and after tests, (tests 2 and 10) show a maximum difference of 2.3% in output across the entire engine speed range tested. The MRT (3200 rpm) and TEP (4800 rpm) variations were 0.54% and 0.21% respectively, as shown in Table 6-7.

Table 6-7 Before and After Repeatability Test

Engine speed	Test 2 - base3		Test 10 - 0827b		difference [Nm]		%	
	Power	Torque	Power	Torque	Power	Torque	Power	Torque
1600 rpm	24.25	143.77	24.34	144.97	0.09	1.21	0.36%	0.83%
2400 rpm	41.57	166.32	41.39	166.38	-0.18	0.06	-0.45%	0.03%
3200 rpm	55.27	164.92	55.70	165.82	0.44	0.89	0.78%	0.54%
4000 rpm	63.71	153.37	64.17	153.49	0.46	0.12	0.71%	0.08%
4800 rpm	66.98	130.74	67.12	133.82	0.14	3.08	0.21%	2.30%

A similar trend can be seen in Table 6-8 for the repetition of Configuration two. The maximum difference is 2.26% for the torque at an engine speed of 4800 rpm. The figures of interest however, MRT and TEP, have variances of 0.22% and 1.24% respectively.

Table 6-8. Configuration Two Repeated

Engine speed	Test 4 - 0812b		Test 5 - 0813		difference [Nm]		%	
	Power	Torque	Power	Torque	Power	Torque	Power	Torque
1600 rpm	24.04	140.35	23.90	142.26	-0.14	1.91	0.58%	1.34%
2400 rpm	39.34	154.78	38.56	153.68	-0.78	-1.10	2.03%	0.72%
3200 rpm	52.27	155.58	52.20	155.91	-0.07	0.34	0.14%	0.22%
4000 rpm	62.12	145.50	62.06	149.65	-0.05	4.15	0.08%	2.77%
4800 rpm	65.40	130.66	64.60	127.77	-0.80	-2.89	1.24%	2.26%

The repetition of configuration 4, the carburettor adapter without any inserts, shows a maximum variation of 4% for the torque at 4800 rpm. However, when we again look at the figures of importance, namely MRT and TEP we see variances of 2.3 % and 3.91%.

Table 6-9. Configuration Four Repeated

Engine speed	Test 9 - 0827a		Test 8 - 0818		difference [Nm]		%	
	Power	Torque	Power	Torque	Power	Torque	Power	Torque
1600 rpm	22.29	130.43	22.37	130.79	0.08	0.36	0.34%	0.28%
2400 rpm	36.01	142.54	35.09	139.34	-0.92	-3.21	2.61%	2.30%
3200 rpm	48.50	145.82	47.78	142.48	-0.72	-3.34	1.51%	2.34%
4000 rpm	59.66	142.55	58.70	139.99	-0.96	-2.56	1.64%	1.83%
4800 rpm	60.94	121.30	58.65	116.59	-2.29	-4.71	3.91%	4.04%

These two figures were used as the worst case for external variance and were used to establish error bars on the trend investigations. In more complex investigations a signal to noise ratio would have been used to this end. The error bars essentially represent the internal noise of the experimental apparatus.

6.5. Analysing the Experiment

The experimental analysis can be either tabular or graphical, both utilising the analysis of means (ANOM) method for identifying the trends. The tabular method shows the degree of change that can be compared across the variable range to identify strong and weak effects in numeric terms. The graphical analysis method shows the direction of the effect very clearly. The gradient of the line represents the degree of effect that the variable or interaction will have on the process.

For tabular analysis the output variable is averaged at each of the levels of a factor, i.e. for factor A, the output variable is averaged for all configurations where A was set at 1, and for all the experimental configurations where A was set at 2. The S/N ratio is determined in a similar fashion if it is determined. Plotting the graph of these values will indicate the significance of the input variable to the output variable. A flat graph will indicate little dependence while a steep graph will indicate a significant dependence.

6.5.1. Tabular Method

The tabular method of analysis takes the form of a table with the average values for each examined variable or interaction level. It is easy then to identify the highest value in each column in the table which then represents the optimum level for that variable. This is done with each of the response variables identified at the beginning of the investigation, namely top-end-power and mid-range-torque.

Case Study One:

Table 6-10 illustrates the optimum configuration for the TEP. The anti-swirl-plate inclusion results in a 4.4 kW improvement in TEP while the inclusion of the baffle plate results in a 2.7 kW improvement in the TEP. The table also indicates a strong interaction effect between the anti-swirl plate and the baffle plate, indicating that the effect should be investigated further.

Table 6-10: Top-End-Power Response Table

Level	Baffle(A)	Anti-Swirl(B)	AxB
1 (in)	65.9	66.8	63.4
2 (out)	63.3	62.4	65.8
difference	2.7	4.4	-2.5

Table 6-11 illustrates that the optimum configuration for the MRT is the same as for the TEP. Inclusion of the anti-swirl plate results in a 9 Nm improvement in the MRT while the inclusion of the baffle plate

results in an average improvement of 5 Nm. Table 6-11 also indicates a strong interaction effect, indicating that the effect should be investigated further.

Table 6-11: Mid-Range Torque Response Table

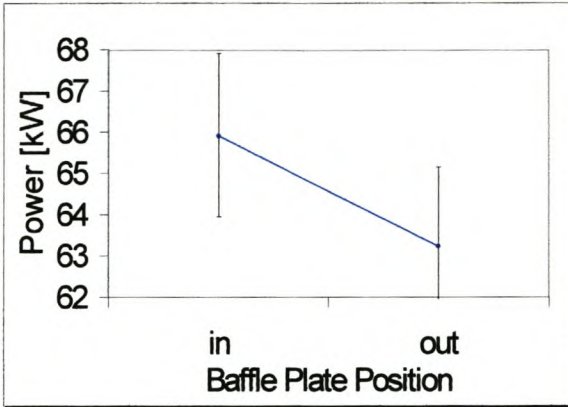
Level	Baffle(A)	Anti-Swirl(B)	AxB
1 (in)	157	159	151
2 (out)	152	150	158
difference	5	9	-7

6.5.2. Graphical Method

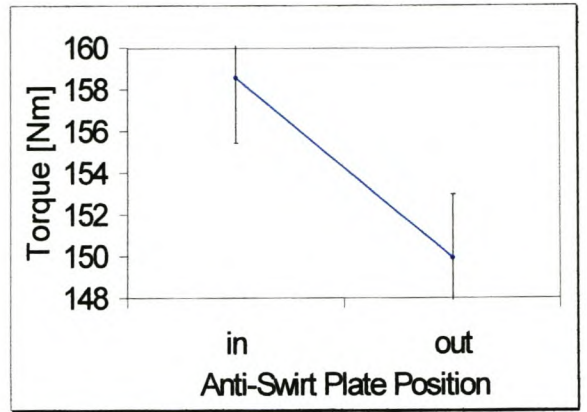
Level analysis graphs provide a graphical representation of the data shown in the tabular method.

Case Study One:

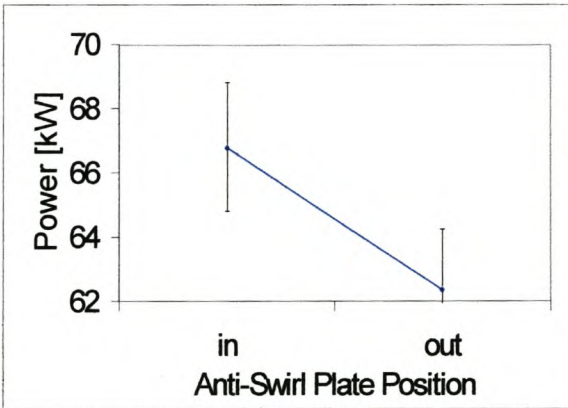
The graphs provide a visual representation of the results. The steepest gradient (biggest effect) is observed for the anti-swirl plates. The inclusion of both the anti-swirl plate and the baffle plate results in increased output for torque and power. It is helpful to include the experimental noise as error bars on the graphs to indicate the strength of the effect with respect to the magnitude of the noise. The error bars on the graphs are percentages as determined in the tabular analysis and repeatability analysis in section 6.4.4



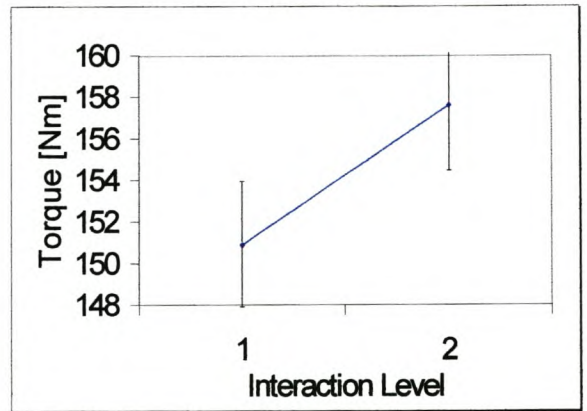
a



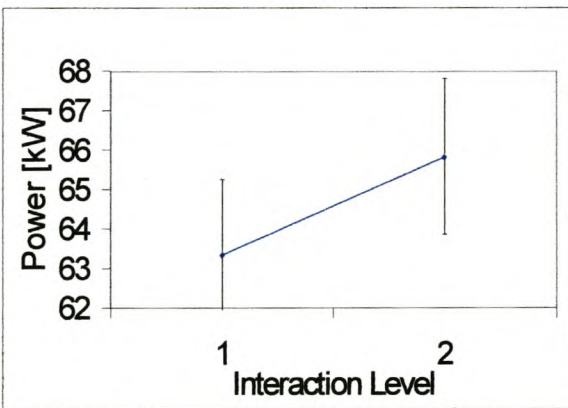
e



b

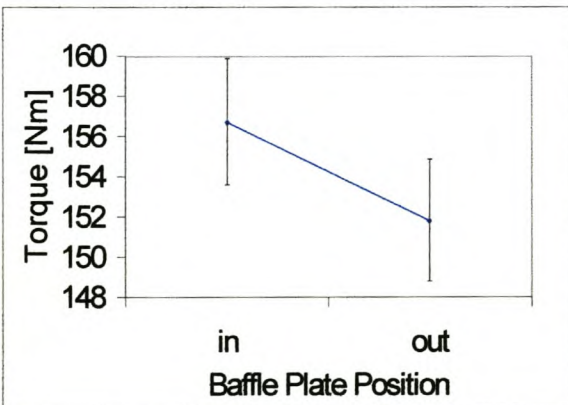


f



c

Figure 6-5 . Level Analysis Graphs for Case Study One. a, b and c are the power graphs for the baffle plate, the anti swirl plate and the interaction respectively. D, e, and f are the torque trends for the same.



d

6.5.3. Interaction Analysis

To be able to determine exactly what the interaction between the plates is, the interaction needs to be analysed using an interaction table. A graph representing the interaction can be drawn from the table to give a graphical representation of the interaction. The tables are calculated as averages of the data at each of the configuration indicated by the headings for the columns and rows. This is best illustrated by the case study.

Case Study One:

The top left number in Table 6-12 is the TEP from the configurations where both the anti-swirl plate and the baffle plate were inserted into the carburettor adapter and gives the highest output response.

Table 6-12. Top-End-Power Interaction Analysis

	Anti-Swirl In	Anti-Swirl Out
Baffle In	66.90	64.95
Baffle Out	66.70	59.80

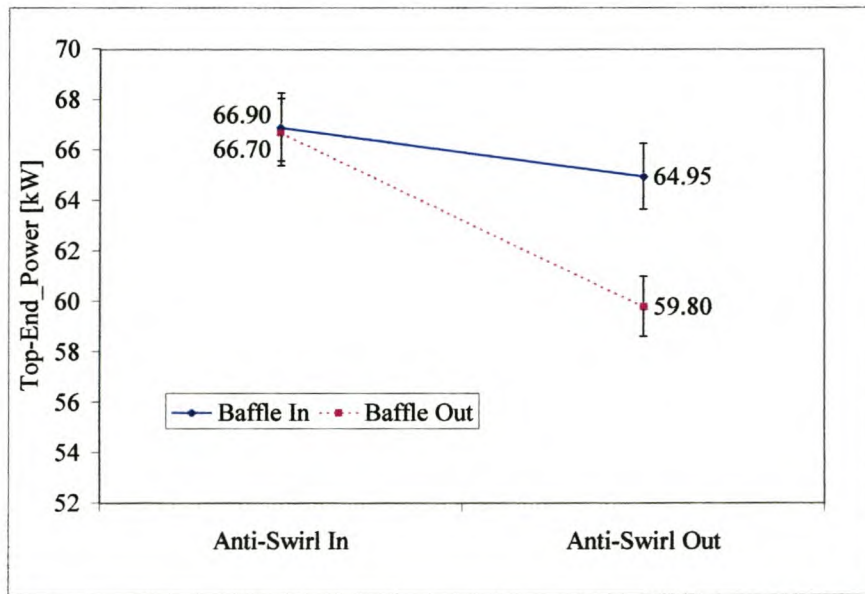


Figure 6-6. Top-End-Power Interaction Analysis

The graphical representation of the power interaction analysis table gives a good indication of the effect in the process. It is often easier to identify the interaction effects from the graphical representation and then quantify them from the tabular representation of the interaction.

Figure 6-6 shows that the effect of the baffle plate is small when the anti-swirl plate is inserted. When the anti-swirl plate is removed from the carburettor adapter, the baffle plate effect is much larger. The effect is that the TEP drops when the baffle plate is removed. The effect of the anti-swirl plate however is significant whether there is a baffle plate in or not. By referring to the tabular representation of the interaction we see that the magnitude of the drop is

$$64.95 \text{ kW} - 59.8 \text{ kW} = 5.15 \text{ kW.}$$

[6-10]

The mid-range-torque interaction analysis is done in the same manner as the top-end-power interaction analysis. The tabular investigation is done first and is shown in Table 6-13.

Table 6-13. Mid-Range-Torque Interaction Analysis

	Anti-Swirl In	Anti-Swirl Out
Baffle In	157.70	155.75
Baffle Out	159.50	144.15

The graphical form of the table is constructed for a more visual effect and to allow for the easy identification of significant interactive effects.

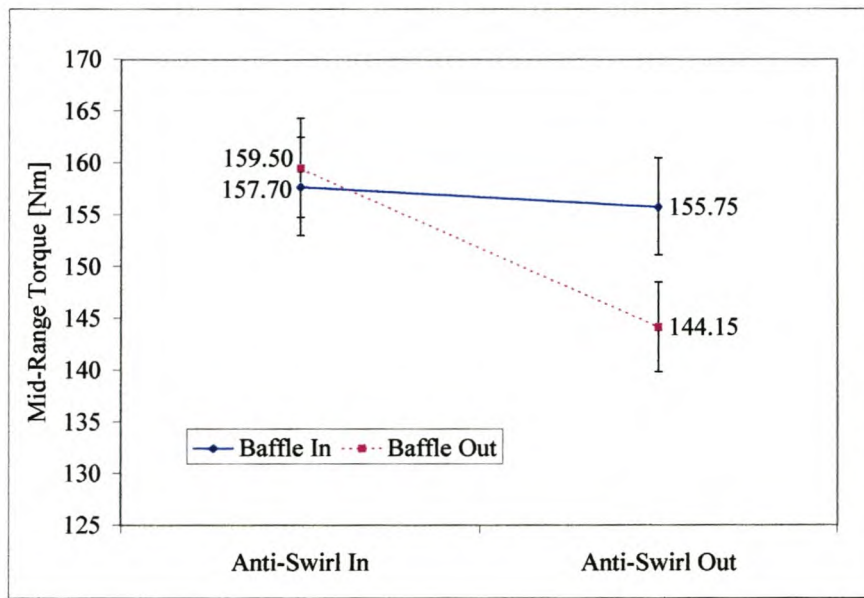


Figure 6-7. Mid-Range-Torque Interaction Analysis

The graph and table show that the baffle plate has a significant effect on the mid-range-torque when the anti-swirl plate is removed from the carburettor adapter. The magnitude of the change is calculated from Table 6-13 as:

$$155.75 \text{ Nm} - 144.15 \text{ Nm} = 11.6 \text{ Nm}$$

[6-11]

However when the anti-swirl plate is inserted into the carburettor adapter then the trend is reversed. The MRT is decreases with the insertion of the baffle plate by 1.8 Nm. This amount is not larger than the error bars but it is a significant finding.

The interaction effect is a negative one in both the TEP and MRT cases. The effect of inserting one of the plates results in a decrease in the effect of inserting the other plate.

6.5.4. Identifying The Strong Effects and the Optimum Levels

The graphs and the tables in the section above are used to determine the significant variables and their optimum level setting.

Case Study One

Based purely on a level analysis of the main effects the TEP and MRT indicate the optimum configuration is with the inclusion of both the baffle and the anti-swirl plates. The interaction is deemed important in both cases, both for the magnitude of the interaction and the fact that it is negative interaction (including one plate decreases the effect of including the other) (Table 6-14).

Table 6-14. Significant Effects

Significant Factors	
Baffle plate	Yes
Anti Swirl Plate	Yes
Interaction	Yes

Based on the further investigation of the interaction effects however, it was seen that the for MRT this is not the case. The interaction investigation shows that the maximum output is actually achieved when the baffle plate is excluded and the anti-swirl plate is included in the carburettor adapter (Table 6-15).

Table 6-15. Optimum Level Settings

	TEP	MRT
Baffle plate	Included	Excluded
Anti Swirl Plate	Included	Included

It must be noted that the TEP inclusion of the baffle plate is based on a 0,2kW difference. The implications of this are discussed later in the chapter.

6.5.5. Prediction Equation

It is important to check both the level effect as well as the S/N ratio in a design for robustness. More often than not, a trade off will have to be made on a variable where the optimum level for the output variable will be different to the optimum level for the S/N ratio. The designer will have to determine which of the effects is more beneficial to the process/product and use that setting.

The prediction equation is calculated by adding the effects of each of the strong variables and interactions to the average of all the experiments (experimental average). When an interaction is included as a significant effect and the sum calculated, the main effects of the two variables in the

interaction need to be subtracted. The reason for subtracting the individual effects of the variables in the interaction is that the interaction effect is comprised of the main effects of the variables involved as well as the interaction effect itself. If the individual effect of the two factors are not subtracted they will be mistakenly included. Even if one of the variables in the interaction are not considered significant, its effect must be subtracted from the interaction effect.

Case Study One:

In this case study there was no S/N ratio investigation included as the focus was on controlling the level of the output variable and not its variance. Only a level analysis prediction equation can therefore be calculated. The experimental average for the power output variable is defined as the average output of the system irrespective of the variable level settings and it is calculated for the top-end-power as:

$$\overline{TEP}_{avg} = \frac{66.9 + 64.95 + 66.7 + 59.8}{4} = 64.59kW \quad [6-12]$$

and for the mid-range-torque as:

$$\overline{MRT}_{avg} = \frac{157.7 + 155.75 + 159.5 + 144.15}{4} = 154.28Nm \quad [6-13]$$

The prediction equation for TEP shown in equations 6.14 and 6.15 and for MRT in equations 6.16 and 6.17 where BF stands for baffle plate and ASP stands for anti-swirl plate. The subscripts indicate the plates inclusion (in) and exclusion (out).

$$\begin{aligned} TEP_{pre} = & \overline{TEP}_{avg} + (\overline{BP}_{in} - \overline{TEP}_{avg}) + (\overline{ASP}_{in} - \overline{TEP}_{avg}) \\ & + [(\overline{BP}_{in} \overline{ASP}_{in} - \overline{TEP}_{avg}) - (\overline{BP}_{in} - \overline{TEP}_{avg}) - (\overline{ASP}_{in} - \overline{TEP}_{avg})] \end{aligned} \quad [6-14]$$

$$\begin{aligned} TEP_{pre} = & 64.59 + (65.93 - 64.59) + (66.8 - 64.59) \\ & + [(66.9 - 64.59) - (65.93 - 64.59) - (66.8 - 64.59)] \\ = & 66.9kW \end{aligned} \quad [6-15]$$

$$\begin{aligned} MRT_{pre} = & \overline{MRT}_{avg} + (\overline{BP}_{out} - \overline{MRT}_{avg}) + (\overline{ASP}_{in} - \overline{MRT}_{avg}) \\ & + [(\overline{BP}_{out} \overline{ASP}_{in} - \overline{MRT}_{avg}) - (\overline{BP}_{out} - \overline{MRT}_{avg}) - (\overline{ASP}_{in} - \overline{MRT}_{avg})] \end{aligned} \quad [6-16]$$

$$\begin{aligned} MRT_{pre} = & 154.28 + (151.83 - 154.28) + (158.6 - 154.28) \\ & + [(159.5 - 154.28) - (151.83 - 154.28) - (158.6 - 154.28)] \\ = & 159.5Nm \end{aligned} \quad [6-17]$$

6.5.6. Confirmation Experiment

The confirmation experiments were included in the initial analysis and found to have outputs exactly as the prediction equation had estimated.

Only through the investigation of the interaction effects did the correct analysis emerge. Two confirmation experiments were needed for this investigation, one for TEP and one for MRT. The two predicted optimums were different and therefore a decision needs to be made as to the global optimum that will be chosen for the system. TEP shows a small difference in value for the two possible configurations and therefore only a small amount of power would be sacrificed if the non-optimum is chosen. MRT however has a more significant difference between the two possible optimum configurations. It is pertinent to note that the MRT optimum is also without one of the inserts and therefore the manufacture of such a carburettor adapter would possibly be easier and cheaper. The chosen optimum is therefore the optimum for the MRT, namely with the baffle plate excluded and only the anti swirl plate in the adapter.

The analysis of the CO% and the exhaust gas temperatures is given in appendix G although no useful information was gleaned from their analysis.

Chapter 7. Case Study One – Traditional Methods vs Taguchi Methods

7.1. Introduction

This chapter examines the Taguchi method used to solve the design problem encountered in Chapter Six and compares the method and results to a conventional method of analysing the data and solving the problem that would otherwise have been used in the absence of the Taguchi Method.

There were four possible combinations of variables and levels in which the carburettor adapter could have been tested. This is the same number as required by the chosen orthogonal array for the Taguchi optimisation process. The Taguchi process can therefore be compared directly with the traditional experimental process without any further experiments. The Taguchi Method was applied to the carburettor evaluation Case Study in Chapter 6. In this chapter a traditional approach is applied to the evaluation of the carburettor adapter and then the results of both methods compared. It must be suggested that Chapter 6 be a prerequisite to this chapter to aid in the understanding.

7.2. Traditional Experimental Method

The term traditional experimental methods refers to the method that is currently used in the investigations. The statistical experimental design methods usually used result in too many experiments to make them feasible. Traditional experimentation methods require the comparison of two tests where only one parameter at a time is varied. The effect of that varied parameter can then be quantified and tested further to determine the optimum level or value for that parameter. This type of investigation relies largely on the experiment designer's knowledge and intuition as to the correct order in which to do the testing, so as to minimise the number of tests needed in determining the trends and optimum settings.

The set of experiments is evaluated as would have been done without Taguchi's Methods. Conclusions are drawn from the available data and presented in table form in Appendices B through F. All possible combinations of the inserts in the carburettor were tested as well as tests of the open configuration (without a carburettor adapter in place) and of the carburettor adapter currently in use.

7.3. Traditional Experimental Analysis

7.3.1. Torque Comparison

The torque data is plotted against engine speed in Figure 7-1.

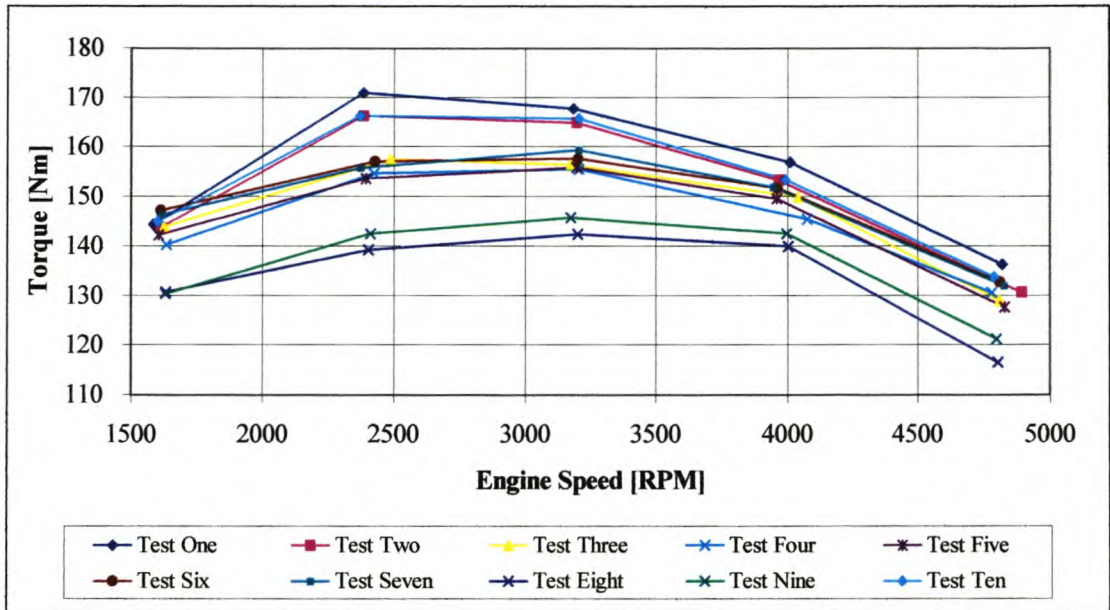


Figure 7-1. Torque Output Comparison

Three distinct groups emerge in the torque output comparison graph in Figure 7-1 (details of the configurations are given in Appendices B and E). The top group, with the highest outputs, are those tests where there is no carburettor adapter or air filter connected to the carburettor (tests one, two and ten). The large jets used in test one expectedly give the most torque due to increased fuelling. Test two and the repeatability test, test ten with the smaller carburettor main jets, have a slightly lower performance. This is as expected since there is no filter, no feed pipe, and no adapter to restrict airflow. The fuel consumption for this group of tests is also higher than the middle body of the tests. As illustrated in Table 7-1 (9 - 20 vs 7 - 19 hg/hr).

Table 7-1. : Fuel Consumption [kg/hr]

Test Number	Test 1	Test 2	Test 3	Test 4	Test 5	Test 6	Test 7	Test 8	Test 9	Test 10
1600 rpm	9.67	9.70	7.73	7.61	7.63	7.61	7.58	6.98	6.83	9.18
2400 rpm	13.68	13.41	11.63	11.46	11.39	11.65	11.19	10.07	10.06	13.16
3200 rpm	16.45	15.93	14.24	14.35	14.47	14.92	14.60	12.79	12.90	15.49
4000 rpm	18.92	17.52	19.50	17.92	17.46	17.89	17.44	15.09	15.58	17.18
4800 rpm	20.94	19.72	19.92	19.77	20.03	19.53	18.84	16.71	16.75	19.11

The group with the lowest torque is that of the empty/open prototype carburettor adapter with no inserts (tests eight and nine). The trend in the graph is as expected but the graph is shifted down approximately 10 Nm. The fuel consumption for this group is much lower (approximately 6 - 16 kg/hr vs 7 - 19 hg/hr) (Table 7-1) than for the other tests. The tests results for the different carburettor adapter inserts lie in between these two groups.

7.3.2. Power Comparison

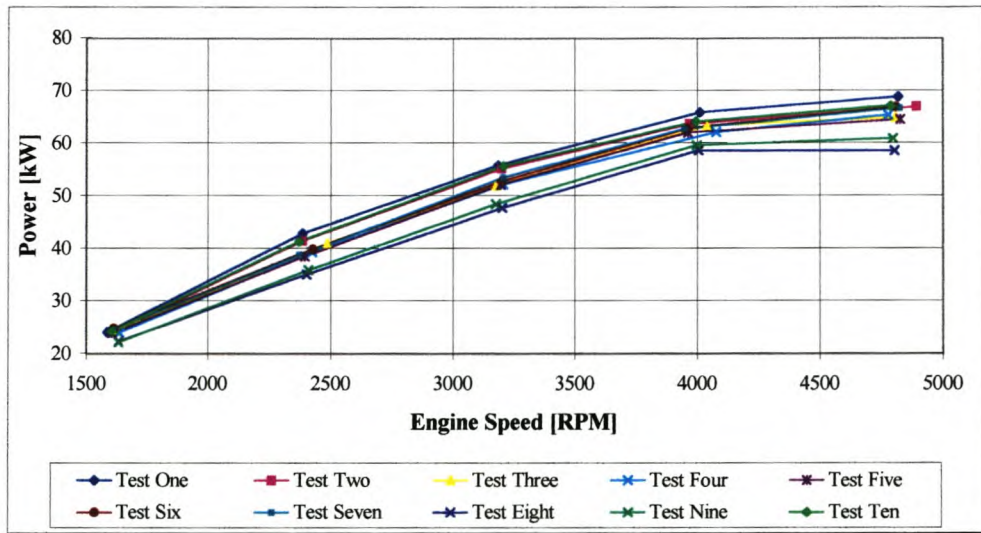


Figure 7-2. Power Output Comparison

The power output comparison curves (Figure 7-2 and Appendix F) follow the same trends as the torque output comparison curves. Three tests stand out at the top (tests one, two, and ten, all with no carburettor adapter) and two are lower (tests eight and nine, both empty carburettor adapter tests) with the rest of the tests bundled together in the middle. The values are difficult to compare due to the proximity of the lines.

7.3.3. Top-End-Power and Mid-Range-Torque Comparison

The power (TEP) and torque (MRT) data of interest are compared in Figure 7-3 for the different experimental configurations.

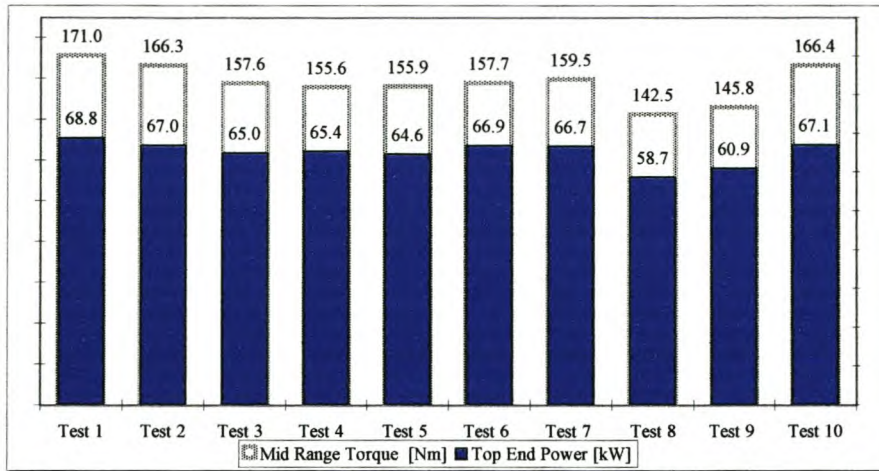


Figure 7-3. Top-End-Power and Mid-Range-Torque Comparison of all Tests

By omitting the no adapter configuration tests numbers one, two and ten and the baseline test three, a comparison can be drawn for the prototype carburettor adapter configurations. It can be seen from Figure 7-4 that tests six and seven are clearly the best configurations as per the considerations of Top-End-Power and Mid-Range-Torque. These tests are the prototype carburettor adapter with a baffle plate and an anti-swirl plate (test six) and the prototype adapter with only an anti swirl plate and no baffle plate (test seven).

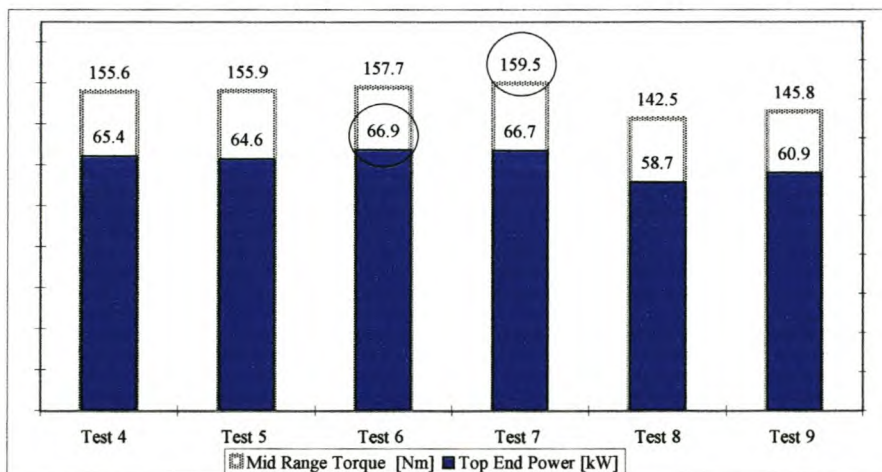


Figure 7-4. TEP and MRT for Prototype Carburettor Adapter Taguchi Investigation

7.3.4. Discussion

From a pure **performance** point of view, the prototype carburettor adapter with the anti-swirl plate and the baffle plate (test six), and test seven with the anti-swirl plate but without the baffle plate, result in the highest TEP and MRT respectively. The question is whether or not to include the baffle plate in the final optimum configuration. The configuration including the baffle plate results in lower low-end-torque but a higher mid-range-torque with top-end-torque approximately the same (see Figure 7-1).

No decision could be made based on the power output curve due to the close proximity of the tests. Fuel distribution for the two tests (test 6 and test 7 as above) is very similar (Table 7-1). From a production point of view, leaving out the baffle plate would result in an easier to manufacture design. Test 7 would therefore be the better choice with only the anti-swirl plate included. The CO% and the exhaust gas temperature analysis yields no further information (Appendices C and D).

7.4. Experimental Evaluation Method - Conclusion

The results of the traditional method are very intuition based while the Taguchi method provides sound reasoning for the choices made. Structured analysis of the interaction and a better understanding of the effect of each of the inserts is achieved with the Taguchi Method. The traditional method did find the same optimum but without adding to the understanding of the system and the effects within it.

Chapter 8. Case Study Two - Optimisation

8.1. Project Background

This project should ideally have been undertaken before Case Study One. However, due to the newness of the Taguchi Method of experimental design to the group, this was not possible. Following the success of, and experience gained from Case Study One, it was decided to use Taguchi Methods to evaluate all the carburettor adapter dimensions simultaneously, rather than the traditional approach used in determining the carburettor adapter dimensions for Case Study One. In this way the method would show its strengths by adding to the knowledge of the system, as well as substantiating the previous work done and highlighting the significance of the interactive effects.

8.2. Traditional Experimental Methods

As indicated previously, traditional experimentation methods require the comparison of two tests where only one input variable is varied at a time. The effect of that input variable can then be quantified and tested further (if necessary) to determine its optimum position. This type of investigation relies largely on the experiment designers knowledge and intuition as to the correct order in which to optimise parameters.

The application of Taguchi methods used in this case study cannot be compared to the traditional method using the testing that was done during the investigation. The experimental matrix dictating the configurations to be tested is too varied and cannot be analysed any way other than as specified by Taguchi Methods level analysis (i.e. statistically).

8.3. Taguchi Method

The experiment was planned and analysed using the Taguchi Method of experimental design. The description of each section/is not included as it was for Case Study One. Only the results are presented. Where necessary however some form of explanation is presented to aid in the explanation of the investigation.

8.4. Planning the Experiment

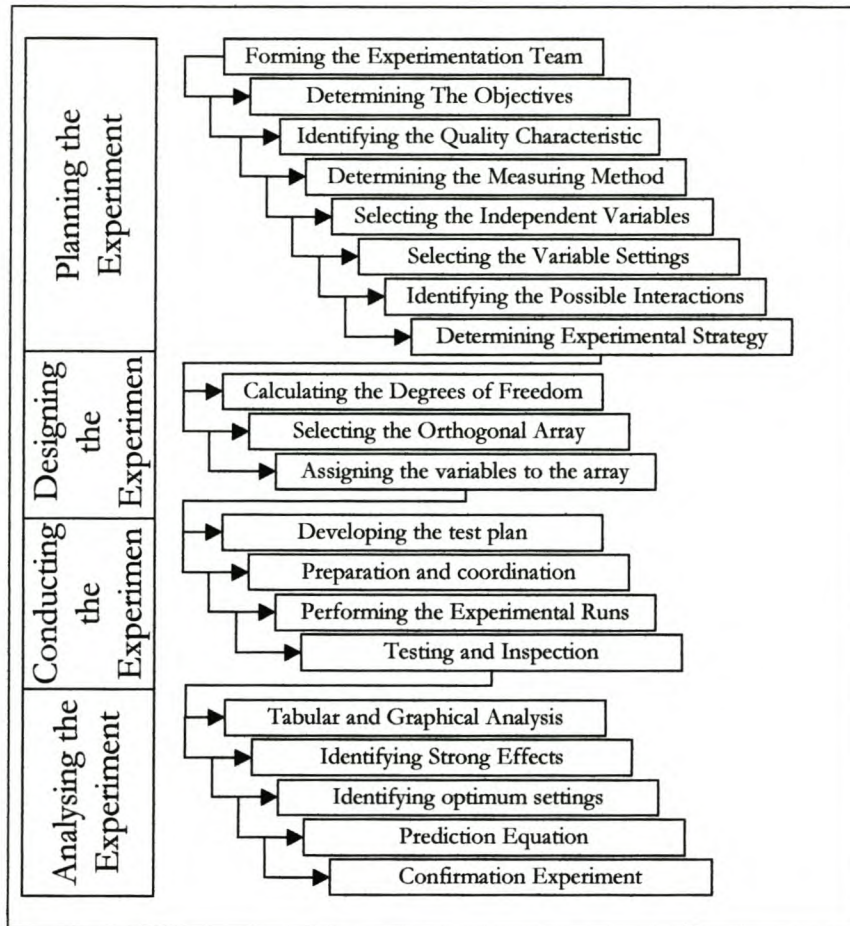


Figure 8-1. Taguchi Methodology

8.4.1. Experimentation Team

Team leader:	Jeremy Green
Management Support:	Dr Andrew Taylor
Technical Support:	Benn Vincent + SMD

8.4.2. Problem Statement: Determining the Objectives

In this case study the objective was predefined as:

- To determine the optimum dimensions for a carburettor adapter and the piping between the air filter and the carburettor adapter.

8.4.3. Identifying the Output Variable

Determining the output variable for such an investigation was complicated by the fact that there were a number of variables that needed to be kept in mind, all of which could be used to determine engine performance, and that all needed to be optimised.

The fuel distribution across the cylinders is very dependent on the flow patterns in the carburettor and is one of the variables that needed investigation. The fuelling distribution can be gauged by one of two other parameters. The CO% in the exhaust gases gives an indication of the degree to which the petrol was burnt. A lean engine with excess air will give a lower CO % (0-2%) compared to a rich engine where the excess fuel will result in a higher CO% (6-7%). A comparison of the CO% levels in the different exhaust cylinder pipes allows for the evaluation of the fuel distribution. Another indication of the fuel distribution between the cylinders is the exhaust temperatures. A lean running engine will result in a higher exhaust temperature than a rich running engine. Both of these variables can be evaluated in terms of an average value and the variance across the four cylinders, to characterise the variation in fuelling that occurs across the cylinders.

Engine performance however can never be ignored in favour of the above two variables, therefore torque, power and specific fuel consumption (SFC) are also used as output variables in the investigation. Mid-range-torque (MRT) and top-end-power (TEP) (as defined in Case Study One) both need to be maximised while the SFC optimum will be a minimum..

8.4.4. Determining the Measuring Methods

The measurement methods needed little determination as the testing procedure for internal combustion engines is a standard procedure at CAE. The equipment that was used in the test is discussed below and in Chapter Three.

The engine that was used in the investigation was a 2 litre, 4 cylinder, engine. It was not in the standard configuration as substantial development had already been completed on the engine by the university. The altered components of the engine included a modified stainless steel inlet manifold and a prototype cylinder head. A prototype low back pressure exhaust was used on a standard exhaust manifold.

The engine was mounted on a standard test bed and connected to a Froude water dynamometer for the control and performance measurement. Data capture was done with ETA (Engine Test Automation) software developed by the CAE. A Bosch CO metre and four gas analyser was used to monitor the CO% and other emission gases such as HC, CO₂ and O₂.

The carburettor adapter simulator (named "Bird-cage" due to its appearance) used in previous test work [Petzer 1996] was used again in this test work. It consisted of two large disks (400mm diameter) forming the top and bottom of the carburettor adapter. The bottom disk had a circular hole cut in the middle through which the carburettor was fed. The plenum walls (1mm galvanised sheeting) were inserted into the area between the plates to form the plenum chamber of variable dimensions. The structure was clamped together by 12 M6 threaded rods. The plenum was connected to the feed pipes by a diffuser which was designed not to provide any pressure reclaiming by changing the kinetic energy of the gas into pressure energy (the diffuser design is discussed briefly in Section 8.6.2). The diffusers and plenum

volumes were all prefabricated to make interchanging them easy during testing. In all, 9 diffusers, and 9 plenum volumes were manufactured for the tests.

8.4.5. Selecting The Independent Variables

The factors that were to be investigated were prescribed at the project conception as:

- Diameter of the carburettor adapter.
- Height of the carburettor adapter.
- Diameter of the feed-pipe.
- Length of the feed-pipe (including the diffuser length).

8.4.6. Selecting the Variable Levels

Before determining the variable levels it was necessary to determine the number of levels to be used for each variable. A two level investigation would identify the main effects but would not indicate whether the relationship of the input variable to the output variable was linear or quadratic. Much of the information for the selection of the levels was based on preliminary investigation by Petzer [1996], and undocumented work by Petzer and Green.

8.4.6.1. Feed-pipe diameter

The standard feed pipe of the engine was 70 mm in diameter. The size of the diffuser that would be required for an increased feed pipe diameter lead to the decision to investigate smaller feed pipe diameters. The gas velocities in the larger pipe would be lower than the standard pipe and would necessitate a larger exit area from the diffuser to the plenum chamber. This would result in the minimum plenum diameter being very large to ensure that it was equal to or greater than the largest diffuser exit width needed. The other two levels were therefore chosen as 60 mm and 50 mm.

8.4.6.2. Feed-pipe length

The standard settings for the feed-pipe (600 mm long and 70 mm diameter) were used as the starting point. Due to possible adjustments to other engine structures, the engine could accommodate a length of 670 mm. A third level 530 mm was chosen to complete the three levels.

8.4.6.3. Carburettor Adapter Height

The relationship between carburettor height and torque and power for an infinite diameter carburettor adapter was developed by Petzer [1996] and is shown in

Figure 8-2. Torque is at an optimum between heights of 40 mm and 55 mm. The effect of reducing the diameter to a finite value was expected to throttle the flow. The additional height levels investigated therefore had to be greater than 40 mm to counter the throttling effect. The possibility of having a chamber height of 30 mm (to include the power peak Petzer identified) was investigated from a geometrical point of view. It was, however, found to be infeasible due to the large diameter plenum that would be needed to match the diffuser from a 70 mm diameter feed-pipe. The throttling effect of the finite diameter was expected to increase the optimum height and therefore starting at 40 mm was deemed sufficient.

Figure 8-2 shows a drop in MRT above 55 mm. The upper height for the carburettor was therefore chosen to be 60 mm. The third level was chosen at 50 mm between the upper and lower limits identified.

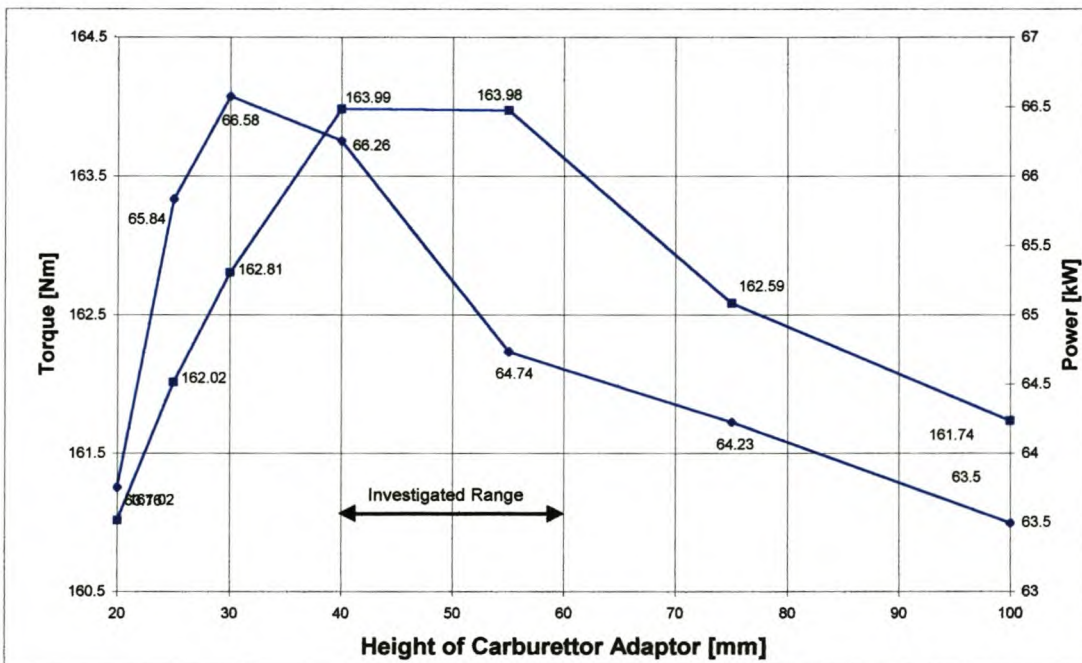


Figure 8-2 MRT and TEP vs Carburettor Height for an Infinite Diameter [After Petzer 1996]

8.4.6.4. Carburettor Adapter Diameter (Plenum Diameter)

The diffuser width at the junction to the plenum was the limiting factor in the choice of the plenum diameter. The largest diffuser width needed to be equal to, or smaller than, the smallest plenum diameter to ensure that the diffuser would fit into the plenum. The carburettor adapter diameter was determined from the volume data accumulated by Petzer [1996] shown in Figure 8-3. The data shows the performance of the tests engine at two plenum heights of 25 mm and 40 mm, and at diameters of 124 mm, 186 mm, 250 mm, and 310 mm. They are compared on a volume basis.

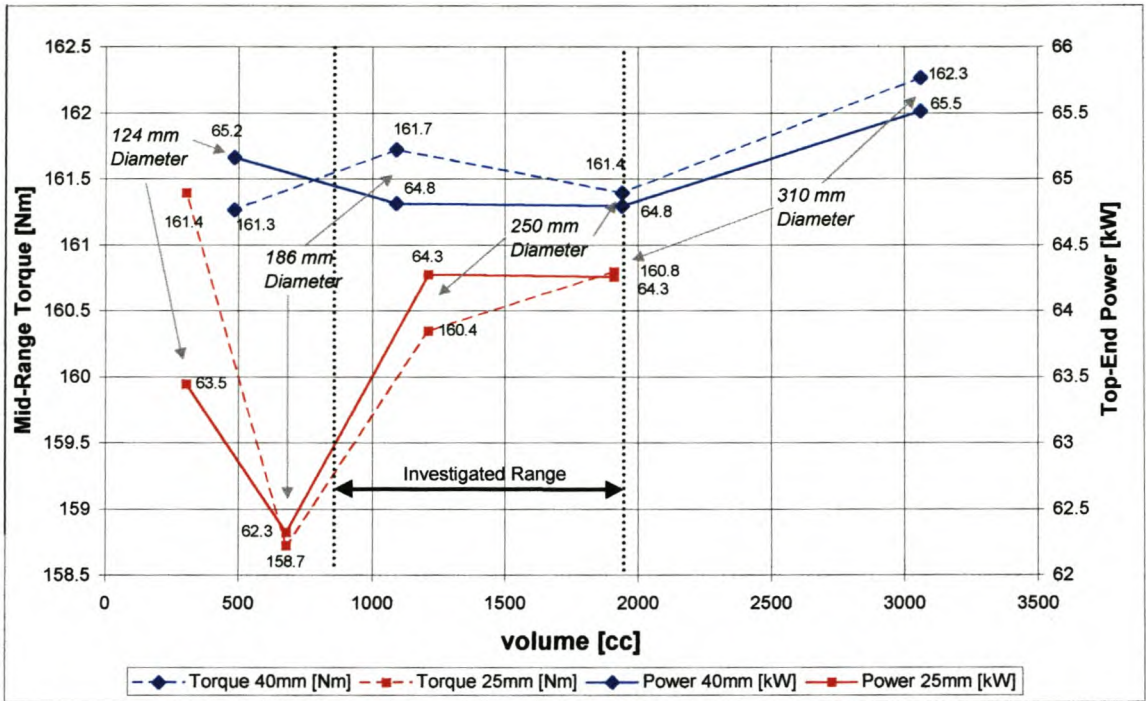


Figure 8-3. TEP and MRT vs Plenum Volume [from Petzer 1996]

The minimum diameter chosen was 161 mm which was the greatest width needed by the diffuser intersection with the carburettor adapter. The additional two levels were chosen around the power peak seen at 1200cc in Petzers results (Figure 8-3).

8.4.7. Identifying Possible Interactions

Interactions were not deemed necessary in the preliminary experimental design, investigating only the main effects. These could be investigated after the experiment with the aid of interaction graphs if deemed necessary. Table 8-1 shows the choice of levels for the birdcage investigation.

Table 8-1. Level Settings for Birdcage Configurations

Level	Feed Pipe Φ	Length	height	Plenum Φ
1	50	530	40	161
2	60	600	50	180
3	70	670	60	200

8.5. Designing the Experiment

8.5.1. Calculating the Degrees of Freedom

There are three levels for each variable and 4 variables in the investigation. 8 DOF's are therefore needed to investigate the main effects. To investigate a single interaction 4 DOF's are needed. There are however no interactions planned for the investigation therefore 8 DOF's are needed in total.

8.5.2. Selecting the Orthogonal Array

The orthogonal array chosen must have at least as many DOF's as there are in the experiment. In this case there are eight DOF's in the experiment so the orthogonal array must have at least eight DOF's. All the variables have three levels in them and therefore the orthogonal arrays available for use are $L_9(3^4)$, $L_{18}(2^1 \times 3^7)$ or $L_{27}(3^{13})$ any higher than this and the number of experiments is excessive (>27). The number of DOF's of the $L_9(3^4)$ orthogonal array is

$$4 \times (3 - 1) = 8 \quad \text{DOF's} \quad [8-1]$$

The number of DOF's in the $L_{18}(2^1 \times 3^7)$ orthogonal array is

$$1 \times (2 - 1) + 7 \times (3 - 1) = 15 \quad \text{DOF's} \quad [8-2]$$

The number of DOF's in the $L_{27}(3^{13})$ orthogonal array is

$$13 \times (3 - 1) = 26 \quad \text{DOF's} \quad [8-3]$$

It would appear that the $L_9(3^4)$ array is most suited for the experimental matrix. The interactions between columns one and two however are confounded with columns three and four. Figure 8-4 shows the linear graph for the $L_9(3^4)$ orthogonal array. The interaction between columns one and two is spread over columns three and four.

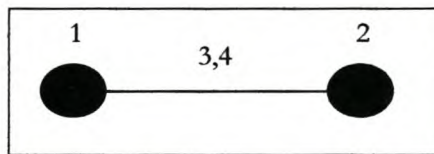


Figure 8-4. Linear Graph of $L_9(3^4)$

Therefore unless one can be sure that there is no interaction between the first two variables, it is wise not to use this matrix. The $L_{18}(2^1 \times 3^7)$ orthogonal array is a specially designed array where there is no confounding of the columns. The linear graph is shown in Figure 8-5.

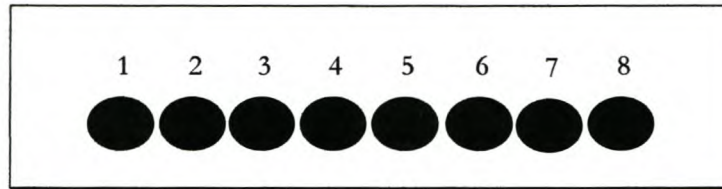


Figure 8-5. Linear Graph of $L_{18}(2^1 \times 3^7)$

The interactions of all the three level columns are more or less evenly spread across all the other three level columns. It is therefore possible to investigate main effects without the interactions confounding them. The additional DOF's will not be wasted as the additional variables can be used to block the experiment into three blocks and the “free” columns can be used as variance checks. These dummy variables should have no trends (be a flat line) as the columns do not represent any variable or other source of variance. If a trend is apparent, it will be representative of the natural variance in the testing method and procedure.

8.5.3. Assigning Variables to the Array

As all the variables were tested at three levels, the first column (two levels) was not used for the input variables, but as an indication of the inherent noise of the experiment and possible random variation in the test method and apparatus. Columns two through five were used for the input variables. Variable six was used as a blocking variable to divide the experiments into three blocks of experiments that could be each completed one a day. The test work could then be completed in three days of experimenting. The experimental variation (uncontrollable variables and noise) as a result of the different days of testing could then be evaluated. Columns seven and eight were used as dummy variables for the same purpose as column one, to determine the level of random variation/noise in the system. The resulting orthogonal test matrix is shown in Table 8-2.

Table 8-2. Orthogonal Array with Assigned Variables and Levels

$$L_{18}(2^1 \times 3^7)$$

Matrix

Level	Var1	Feed Pipe Φ	Length	height	Plenum Φ	Block	Var7	Var8
1	1	50	530	40	161	1	1	1
2	2	60	600	50	180	2	2	2
3	-	70	670	60	200	3	3	3

Experiments

Config	Var1	Feed Pipe Φ	Length	height	Plenum Φ	Block	Var7	Var8
1	1	50	530	40	161	1	1	1
2	1	50	600	50	180	2	2	2
3	1	50	670	60	200	3	3	3
4	1	60	530	40	180	2	3	3
5	1	60	600	50	200	3	1	1
6	1	60	670	60	161	1	2	2
7	1	70	530	50	161	3	2	3
8	1	70	600	60	180	1	3	1
9	1	70	670	40	200	2	1	2
10	2	50	530	60	200	2	2	1
11	2	50	600	40	161	3	3	2
12	2	50	670	50	180	1	1	3
13	2	60	530	50	200	1	3	2
14	2	60	600	60	161	2	1	3
15	2	60	670	40	180	3	2	1
16	2	70	530	60	180	3	1	2
17	2	70	600	40	200	1	2	3
18	2	70	670	50	161	2	3	1

8.6. Conducting the Experiment

8.6.1. Developing the Test Plan

All tests were done at wide open throttle to get peak engine performance and at two different engine speeds, 4800 rpm for TEP and 3200 rpm for MRT. It was planned to do all the testing according to the block variable, changing the birdcage configuration between each run. Three full days of testing was therefore needed to complete all the manual labour in changing the “birdcage” configuration between test runs. All the testing had to be completed during work hours and with the same batch of fuel to remove possible fuelling variations. Any experimental noise in the system would be reflected in the dummy variables in columns one, seven and eight.

8.6.2. Preparation and Co-ordination

In the investigation an adapter was needed to join the feed pipe to the carburettor adapter plenum. This adapter had the ability to act as a pressure recovery diffuser and aid in the breathing of the engine by providing a raised pressure at the carburettor throat and thus increased density and increased fuelling. This effect needed to be cancelled out (or made equal) for all the various configurations that existed in the experimental matrix. This ensured that the diffuser did not provide unequal gain to individual

configurations, and thereby add noise to the data. All the diffusers were designed to produce equal effects for all configurations across all engine speeds. In so doing the diffuser pressure recovery effect was removed as a variable and held constant for all engine speeds and all birdcage configurations.

The engine was first run on a carburettor to check that the engine was functioning correctly and to check all the support equipment. DUPEC Engine Control Unit (ECU) was then added to control the added fuel injection system and to control the spark advance to the spark plugs. The design and manufacture of all the diffuser and carburettor adapter pieces was completed before testing commenced to keep the change over time between engine configurations and tests to a minimum.

8.6.3. Performing the Experimental Runs

Testing was undertaken in three blocks over three days without incident. For each experimental configuration the engine was run at the two test speeds until equilibrium (base on stable exhaust temperatures) was reached. Data was recorded for the duration of the test both electronically and manually (as a back up and across checking precaution).

8.6.4. Testing and Inspection

The data recorded during each test was analysed electronically. A region of stable operation at each engine speed for each test was identified, and all the electronically stored data averaged over that time period. The results from the averaging were then graphically represented to determine if all the tests could be considered accurate and feasible with no spurious data points. This process also allowed for data integrity checks, i.e. identifying an inaccurate averaging effect or a mistyped reference in the results calculations where they differed from the results recorded manually during the testing. Examples of these inspection graphs are recorded in Appendix H for engine speed, dynamometer and engine water temperature and air temperature (wet and dry bulb). A complete table of results at both the engine test speeds for all the tests is shown in Appendix I.

8.7. Analysing the Experiment

A level average analysis was performed on the results using MRT, TEP and SFC as performance measures and CO% and exhaust temperature average and variance values as an indication of fuelling distribution. These results are presented in Appendix J .

Identifying the strong interactions and their optimum levels proved more difficult than anticipated for this case study. In most cases the block variable was found to be the major contributor to the variance. This means that the output parameter was most influenced by the day on which the experiment was conducted as opposed to any of the input variables. The variance analysis also showed that the empty

variables representing the random intrinsic variance in the experimental procedure and method were significant, in most cases more so than the input variables. Figure 8-6 shows the level analysis of the specific fuel consumption at 3200 rpm. The block variable is clearly the most significant variable with all the other being relatively insignificant (close to straight lines).

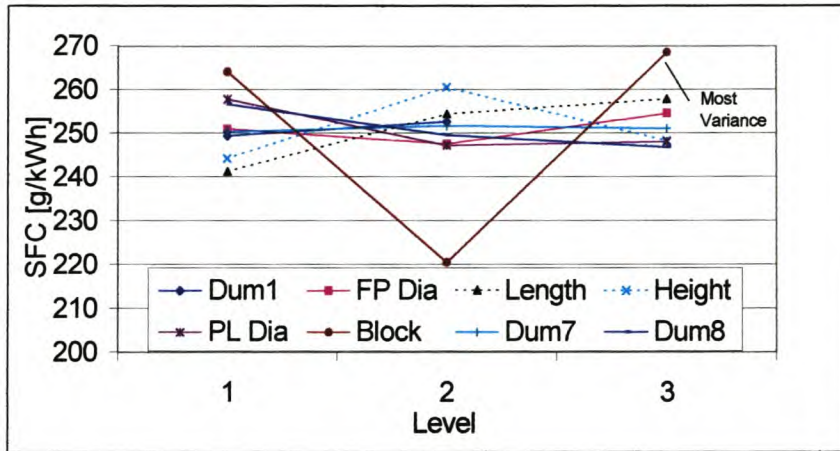


Figure 8-6. SFC Output Variable @ 3200 rpm

Figure 8-7 shows the level analysis of TEP. The block variable again represents the greatest effect on the output parameter. The length and height variables also show trends but they are smaller than the variance as a result of the day on which the experiment was conducted.

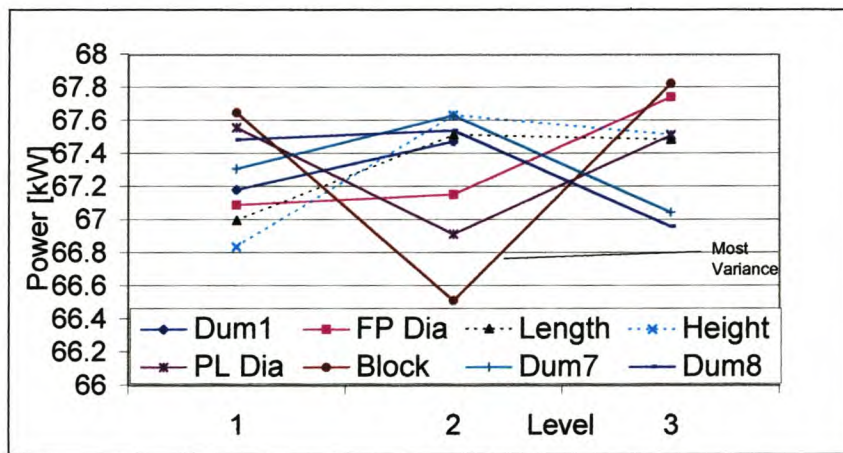


Figure 8-7. Power Output @ 4800 rpm (TEP)

One of the fundamental properties of the orthogonal array based design is that the effect of each variable is determined independently of any of the other variable trends. The trends in variables are therefore independent of the block variation. This can be shown by attempting to correct for the block variance. This involved adding and subtracting from the results obtained each day such that the resulting variance of the block variable was zero. The results of this effort are shown in Figure 8-8. Correcting for the variance in the blocks did not effect the response trends of the other variables in any way. This shows that the response due to each variable is irrespective of the trends in the other variables.

Statistically the trends identified are correct, but they are not significant in comparison to the random variance that was identified in the 'empty' variables 1, 7 and 8.

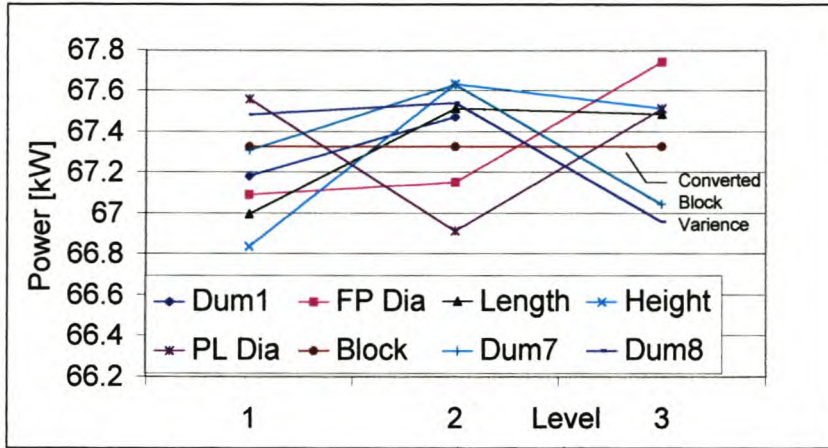


Figure 8-8. Power Output for Corrected Block Variance @ 4800 rpm

Trying to determine the optimum configuration from these trends is a fruitless exercise as the random variance within the experiment is in most cases more significant than the trends that can be attributed to the input variables. This indicates that although the trends are statistically correct, they could be attributed to the systems variation and not due to the input variables changing values.

8.7.1. Prediction Equation and Confirmation Experiment

The prediction equation was not calculated as there was no value to be added by the exercise and therefore there was also no need for a confirmatory experiment.

8.8. Experimental Method Evaluation

In the case study the experimental noise was too great to determine any trends in the input variables. Therefore the next step in the quality engineering optimisation process shown in Figure 5.1, namely, tolerance design is required. The parameter design optimisation was unsuccessful due to the high noise levels and the tolerance design (which may involve spending large sums of money) aims to address those shortfalls that prevented a successful optimisation taking place. Some of the identified short comings of the experimental process are discussed further.

The measuring method was not accurate enough to determine the trends in the input variables as the noise in the engine data created too much random variance. The best solution to this problem is to remove the source of the variance, the engine. Testing the carburettor adapter in a more stable environment would enable the subtle trends in the airflow to be quantified, and the understanding developed before applying it to the engine configuration. Another issue that needs to be addressed is the exhaust temperature measurement. It is very sensitive to the probe position and more care must be

taken to ensure that it is accurately representative of the output gas temperatures. Also the CO% should be logged electronically to enable the actual trends to be determined and remove the guesswork from recording the reading from the gas analyser. An indication of the variation would then also be possible to determine.

The Taguchi Method was unsuccessful in this application due to the noisy environment. The trends were in the region of 1% change in the output parameter which demands very accurate control and measurement. The major disadvantage of Taguchi Methods is illustrated. The knowledge is only available after all the experimentation is complete and the data analysis finished. Had the traditional experimentation methods been used, the deficiencies in the system would possibly have been identified earlier and the effort not been wasted in further testing of the system.

Chapter 9. Case Study Three - Modelling and Simulation

9.1. Case Study Background

In this case study a modelling and simulation investigation was undertaken to determine the prototype dimensions of the inlet manifold for a 1600cc engine. The engine and its components were modelled and simulated using ESA (Engine simulation Analysis ver 1.07 beta), an engine simulation package developed by CAE. Taguchi methods were used in the modelling matrix design, result analysis and trend examination as well as the determination of theoretical optimum dimensions for the inlet manifold in terms of torque at 2800 rpm (low end torque, LET) and power at 5300 rpm (top-end-power, TEP). A number of camshafts were evaluated. The camshafts were described using the minimum number of parameters and levels and then analysed in the Taguchi investigation to determine the best performing camshaft at the optimised inlet manifold configuration and valve timing.

9.2. Introduction

CAE was commissioned to assist in an engine upgrade project to modify a 1600cc engine to meet specific performance targets. These targets are outlined in Table 9-1.

Table 9-1. Design Performance Targets

	Output variable	Performance Criteria	Performance Targets
Target	Torque @ 2800 rpm	>135 Nm + 5%	>141.74 Nm
Restriction	Power @ 5300 rpm	<64 kW + 5%	<67.2 kW

A 1600cc engine was provided for the project, as well as the previously designed dual length high performance inlet manifolds to aid in the adaptation design. A number of cam shafts were also provided to evaluate and identify the best performing camshaft when coupled with the inlet manifold design. There were a vast number of possible configurations for the engine and these needed to be reduced. The engine simulation software was used to determine the most feasible region in which the optimum configuration would occur. The prototype testing and manufacture could then be focused on the optimum region and reduce time and costs. Taguchi's method of experimental design and evaluation was used to design a modelling matrix, thereby reducing the number of simulations necessary to determine the optimum variable positions and identify the trends associated with these variables theoretically. Full factorial designs are usually used to determine the modelling matrix for computer

simulations, but they demand extensive computing power to run the simulations and time to construct the simulation files and analyse the results afterwards. By using a Taguchi orthogonal array to dictate the simulations to be run, the time spent constructing the input files, analysing the results, and running the simulations was greatly reduced and the turnaround time for results therefore also greatly reduced.

9.3. Experiment Planning Following Dr Taguchi's Method

9.3.1. Experimentation team

Team leader:	Jeremy Green
Management Support:	Dr Andrew Taylor
Project Manager:	Paul Williams
Programmer:	Christie Van Vuuren

9.3.2. Problem Statement - Determining the Objectives

The objective of the study was to reduce the uncertainty regarding the optimum operating region for the prototype design, manufacture and testing. By theoretically evaluating the engine performance under the different variable configurations, the theoretical optimum was determined prior to testing. Thus avoiding unnecessary prototype manufacture and testing to determine the optimum operating regime.

The objectives were:

- To determine the optimum inlet manifold dimensions and,
- To select the best camshaft from the supplied camshafts.

The objective for the development was to maximise low-end torque (LET), namely, torque at 2800 RPM. The design target was 135 Nm + 5% (141.74 Nm) at 2800 RPM. This was subject to a restraint on top-end power of less than 64 kW + 5% (67.2 kW) at 5300 rpm. Although it was possible that the optimum camshaft dimensions as calculated from the simulation and the Taguchi analysis would not correspond to one of the supplied camshafts, it was hoped that this would not be the case.

9.3.3. Identifying the Quality Characteristic (Output Variable)

The performance targets as described in the objectives prescribed the output variable for the test work. For the results of this test work however, the output variables of torque and power were initially maximised and then checked against the performance restraints. Analysis was therefore easier and LET was the main output variables used in the results analysis. It was presumed that the trends identified through the simulation investigation would mirror the true situation, although the values of the outputs would not be absolute. Specific output measurement would only be made during the prototype manufacture and testing stage.

9.3.4. Determining the Measuring Methods

The in-house designed engine simulation software, ESA (Engine Simulation Analysis) was used to evaluate the variables as prescribed by the Taguchi experimental design. ESA is a simulation package that uses CFD, heat and mass transfer equations and a combustion model to simulate an internal combustion engine from inlet to exhaust. Results of the simulation runs were analysed according to the methodology as prescribed for Taguchi experimental design. A level averaging method for “maximum is best” method was used [Peace 1993].

9.3.5. Selecting the Independent Variables (Input Variables)

The instructions from the client for the experimental investigation were to investigate the parameters of the inlet manifold, i.e. length and diameter, and investigate the different camshafts that were supplied to determine the optimum engine configuration. The first two variables were therefore the inlet manifold’s pipe diameter and length. The remaining variables were chosen to represent the array of camshafts that were supplied for investigation. This was closely linked to the selection of levels of each variable and is therefore included in Section 9.3.6.

9.3.6. Selecting the Variable Levels

The camshafts supplied to CAE for evaluation were pre-manufactured and so the variables used to describe them needed to be selected carefully. It can be seen from Table 9-2 that there was a vast range of both inlet valve and exhaust valve opening positions, in total nine levels of each. The positions could not be used as input variables, as nine levels is excessive for a standard Taguchi Methods investigation.

Table 9-2. Supplied Camshafts

Camshaft No.	Cam Profile No.	Cam Profile Group	Valve Lift [mm]	Tot. Duration [°CA]	IVO [BTDC]	IVC [ABDC]	EVO [BBDC]	EVC [ATDC]	Duration [°CA] (1mm)
026 109 101L	026 109 113D	2	10	284	29	75	71	33	216
026 109 101M	026 109 113B	1	8.6	269	23	66	51	38	201.6
037 109 101B	035 109 113D	3	10.2	289	23.6	85.4	63.6	45.4	220.2
048 109 101G	048 109 113A	3	10.2	285	14.7	90.3	62.7	42.3	218.2
048 109 101H	048 109 113A	3	10.2	285	19.7	85.3	67.7	37.3	218.2
050 109 101A	050 109 113B	4	10.6	278.4	22.35	76.05	64.35	34.05	216.25
050 109 101B	050 109 113B	4	10.6	278.4	18.95	79.45	60.95	37.45	216.25
050 109 101D	050 109 113B	4	10.6	278.4	17.35	81.05	64.35	34.05	216.25
050 109 101E	050 109 113B	4	10.6	278.4	17.35	81.05	59.35	39.05	216.25

There were 5 main cam profiles present in the selection of camshafts. The only other characteristic that varied was the position of the lobes in relationship to each other (the inlet and exhaust cam profiles were identical on each camshaft). The profiles differed in both lift and duration from one camshaft to the next. Therefore by choosing the lift to describe the profile, all 5 were uniquely identified. The camshaft

Which is sufficient for the investigation so no further arrays were considered. The chosen orthogonal array for the experimental configurations is shown in Table 9-8.

Table 9-8. $L_{16}(4^5)$ Orthogonal Array

$L_{16}(4^5)$
Experiments

Test	Cam lift	IVO	DIFFANG	Length	Diameter
1	1	1	1	1	1
2	1	2	2	2	2
3	1	3	3	3	3
4	1	4	4	4	4
5	2	1	2	3	4
6	2	2	1	4	3
7	2	3	4	1	2
8	2	4	3	2	1
9	3	1	3	4	2
10	3	2	4	3	1
11	3	3	1	2	4
12	3	4	2	1	3
13	4	1	4	2	3
14	4	2	3	1	4
15	4	3	2	4	1
16	4	4	1	3	2

9.4.3. Linear Graphs

There are two possible linear graphs for the $L_{16}(4^5)$ orthogonal array. In the first graph two main effects are investigated and their interaction was spread over the other three columns (Figure 9-1). The one used for this investigation, was simply 5 dots representing the five main effects (Figure 9-2), as interactions were not integral to this investigation and the assumption was made that the interaction between camlift (being representative of the camshaft profile) and the IVO would not be significant and therefore no significant aliasing would occur..

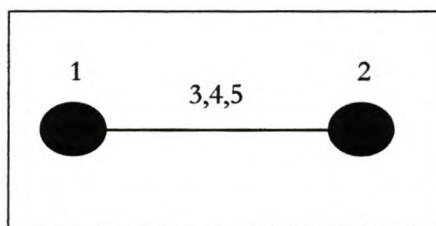


Figure 9-1. Alternative Linear Graph of $L_{16}(4^5)$

with a lift of 10.2 had two different durations, 289° and 285° which are not significantly different with respect to the other camshafts durations. Grouping these together for modelling purposes (and taking the duration as 285° for both) reduced the levels needed by one, resulting in four unique cam profiles. The camshaft profile differentiation is shown in Table 9-3 as taken from Table 9-2.

Table 9-3. Camshaft Profile Levels

Level Group	Profile ID	Total Duration [°]	Valve Lift [mm]
1	026 109 113B	269	8.6
2	026 109 113D	284	10
3	048 109 113A/035 109 113D	285 (289)	10.2
4	050 109 113B	278.4	10.6

By examining the inlet valve opening (IVO) angle, it is apparent that there are four distinct groups of similar values. The average of the values in each group resulted in four levels of IVO. These are shown in Table 9-4. ESA could only deal with integer values for the IVO and thus the numbers were rounded off to the nearest integer.

Table 9-4. IVO Level Determination

Level Group	Angles [°BTDC]	IVO Average [°BTDC]
1	(14.7)	15
2	(17.35)(17.35)(18.95)(19.7)	18
3	(22.35)(23)(23.6)	23
4	(29)	29

In an investigation of the difference between the position of inlet valve opening (IVO) angle and the position of exhaust valve opening (EVO) angle, it was apparent that there were five unique positions i.e. 492, 493, 498, 500, 512 (Table 9-5). The IVO is before top dead centre while the EVC is before bottom dead centre and there is a full engine cycle in between the two. The angle between the two events (DIFFANG) is therefore:

$$DIFFANG = IVO + 360^\circ + (180^\circ - EVO) \quad [9-1]$$

For cam one the calculation is

$$DIFFANG = 29^\circ + 360^\circ + (180^\circ - 71^\circ) = 498^\circ \quad [9-2]$$

Table 9-5. Calculation of DIFFANG

IVO [BTDC]	IVC [ABDC]	EVO [BBDC]	EVC [ATDC]	Duration [°CA] (1mm)	DIFFANG °
29	75	71	33	216	498
23	66	51	38	201.6	512
23.6	85.4	63.6	45.4	220.2	500
14.7	90.3	62.7	42.3	218.2	492
19.7	85.3	67.7	37.3	218.2	492
22.35	76.05	64.35	34.05	216.25	498
18.95	79.45	60.95	37.45	216.25	498
17.35	81.05	64.35	34.05	216.25	493
17.35	81.05	59.35	39.05	216.25	498

By grouping 492 and 493 (the values are not significantly different from each other) to give an average of 492.5, four levels were needed to completely describe all the DIFFANG configurations. The DIFFANG levels are shown in Table 9-6

Table 9-6. DIFFANG Level Determination

Level Group	Number in Level Group	DIFFANG [°]
1	3	492.5
2	4	498
3	1	500
4	1	512

The three variables, camlift, IVO and DIFFANG were all reduced to four levels that completely described the range of camshafts supplied. The length and diameter variables therefore, were also assigned four levels each so that all the variables would have an equal number of levels. The spatial constraints of the engine compartment restricted the length variable to a minimum of 339 mm and a maximum of 680 mm. The internal levels were equally spaced at convenient intervals between the two extremes. The diameter variable standard value was 33 mm. Two additional levels were added either side of that, 2mm away. The level values were extended to either side of this value to include an increase and decrease of the wall friction index (dependant on the amount of surface area the flowing air comes into contact with) and air velocity, that would accompany a change in pipe diameter. The fourth level

was added to the top of the three, separated by the same distance (2 mm) as the other 3. The final level choices are shown in Table 9-7.

Table 9-7. Length and Diameter Level Determination

Level Group	Length [mm]	Diameter [mm]
1	339	31
2	480	33
3	580	35
4	680	37

9.3.7. Identifying Possible Interactions

No interactions were investigated in this application. The important aspect was the investigation of the main effects, and therefore the interactions were deemed unimportant in the investigation. It was important however not to confound the main effects with any first order interactive effects and this was kept in mind when choosing the orthogonal array.

9.4. Designing the Experiment

9.4.1. Calculating the degrees of Freedom

Each variable has 4 levels and therefore needs three DOF's. The investigation therefore needs 15 DOF's to investigate the main effects. Each interaction investigated would need an additional 9 DOF's. There are no interactions investigated in this investigation, therefore the total DOF's required is 15.

9.4.2. Selecting the Orthogonal Array

The Taguchi experimental matrix was chosen using the calculation of the number of DOF's for the experiment and matching that with the most appropriate orthogonal array. The linear graph of the chosen orthogonal array was compared to the desired variable investigation. The simplest orthogonal array with 4 levels per variable is $L_{16}(4^5)$. The orthogonal array chosen must have at least as many DOF's as there are in the experiment. In this case there are fifteen DOF's in the experiment so the orthogonal array must have at least fifteen DOF's.

The number of degrees of freedom of the $L_{16}(4^5)$ orthogonal array is

$$5 \times (4 - 1) = 15 \quad \text{DOF} \quad [9-1]$$

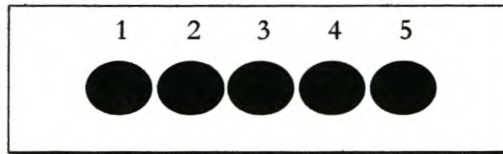


Figure 9-2. Chosen Linear Graph of $L_{16}(4^5)$

9.4.4. Assigning Variables to the Array

The variable levels chosen in Section 9.3.6 are shown in Table 9-9

Table 9-9. Variable Parameters and Levels

$L_{16}(4^5)$
Matrix

Level	Cam lift	IVO	DIFFANG	Length	Diameter
1	8.6	15	492	339	31
2	10	18	498	480	33
3	10.2	23	500	580	35
4	10.6	29	512	680	37

The corresponding orthogonal array for these variables and levels is shown in Table 9-10. The exhaust valve opening (EVO) angle is required as an input variable for ESA. EVO is a function of IVO and DIFFANG and was calculated and included in the modelling matrix.

Table 9-10. Modelling Matrix

$L_{16}(4^5)$
Experiments

Test	Cam lift	IVO	DIFFANG	EVO	Length	Diameter
	mm	°BTDC	°	°BBDC	mm	mm
1	8.6	15	492	63	339	31
2	8.6	18	498	60	480	33
3	8.6	23	500	63	580	35
4	8.6	29	512	57	680	37
5	10	15	498	57	580	37
6	10	18	492	66	680	35
7	10	23	512	51	339	33
8	10	29	500	69	480	31
9	10.2	15	500	55	680	33
10	10.2	18	512	46	580	31
11	10.2	23	492	71	480	37
12	10.2	29	498	71	339	35
13	10.6	15	512	43	480	35
14	10.6	18	500	58	339	37
15	10.6	23	498	65	680	31
16	10.6	29	492	77	580	33

9.5. Conducting the Experiment

9.5.1. Developing the Test Plan

The test planning included determining the modelling matrix from which the multi-simulation files could be constructed and programmed. Each engine configuration needed to have the manifold configuration programmed into a separate file and made available to the simulation programme to retrieve when needed. The simulation would then be run on a debugged version of the software on a sufficiently powerful computer to reduce the necessary computing time. The results would then be analysed to determine the optimum configuration of the camshafts and the inlet manifold. This information would then be passed on to the next phase of the project for prototype manufacture and testing. If the optimum camshaft identified was not in the available camshaft selection then this would be conveyed to the client and the likelihood of obtaining such a camshaft explored.

9.5.2. Preparation and Co-ordination

All components of the simulation program needed to be functioning correctly to make the model simulation and analysis feasible. Computer time was booked on a sufficiently powerful computer and all the necessary files were created and loaded into the correct folders.

9.5.3. Performing the Experimental Runs

The program was run one configuration at a time and the results transferred to the results file before the next configuration was run. This process was automated in a multi-simulation run file. On completion, all the data was in one file which allowed easy transfer from the programme to the data analysis package. Simulations were run at speeds of 2800 rpm and 5300 rpm to generate the LET and TEP data needed for the analysis.

9.5.4. Testing and Inspection

The simulation data was checked for authenticity by making sure that it was feasible. Appendices K and L shows the results from the simulation runs. Reproducibility was not an issue in this application as there were no errors in variation that could occur within the experimental matrix.

9.5.5. Results

Results from the simulation modelling for the speeds 5300 rpm and 2800 rpm are shown in

Table 9-11 and Table 9-12 respectively. A complete set of results is given in Appendix K and L.

**Table 9-11. Simulation Results @ 5300 RPM
(TEP [kW])**

Test	Speed	Torque	Power
1	5300	125.2	69.5
2	5300	128.6	71.4
3	5300	116.0	64.4
4	5300	113.8	63.2
5	5300	134.9	74.9
6	5300	125.3	69.5
7	5300	134.4	74.6
8	5300	133.9	74.3
9	5300	122.9	68.2
10	5300	117.7	65.3
11	5300	147.3	81.7
12	5300	134.4	74.6
13	5300	143.6	79.7
14	5300	130.9	72.6
15	5300	123.8	68.7
16	5300	116.7	64.8

**Table 9-12. Simulation Results @ 2800 RPM
(LET [Nm])**

Test	Speed	Torque	Power
1	2800	125.4	36.8
2	2800	134.1	39.3
3	2800	137.1	40.2
4	2800	143.8	42.2
5	2800	120.3	35.3
6	2800	132.3	38.8
7	2800	120.2	35.2
8	2800	134.5	39.4
9	2800	129.9	38.1
10	2800	130.5	38.3
11	2800	117.6	34.5
12	2800	119.9	35.2
13	2800	118.7	34.8
14	2800	115.7	33.9
15	2800	136.3	40.0
16	2800	136.4	40.0

9.6. Analysing the Experiment

9.6.1. Tabular Method

The tabular results of the Taguchi analysis are shown in Table 9-13 through Table 9-16. The average output of each level of each variable is recorded to give a view of the trends. The difference between the maximum and minimum values of each variable was calculated (delta). The % that each variable contributed to the total variance of the output variable was then calculated (%). The maximum output per variable is then identified and the corresponding level and its value recorded in the last three columns of the table.

Table 9-13. Torque Response Table @ 5300 rpm

Variable	Output [Nm]				Variance		Optimum		
	L1	L2	L3	L4	delta	%	Max	Level	Setting
Cam lift	120.90	132.11	130.57	128.71	11.21	24.25	132.11	2	10.0 mm
IVO	131.61	125.62	130.36	124.70	6.91	14.95	131.61	1	15 °BTDC
DIFFANG	128.60	130.41	125.91	127.37	4.51	9.75	130.41	2	498 °
Length	131.20	138.33	121.32	121.43	17.01	36.80	138.33	2	480 mm
Diameter	125.13	125.62	129.82	131.71	6.58	14.24	131.71	4	37 mm
	1	2	3	4	100				

Table 9-14. Power Response Table @ 5300 rpm (TEP)

Variable	Output [kW]				Variance		Optimum		
	L1	L2	L3	L4	delta	%	Max	Level	Setting
Cam lift	67.10	73.32	72.46	71.44	6.219	24.3	73.32	2	10.0 mm
IVO	73.04	69.72	72.35	69.21	3.833	14.9	73.04	1	15 °BTDC
DIFFANG	71.37	72.38	69.88	70.69	2.5	9.75	72.38	2	498 °
Length	72.82	76.77	67.34	67.40	9.438	36.8	76.77	2	480 mm
Diameter	69.45	69.72	72.05	73.10	3.654	14.2	73.10	4	37 mm
	1	2	3	4	100				

Table 9-15. Torque Level response @ 2800 rpm (LET)

Variable	Output [Nm]				Variance		Optimum		
	L1	L2	L3	L4	delta	%	Max	Level	Setting
Cam lift	135.09	126.83	124.47	126.74	10.62	23.62	135.09	1	8.6 mm
IVO	123.55	128.12	127.79	133.66	10.11	22.48	133.66	4	29 °BTDC
DIFFANG	127.92	127.64	129.29	128.27	1.65	3.66	129.29	3	500 °
Length	120.30	126.22	131.05	135.55	15.25	33.90	135.55	4	680 mm
Diameter	131.67	130.15	126.99	124.32	7.35	16.34	131.67	1	31 mm
	1	2	3	4	100				

Table 9-16. Power Response Table @ 2800 rpm

Variable	Output [kW]				Variance		Optimum		
	L1	L2	L3	L4	delta	%	Max	Level	Setting
Cam lift	39.61	37.19	36.50	37.16	3.11	23.62	39.61	1	8.6 mm
IVO	36.23	37.57	37.47	39.19	2.96	22.48	39.19	4	29 °BTDC
DIFFANG	37.51	37.43	37.91	37.61	0.48	3.66	37.91	3	500 °
Length	35.27	37.01	38.43	39.75	4.47	33.90	39.75	4	680 mm
Diameter	38.61	38.16	37.23	36.45	2.15	16.34	38.61	1	31 mm
	1	2	3	4	100				

9.6.2. Graphical Method

The graphical representation of the data is presented in Figure 9-3 through Figure 9-6. The trends for each variable can easily be seen and the optimum level identified. From these two representations of the results it is possible to comment on the prototype configuration that would warrant manufacture and testing.

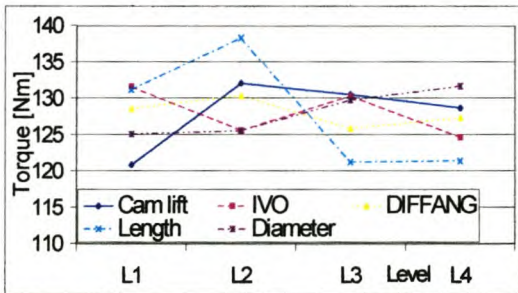


Figure 9-3. Torque @ 5300 rpm

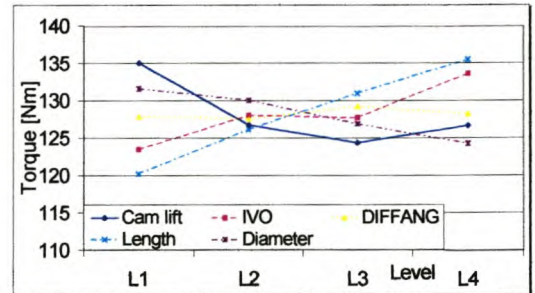


Figure 9-5. Torque @ 2800 rpm (LET)

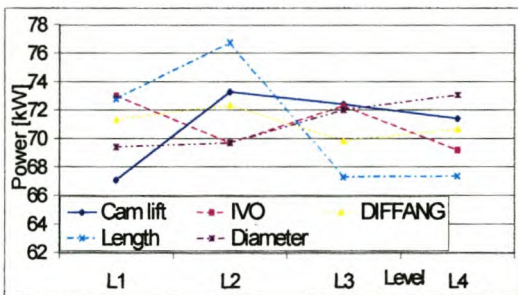


Figure 9-4. Power @ 5300 rpm (TEP)

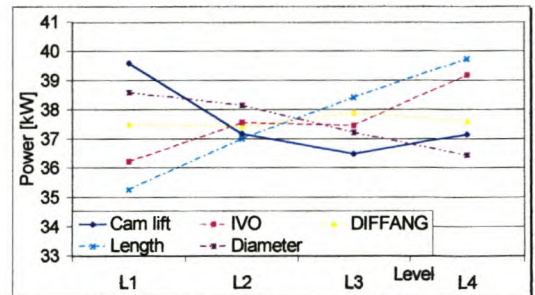


Figure 9-6. Power @ 2800 rpm

9.6.3. Identifying Strong Effects and their Optimum

The main effects of all the output variables were identified as the inlet pipe length and the camshaft lift (which is linked to the valve duration). The trends identified in the analysis are as follows for the investigations at 5300 rpm and 2800 rpm.

9.6.3.1. Inlet length

In the low-end-torque (2800 rpm) investigation the trend in inlet manifold length follows known trends (see Section 2.6.2.1.). The **longer inlet pipe** provides more kinetic energy to the incoming gas and the inertial ramming effect can be used to maximise output. The effect of the inlet length is quantified in Table 9-15 for the torque (Figure 9-5) and Table 9-16 for the power (Figure 9-6). The inlet length is identified as the strongest parameter with 33.9 % of the torque effect contributed to it translating to a variation of 15.25 Nm and 4.47 kW across the investigation spectrum.

For the top-end-power (5300 rpm) investigation, both the torque and power level analysis (Figure 9-3, Figure 9-4, Table 9-13 and Table 9-14) show that the **second level** provides the maximum performance. This could be attributed to the increased friction of long pipes with increased gas velocity and the pulse effects of the engine running at high speeds. It can be seen from the response tables that the length is the strongest parameter of the investigation providing 36.8 % of the overall variation. The torque effect is 17.01 Nm and the power effect can be quantified as a 9.4 kW contribution to variation.

9.6.3.2. Inlet Diameter

The diameter shows expected trends of large diameter pipes (Section 2.6.2.2.) having a low resistance to flow at high speeds (5300 rpm) and the small diameter pipe as optimum at low speeds so that the kinetic energy of the air remains high. For the TEP investigation the 37 mm diameter (**Level 4**) showed best results and for the LET investigation the 31 mm diameter (**level 1**) showed the best results as seen in Table 9-13 through Table 9-16. The diameter contribution was not identified as a main effect in either of the two investigations. The effect however should not be ignored as they were 14% and 16% contributors for the 5300 rpm and 2800 rpm investigations respectively.

9.6.3.3. Cam Lift

The cam-lift parameter was chosen as a representation of the cam-profile in its entirety (Section 9.3.6). Both the valve open duration and the valve lift were described by a single variable. In the LET investigation the breathing requirements are lower and the timing slower for the valves. The optimum level (one) was the one

breathing requirements are lower and the timing slower for the valves. The optimum level (one) was the one with the **lowest lift** and the **shortest duration**. It contributed 24% to the overall variation of the LET. The TEP investigation also showed the camshaft lift as being a major contributor to the output variable, also with 24% contribution. The optimum level here however was identified as **level 2**, the configuration with the **longest duration**. This would be the configuration where the pulses in the manifold pipes contribute most to the engine performance.

9.6.3.4. IVO

For the TEP investigation the IVO optimum level was **level 1** (15°BTDC). It was the third most dominant effect of the investigation with a 6.91 Nm (3.8 kW) effect on engine performance. For the LET investigation **level 4** was found to be the optimum setting (29°BTDC). It was again the third most dominant effect in the investigation although in this instance it had 22% of the variance attributed to it. (10.11 Nm and 2.96 kW).

9.6.3.5. DIFFANG

The % variance for the LET investigation was negligible (4%) and though it is higher for the TEP investigation (9.7%) it is still not significant. The optimum setting for TEP investigation was **level 2** (498°) and for the LET investigation the best performance was gained at **level 3** (500°) with only 0.48 kW and 1.65 Nm difference in engine performance.

The identified optimum levels are summarised in Table 9-17.

Table 9-17. Optimum Level Settings

Variable	2800 rpm		5300 rpm	
Cam Lift	1	8.6mm	2	10mm
IVO	4	29°BTDC	1	15°BTDC
DIFFANG	3	500°	2	498°
Length	4	680mm	2	480mm
Diameter	1	31mm	4	37mm

The optimum configuration for target torque is therefore achieved with a cam with the properties of :*IVO of 29°BTDC, EVO of 69°BBDC, a lift of 8.6mm and duration of 269°*, and an inlet manifold *680mm long with a diameter of 31mm*.

The only camshaft from the selection with an 8.6mm lift has an IVO of 23°BTDC. The best option would be to try and get another camshaft manufactured to these optimum specifications.

9.6.4. Prediction Equation

The prediction equation is calculated from the average effect of the significant factors and their optimum settings. LET was the significant factor in the investigation and the calculation is as follows. The DIFFANG contribution to the output variable was the only parameter to be ignored, as its influence was deemed insignificant in comparison to the other four which all achieved in excess of 15% in the investigation.

$$V_{pre} = OV_{avg} + (CL_1 - OV_{avg}) + (IVO_4 - OV_{avg}) + (L_4 - OV_{avg}) + (D_1 - OV_{avg}) \quad [9-3]$$

Where: V_{pre} = output variable predicted value;

OV_{avg} = The average result of the output variable over all the tests conducted in the investigation; ie the average output of the system irrespective of the level settings.

CL_i = The output variable average of Camlift at level i ;

IVO_i = The output variable average of Inlet Valve angle at level i ;

L_i = The output variable average of Inlet Pipe Length at level i ;

D_i = The output variable average of Inlet Pipe Diameter at level i ;

i = the optimum level of the parameter.

For the Torque @ 2800 rpm the prediction equation yields:

$$V_{out} = 1283 + (1351 - 1283) + (1337 - 1283) + (1356 - 1283) + (1317 - 1283) = 151 Nm \quad [9-4]$$

This is above the required 142 Nm asked for at the outset of the experiment and is acceptable.

The corresponding value of the TEP at the same variables levels is:

$$V_{out} = 71.1 + (67.1 - 71.1) + (69.21 - 71.1) + (67.4 - 71.1) + (69.5 - 71.1) = 60 kW \quad [9-5]$$

which is below the prescribed 67kw maximum.

9.7. Conclusions

It can be seen that the four experiments resulted in different optimum settings for the variables depending on the speed at which the investigation took place. Torque and power at each speed generated the same

optimised configuration. That made it unnecessary to investigate both torque and power at the two speeds. In further investigations only the torque investigation need to be done.

The optimum camshaft for the LET requirement results in a very low TEP. Although this meets with the initial requirements the client may feel that the TEP is too low and rather have a trade off whereby one of the variables is changed to improve the TEP and decrease the LET.

The prototype manifold can be manufactured to the above specifications. A possible further investigation would be to model the available camshafts with the suggested optimum inlet manifold and determine which performs the best. Confirmation testing of the engine with different camshafts and the prototype manifold can be compared to determine the best operating camshaft among the camshafts available if the recommended camshaft design cannot be manufactured.



Figure 9-7. Prototype Inlet Manifold

The optimum camshaft is not found in the available selection. The prediction equations for the closest camshaft profile with a lift of 8.1mm and an IVO of 23° predict an LET of 145Nm and a TEP of 63 kW. The LET is lower than for the optimum conditions but still within design constraints. The TEP delivered is higher with this configuration. It was at the clients discretion which option to utilise. It is recommended that the above option be explored initially during the prototyping phase.

Chapter 10. Case Study Four - Taguchi vs Full Factorial

This case study is a comparison of the performance of the Taguchi Method of experimental analysis with the comprehensive full factorial method of the same investigation and is an extension of Case Study Three described in Chapter 9. The full factorial analysis tests all the possible combinations of the variables under investigation while the Taguchi Matrix uses minimal experiments applying an orthogonal array in the design. Due to the extended experimental times needed for the full factorial, only one engine speed (5300 rpm) was used for the comparison. Torque and power were not both needed as output variables. Case Study Three showed that the two delivered the same results as power is a function of torque and engine speed. Therefore if engine speed is not varied, power is a function of torque and both variables do not need to be investigated. Only power was used as an output variable in this case study.

10.1. Preparation

The problem from Case Study Three was used for the comparison of experimental methods. The model design was complete and the only additional programming that was necessary was the creation of multiple simulation files needed for the large number of simulations for the full factorial. The simulation package development had progressed and a newer version was used for this analysis. The results therefore are not directly comparable and a new Taguchi analysis was undertaken for the comparison investigation.

Five input variables were investigated; Cam-shaft Lift (camlift), Inlet valve opening angle (IVO), the difference between the inlet valve and the exhaust valve opening angles (DIFFANG), the length of the inlet manifold pipe (length) and the diameter of the inlet manifold pipe (diameter), each at four levels. It was decided to use evenly distributed levels for each of the variables (except for diameter that would use the standard diameter of the engine in Case Study Three as one of the points), to generate evenly spaced points on the output variable trend graphs, as shown in Table 10-1.

Table 10-1. Levels of the input Variables

L16(45)
Matrix

Level	Cam lift	IVO	DIFFANG	Length	Diameter
1	8.6	15	494	600	33
2	10	20	498	640	34.5
3	10.2	25	502	680	36
4	10.6	30	506	700	37

10.2. Taguchi Investigation

The Taguchi simulation runs were conducted as in Chapter 9 using the same orthogonal array with the new variable levels as shown in Table 10-2. The 16 simulations took almost 4 hours to run, at approximately 15 minutes each.

Table 10-2. Orthogonal Array used in the Taguchi analysis.

L16(4⁵)
Experiments

Test	Cam lift	IVO	DIFFANG	Length	Diameter
	mm	°BTDC	°	mm	mm
1	8.6	15	494	600	33
2	8.6	20	498	640	34.5
3	8.6	25	502	680	36
4	8.6	30	506	700	37
5	10	15	498	680	37
6	10	20	494	700	36
7	10	25	506	600	34.5
8	10	30	502	640	33
9	10.2	15	502	700	34.5
10	10.2	20	506	680	33
11	10.2	25	494	640	37
12	10.2	30	498	600	36
13	10.6	15	506	640	36
14	10.6	20	502	600	37
15	10.6	25	498	700	33
16	10.6	30	494	680	34.5

The tabular results of the Taguchi analysis are shown in Table 10-3. The average output of each level of each variable is recorded to give a view of the trends. The difference between the maximum and minimum values of each variable was calculated (delta). The % that each variable contributed to the total variance of the output variable was then calculated (%). The maximum output per variable was then identified and the corresponding level and its value recorded in the last three columns of the table as in Chapter 9.

Table 10-3. Taguchi Analysis Power Response Table @ 5300 rpm

Variable	Output [kW]				variance		Optimum		
	L1	L2	L3	L4	delta	%	Max	Level	Setting
Cam lift	60.12	64.27	65.13	67.05	6.9	24.2	67.05	4	10.6 mm
IVO	60.23	63.71	66.34	66.29	6.1	21.3	66.34	3	25 °BTDC
DIFFANG	65.03	65.37	64.34	61.82	3.6	12.4	65.37	2	498 °
Length	69.67	64.01	61.43	61.45	8.2	28.8	69.67	1	600 mm
Diameter	62.41	62.77	65.18	66.22	3.8	13.3	66.22	4	37 mm
	1	2	3	4	28.7	100	actual		

Figure 10-1 is a graphical representation of the data shown in Table 10-3, indicating visually the significant trends and optimum level settings.

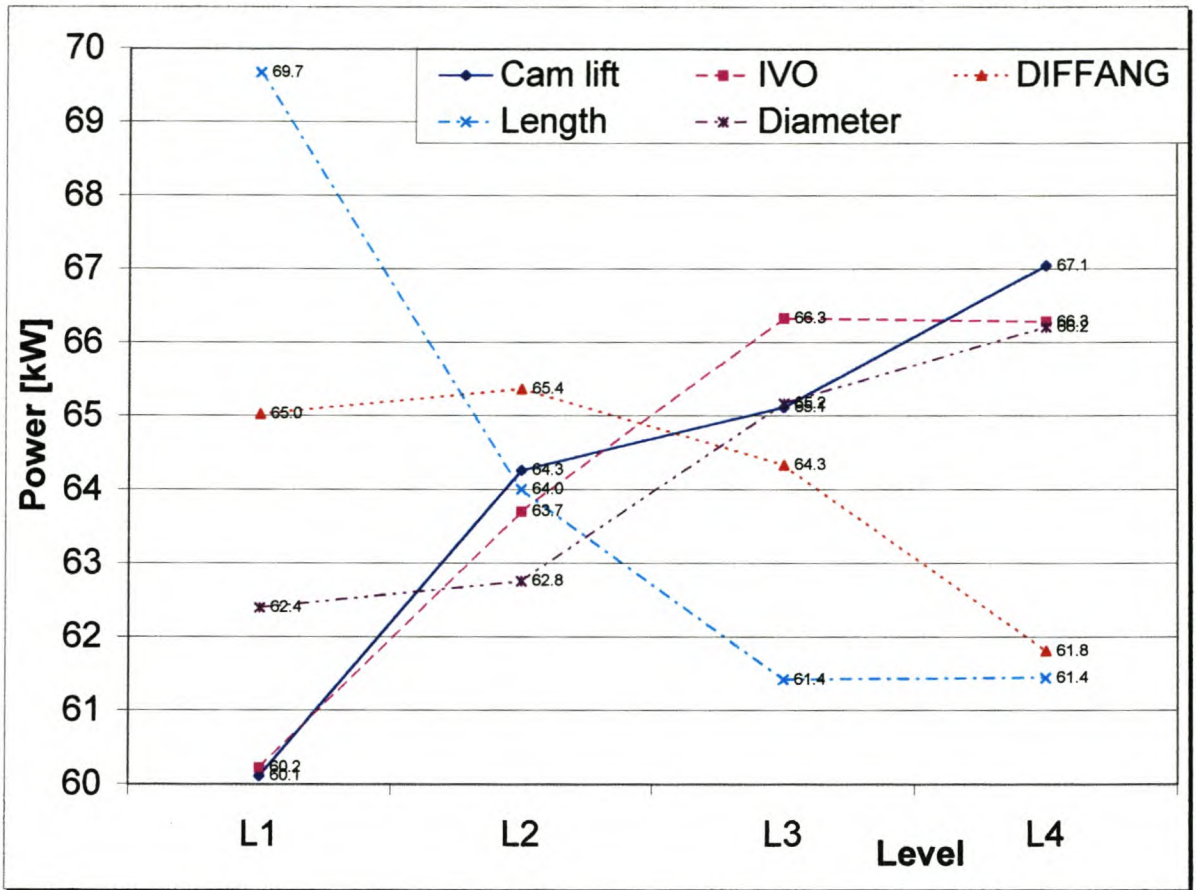


Figure 10-1. Taguchi Power Response Results @ 5300 rpm

10.3. Full Factorial

The full factorial matrix was constructed as per the description in section 4.5 and the 1024 (45) possible configurations were programmed into blocks of 100, the maximum that the simulation package could handle in one multi-simulation run. The 1024 configurations, at an average of 15 minutes each, took approximately 10 full days of processing time to complete. Great care was taken when reconstructing the results matrix that no data was misplaced or corrupted that could lead to skewed results. The level averaging technique used in the Taguchi analysis was also used in the analysis of the full factorial results. It should be noted that the pivot table report function in Microsoft Excel® would have done the analysis very quickly without the possibility of a typing error and the author recommends this method of results analysis for future uses of Taguchi method applications.

Table 10-4. Full Factorial Power Response Table @ 53200 rpm

Variable	Output [kW]				Variance		Optimum		
	1	2	3	4	delta	%	Max	Level	Setting
Cam	60.35	64.37	64.71	66.84	6.5	26.20	66.84	4	10.6 mm
IVO	61.29	63.56	65.27	66.15	4.9	19.60	66.15	4	30 °BTDC
Diffang	65.14	64.69	63.82	62.62	2.5	10.17	65.14	1	494 °
Length	68.94	63.71	61.80	61.82	7.1	28.79	68.94	1	600 mm
Diameter	62.11	63.38	64.89	65.89	3.8	15.23	65.89	4	37 mm
	1	2	3	4	24.79	100			

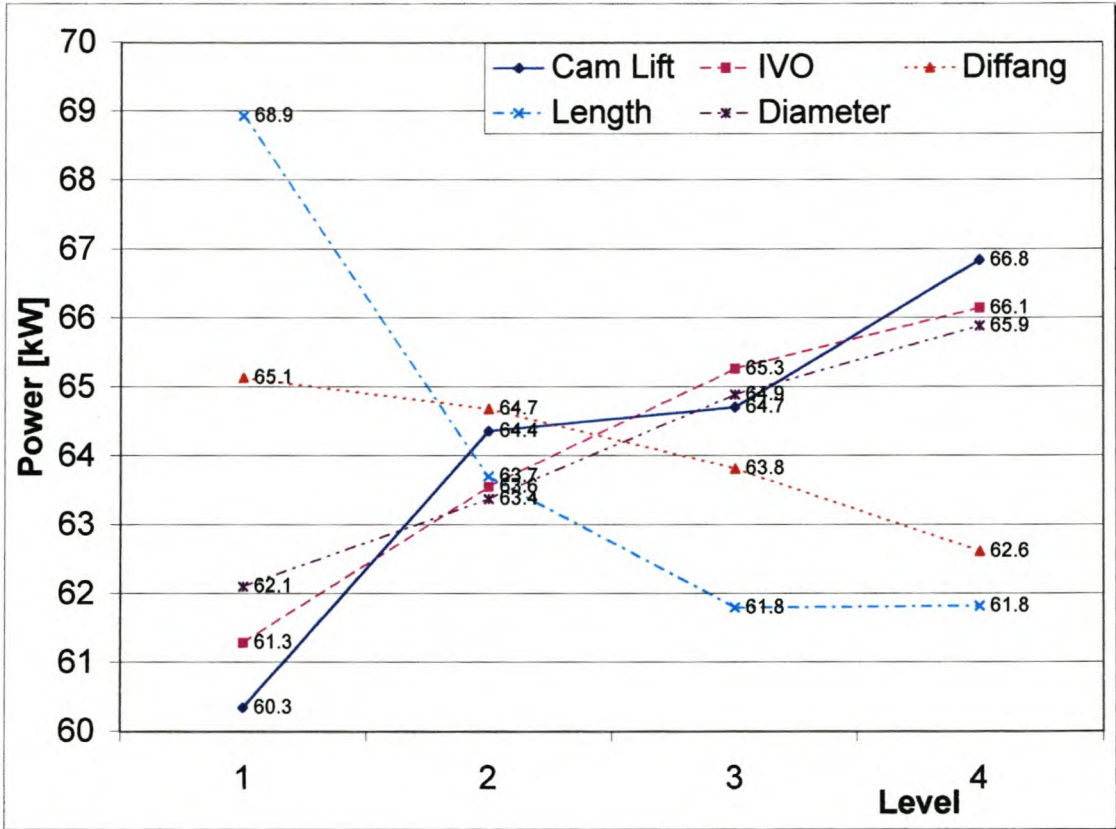


Figure 10-2. Full Factorial Power Response Results @ 5300 rpm

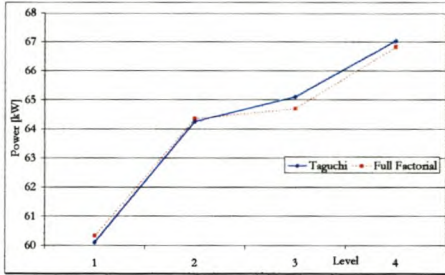
10.4. Comparison

A comparison of the results using the different methods of analysis is shown in tabular form in Table 10-5 and in graphical form in Figure 10-3. The figures show that the Taguchi matrix is a very good approximation of the full factorial design.

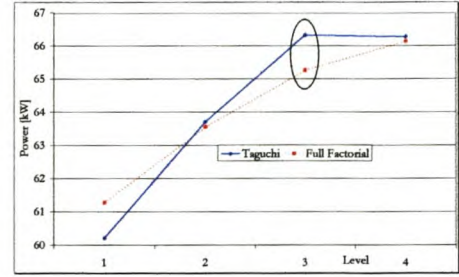
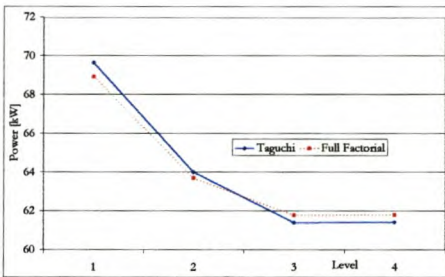
Table 10-5. Comparison of Full Factorial and Taguchi Results

Taguchi Analysis Table, Power @ 5300				
Level	L1	L2	L3	L4
Cam lift	60.12	64.27	65.13	67.05
IVO	60.23	63.71	66.34	66.29
DIFFANG	65.03	65.37	64.34	61.82
Length	69.67	64.01	61.43	61.45
Diameter	62.41	62.77	65.18	66.22

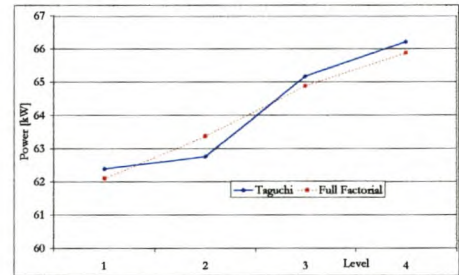
Full Factorial Power @ 5300				
Level	1	2	3	4
Cam lift	60.35	64.37	64.71	66.84
IVO	61.29	63.56	65.27	66.15
DIFFANG	65.14	64.69	63.82	62.62
Length	68.94	63.71	61.80	61.82
Diameter	62.11	63.38	64.89	65.89



CamLift

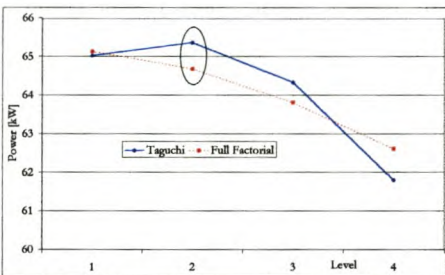


IVO



Diameter

Length



DIFFANG

Figure 10-3. Comparison of Full Factorial and Taguchi Analysis Trends

There are two variables of concern where the Taguchi approximation of the trends results in a different optimum level to the full factorial. The IVO variable (Figure 10-3) show a possible difference in the optimum level determination between the two solutions. Although there is only a 0.6% difference in the value for level three between the two methods, this is sufficient for the resulting data to indicate a different optimum level. The Taguchi analysis indicates the optimum could be at level three or four, as the trend plateau's out at those two levels. The full factorial however leaves no doubt as to the optimum being level four.

DIFFANG in Figure 10-3 shows that although there is only a 1% difference in the value for level two between the Taguchi solution and the full factorial solution, the difference is sufficient to change the

predicted optimum level setting. The full factorial predicts an optimum at level one while the Taguchi solution predicts an optimum at level two. This is of little consequence in the prediction equation as in both cases the DIFFANG would have not been used as it is a very low contributor to the overall variance and its level would have been convenience based and not dependent on the investigations findings.

Table 10-6. Difference Between Full Factorial and Taguchi Results

Power @ 5300 Difference				
Level	1	2	3	4
Cam lift	0.23	0.10	-0.41	-0.21
IVO	1.06	-0.15	-1.06	-0.14
DIFFANG	0.11	-0.68	-0.52	0.81
Length	-0.74	-0.30	0.37	0.37
Diameter	-0.29	0.62	-0.29	-0.33

Power @ 5300 % Difference				
Level	1	2	3	4
Cam lift	0.38%	0.15%	-0.64%	-0.31%
IVO	1.75%	-0.24%	-1.62%	-0.21%
DIFFANG	0.17%	-1.05%	-0.82%	1.30%
Length	-1.06%	-0.47%	0.60%	0.61%
Diameter	-0.47%	0.98%	-0.44%	-0.50%

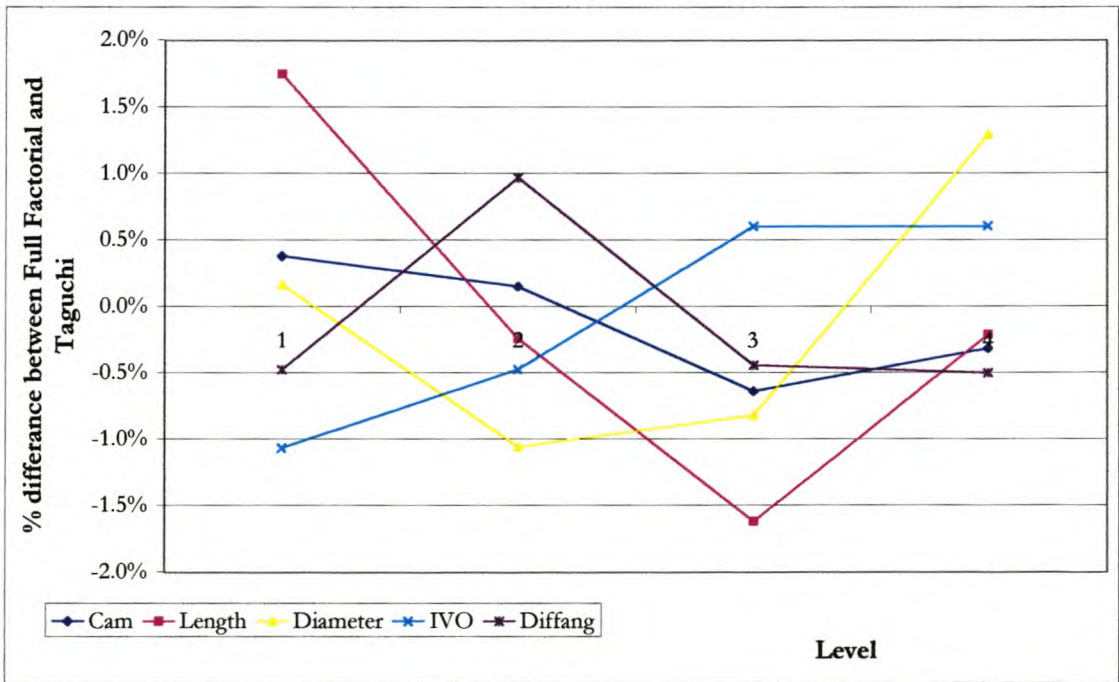


Figure 10-4. Taguchi and Full Factorial Difference

Table 10-6 and Figure 10-4 show the differences between the Taguchi solution and the full factorial solution as a percentage. The maximum variance is 1.75% with the average difference being only 0.69%. The Taguchi approximation of the variable trends is therefore very good, especially at the reduced experimentation time needed to generate the necessary data. If this exercise was extended into the experimentation arena then the benefits in terms of time and cost saving would be enormous.

It must be noted however that where a variable plateau exists in a Taguchi analysis it could mean that either of the values on the plateau could be the true optimum and need to be investigated further.

10.5. Prediction Equation

Based on the results of the Taguchi matrix investigation a prediction equation was generated to predict the performance of the optimum configuration. The prediction equation takes into account the variables that were deemed significant in the analysis. All the variables, bar DIFFANG, were deemed significant and therefore all, bar DIFFANG, were included in the prediction equation.

$$V_{out} = P_{avg} + (CL_i - P_{avg}) + (IVO_i - P_{avg}) + (L_i - P_{avg}) + (D_i - P_{avg}) \quad [10-1]$$

Where, P_{avg} = The average power output for the experimental investigation;

CL_i is the average power output of the camlift at the i th level;

IVO_i is the average power output of the camlift at the i th level

L_i is the average power output of the Length at the i th level;

D_i is the average power output of the diameter at the i th level;

i is the level at which the variable is being evaluated (the maximum for the optimum prediction equation)

Substituting in to the equation yields:

$$V_{out} = 64.14 + (67.05 - 64.14) + (66.34 - 64.14) + (69.67 - 64.14) + (66.22 - 64.14) \quad [10-2]$$

$$V_{out} = 76.85 \quad [10-3]$$

The optimum levels for the confirmation experiment were. Camlift 4; IVO 3; Length 1; Diameter 4; DIFFANG 2. The full factorial investigation included this simulation run and the results could therefore be compared. V_{outFF} is the output power of the confirmatory simulation run which resulted in a 0.55% difference from the prediction equation as shown in the calculation below.

$$V_{outFF} = 76.43 \quad [10-4]$$

$$\frac{V_{out} - V_{outFF}}{V_{out}} \times \frac{100}{1} = \frac{76.85 - 76.43}{76.85} \times \frac{100}{1} = 0.55\% \quad [10-5]$$

The maximum output generated by the full factorial was found by searching the full factorial investigation results for the maximum power output. The levels for the parameters of the maximum power output were; Camlift 4; IVO 4; DIFFANG 2; Length 1 and Diameter 4; with a power output of 76.76 kW. A comparison of the Taguchi predicted output with the confirmatory simulation run, the full factorial predicted output with the confirmatory simulation run, and the actual maximum output configuration is given in Table 10-7.

Table 10-7. Final Comparison

Full factorial Analysis			Taguchi Method			FF Search	
Max	Level	Setting	Max	Level	Setting	Level	Variable
66.84	4	10.6 mm	67.05	4	10.6 mm	4	Cam
66.15	4	30 °BTDC	66.34	3	25 °BTDC	4	IVO
65.14	1	494 °	65.37	2	498 °	3	Diffang
68.94	1	600 mm	69.67	1	600 mm	1	Length
65.89	4	37 mm	66.22	4	37 mm	4	Diameter
Confirmatory	76.29 kW					76.76 kW	
Predicted	75.61 kW					76.85 kW	

10.6. Conclusions

Table 10-7 indicates the effectiveness of the Taguchi Method. The two factors that were mis-optimised (IVO and DIFFANG) had little effect on the power output. The IVO was at the top end of its range and had plateaued to a constant value and thus had little effect on the prediction equation. DIFFANG was a very complicated variable representing many effects simultaneously. In both the Taguchi analysis and the full factorial it was deemed to be insignificant in the final analysis as it contributed very little to the overall variance. The full factorial analysis estimate of the optimum output was further away from the actual maximum output than the Taguchi prediction which over-predicted the power by 0.1 kW. The Taguchi Investigation was completed in 16 simulations vs the 1024 simulations used in the full factorial yet still produced arguably better results.

It must be noted that in a Taguchi investigation care must be taken where the analysis shows a plateau in the variable trend. The Case Study has shown that both variables in the plateau could represent the optimum and thus all possibilities should be investigated. It also is apparent from this case study that error bars are necessary to determine the reliability that can be given to a “maximum”. The error bars would have brought attention to the reliability of the plateau and thus not left error in the analysis.

Chapter 11. Conclusions and Recommendations

Taguchi Methods successfully reduced the amount of experimentation needed during automotive engine research by employing statistical design of experiments in a simplistic form. This did not demand a comprehensive grasp of the statistics needed to design the orthogonal arrays for the applications. In the case studies included in this work, a wide range of applications were evaluated and all of them were successful to varying degrees.

Case study one investigated the inclusion of flow diverters in a carburettor adapter prototype. The experimental design as determined using the Taguchi Method was a simple one and allowed comprehensive but easy comparison to be made with the traditional approach. In this case the traditional approach was to undertake a full factorial investigation where all possible combinations were tested. Results showed that information about the interaction of the flow diverters with each other was highlighted using the Taguchi Method of experimental design versus the traditional approach. Although the traditional method may have identified the interaction, the ability of the Taguchi method to put a value to it is a significant advantage. The structured data analysis procedure of the Taguchi methodology also ensures that the interaction is not missed. The Taguchi Method could also quantitatively attach a benefit to the inclusion of the various adapters that could be offset against the cost of its inclusion. The effect of the inclusion of the baffle-plate was to increase the Mid-Range-Torque by an average of 5 Nm.

Case study two expanded the investigation of the first case study to examine the geometrical configuration of the carburettor adapter and the interactions of the investigated variables with each other. The carburettor adapter diameter and height were analysed as well as the diameter and length of the feed pipe from the air filter to the carburettor adapter. The measurement of the engine outputs was comprehensive and resulted in a complex analysis of the data. Torque and power were measured at different engine speeds as well as emissions data for each test point. The measurement of the emissions data however was deemed to be insufficiently accurate to enable useful analysis. This was also shown in the data analysis where no consistent or significant trends could be reliably identified. The major difficulty encountered during the experimentation was that the natural variation of the system (noise) was just as significant as the trends identified. This could have been overcome by either reducing the natural variation or increasing the range of the input variables such that there was significant variation in the output values. This knowledge in itself was valuable however and would not have been available in a traditional approach of one step at a time experimentation.

Case study three then went on to an investigation where experimental variation would have no impact on the investigation. A computer simulation programme was used to investigate a number of interactive components of the engine. The camshaft valve opening angles were examined using calculated variables describing the inlet and exhaust valve opening and closing angles and the valve lift. The inlet pipe

diameter and length were the final two variables included in the investigation. The output of the engine was measured and analysed at two engine speeds that resulted in a multiple response variable optimisation problem. This resulted in different optimum configurations for the two engine speeds. A trade off needed to be made between optimum variable levels at the two engine speeds to determine the overall optimum design.

Case study four was a continuation of case study three and compared the results of the Taguchi Methods analysis to a comprehensive analysis (full factorial) using the same computer programme and the same variable levels. The comparison showed conclusively that the loss of accuracy resulting from the reduced number of experiments of the Taguchi Method was almost insignificant. The largest difference on one point in the analysis was 1.5% while the trend differences were minimal.

Generally the results obtained from the Taguchi Method experiments were superior and resulted in more information about the process being analysed. This information was also obtained using less experimental work.

The major disadvantage of the Taguchi Method is not obvious from the case studies. Taguchi Methods demand that all the experiments are completed and then analysed before any information is fed back to the experimenter. This means that if there is a problem during the experimentation runs, then it only becomes evident after the data analysis. It also means, as in case study two, that where there is no significant trend present this is only identified after the data analysis has been completed. All the experimental runs completed are therefore superfluous and wasted time and money. The traditional method however may have shown the problem earlier in the experimental programme. This single point may cause resistance to the method and can only be overcome by fastidious experimental execution. But as fastidious experimental execution is important to any experimentation programme, this fact should discourage the use of Taguchi methods. It can be conclusively stated that Taguchi Methods result in more information for less effort without exception, provided sound experimental procedures are used to identify significant trends.

GLOSSARY

Aliasing	When the effect of a variable or interaction cannot be separated in the analysis from the effect of another interaction then the two effects are said to be aliased.
ANOVA	Analysis of variance, Statistical tool for identifying relationships between variables.
Combustion Chamber:	The area above the piston and below the cylinder head in which combustion occurs.
Confounding	When the main effects or interactions are aliases with a blocking variable or interaction effects
Dependent Variable	A variable (usually an output variable) whose value is dependent on another (independent) variable (b where $b=f(x)$)
Exhaust Blow Down:	The rushing out of combustion products that occurs when the exhaust valve opens.
Identity	Or generator. The defining term that shows all possible aliasing combinations in an experimental design.
Independent Variable	A variable (usually an input variable) whose setting influences the value of another (dependent) variable (x where $b=f(x)$)
Induction system	For the purpose of this investigation, the induction system of the engine is defined to include all the parts of the engine from the air intake to the inlet valves of the combustion chamber. This includes such components as the air filter and associated piping, carburettor adapter, carburettor, inlet manifold and ports in the cylinder head.
IO PAK	The input output module of the computer control system
Levels	(of a variable) The discrete values at which the variable are tested in an experimental design.
Naturally Aspirated	An engine that is not super charged or turbo charged
Pancake air filter	The type of air filter commonly used outside of South Africa. The large air inlet area results in lower flow losses increased engine efficiency.
Quality Characteristic	Another name used for the output variable that is to be used in the optimisation or investigation project.

Residual gases		The burnt gases that are not vented from the combustion chamber before the exhaust valve closes.
Response parameter:		See quality Characteristic.
Reversion		The phenomenon that occurs when combustion products flow into the inlet pipes when the inlet valve opens. It occurs as a result of the combustion chamber pressure being higher than the pressure in the inlet pipe.
Specific Fuel Consumption (SFC)	Fuel	A measure of an engine efficiency that is normalised for the size (power output) of an engine [g/kwh]
Traditional Experimental Methods		This is the method currently employed by the majority of experimenters. Usually one variable at a time is varied without changing anything else in the tested system and the effect on the system compared (This is in contrast to other possible 'traditional' experimental designs such as a full factorial).
Volumetric Efficiency		A ratio of air in the combustion chamber vs the air that would fill the displaced volume under atmospheric conditions.

REFERENCES

- Bandurek**, G, Disney, J., Bendall, A, 1988, *Application of Taguchi methods to surface mount process*. Quality and Reliability Engineering International, 4, 171-81
- Barker**, T.B., 1986, *Quality Engineering by Design: Taguchi's philosophy*. Quality Progress, 19,12
- Bendel A**, A, Disney, J., Pridmore, W. A., 1989, *Taguchi Methods: Applications in World Industry*. IFS Publications, London, UK
- Beveridge**, G.S.G., Schechter Robert S, 1970, *Optimization: Theory and Practice*. McGraw-Hill, New York
- Biles**, W.E., Swain James J, 1980, *Optimization and Industrial Experimentation*, Wiley, New York
- Box**, G.E.P., Davis O.L, 1967, *Statistical Methods in Research and Production: With special reference to the chemical Industry*. Oliver and Boyd, London
- Box**, G.E.P., Draper N.R., 1969, *Evolutionary Operation: a statistical method for process improvement.*, Wiley, New York
- Box**, G.E.P., Jenkins, G.M., 1976, *Time Series Analysis: Forecasting And Control*. Holden Day, San Francisco California
- Box**, G.E.P. 1978, *Statistics for Experimenters: An Introduction to design, data analysis and model building*.
- Box**, G.E.P., Draper, N.R. 1987, *Empirical Model Building and Response Surfaces*. Wiley, New York
- Box**, G.E.P., Tiao G.C., 1992, *Bayesian Interference in Statistical Analysis*. Wiley, New York
- Box**, G.E.P, Wu chien-Fu, Leonard, Tom, 1983, *Scientific Interference, Data Analysis and Robustness*. Academic Press, New York
- Box**, G.E.P, Wilson, K.B, 1951, *On the Experimental Attainment of optimum conditions*. Roy. Stat. Soc, Ser, B 13, 1
- Box** , G.E.P, 1966, *A note on Augmented Designs*. Technometrics, 8, 184
- Box** , G.E.P, Bisgaard, S., Fung, C., 1988, *An explanation and critique of Taguchi's contribution to quality engineering*. Quality and Reliability Engineering International, 4, 123-31
- Box** , G.E.P, Hunter J.S, *The 2^{**}(k-p) factorial designs*. Technometrics, 3, 311, 449
- Bryne**, D.M., Taguchi, S., 1986, *The Taguchi approach to parameter design*, American Society for Quality Congress, Anaheim,CA
- Chamberlin** , W.B., Mozdzen E.C., Gordon C. L., 1990, *Extending Injector Life in Methanol-Fueled DDC Engines Through Oil and Fuel Additives*. SAE, 902227
- Clarke**, F.H, 1983, *Optimization and Nonsmooth Analysis*. Wiley, New York
- Cohon**, Jared L, 1978, *Multiobjective Programming and Planning*. Academic Press, London
- Danial**, C, 1971, *Fitting Equations to Data: computer analysis of multifactorial data for scientists and engineers*. Wiley, New York
- Danial**, C, 1980, *Fitting Equations to Data: Computer analysis of multifactorial data*. Wiley, New York
- Daniel**, C, 1962, *Sequences of fractional replicates in the 2^{**}(p-q) series*. J. Am. Stat. Soc., 58, 403
- Daniel**, C, 1976, *Applications of Statistics to Industrial Experimentation*. Wiley, NewYork
- Davies**, O.L., Hay W.A, 1950, *The Construction and use of fractional factorial designs in industrial research*. Biometrics, 6, 233
- Dohi** , M., Maruyama Y, 1990, *Ride Comfort Optimization for Commercial Trucks*. SAE, 902266
- Draper**, N.R., Hunter, W.G, 1966, *Design of experiment for parameter estimation in multi response situations*. Biometrika, 53, 525

- Ferguson, C.R.**, 1986, *Internal Combustion Engines, Applied Thermosciences*. Wiley, New York
- Fitton, J.**, *Knock in internal combustion engines*. MSc thesis, University of Cape Town
- Fletcher, R.**, 1980, *Practical Methods of Optimization*. Wiley, New York
- Gardener, T.P.**, 1992, *Investigation of the effects of Engine Design Parameters on Diesel Combustion and Emissions Using Taguchi Methods*. SAE, 920116
- Heath, W.A.**, 1996, *The Effect of Valve Angles on Engine Performance*. Final Year Project, Mech Eng. University Of Stellenbosch,
- Heisler, H.**, 1995, *Advanced Engine Technology*, Edward Arnold, London
- Hunter, J.S., Naylor, T.H.**, 1971, *Experimental design for computer simulation experiments*. Management Science, 16, 422
- Hunter, C.E., Gardner T.P., Zakrajsek, C.E.**, 1990, *Simultaneous Optimization of Diesel Engine Parameters for Low Emissions Using Taguchi Methods*. SAE, 902075
- Hunter, W.G.**, 1967, *Estimation of unknown constants from multiresponse data*. Ind. Eng. Chem Fundam., 6. 461
- Kailash, C.K.**, *Product and Process design Optimization by design of experiments using Taguchi Methods.*, SAE, 880821
- Khuri, A.I, Cornell John A.**, 1996, *Response Surfaces Designs and Analysis, 2nd edition*. Marcel Dekker, Inc, New York
- Lochner, R.H., Matar J. E.**, 1990, *Designing For Quality: An introduction to the best of Taguchi Methods and Western Methods of Statistical Experimental Design*. Quality Resources, White Planes, NY
- Logo**, 1990, *The Box-Cox Transformations and the Taguchi Method*. Applied Statistics JRSS©, 39, 31-48
- Logothetis, N.**, 1988, *The role of data- transformation in the Taguchi analysis*. Quality and Reliability Engineering International, 4, 49-61
- Logothetis, N., Haigh, A.D.**, 1987, *The Statistical flexibility of the Taguchi Method in the optimisation of multi-response processes*. Professional Statistician, 7, 6
- Logothetis, N.**, 1992, *Managing for total Quality: From Demming to Taguchi and SPC*. Prentice Hall, UK
- Lunneborg, C.E.**, 1994, *Modelling Experimental and Observed Data*. Duxbury Press, California
- Manton, S.M.**, 1988, *Engineering For Quality*. Proceedings of the Institute of Mechanical Engineers, Part B, 202, 19,1988
- Marquardt, D.W.**, 1963, *An algorithm for least squares estimation of non-linear parameters*. J. Soc. Ind. Appl. Math. 2, 431
- Muller, C.A.**, Jan-95, *Design of Inlet Manifold with Fuel Injection using Siamesing*. Mechanical Engineering, University of Stellenbosch
- O'Connor, P.D.T.**, 1991, *Practical Reliability Engineering Third Edition*. Wiley, London
- Orr, S, Folsom**, 1987, *Optimisation of electroplating process for 434 stainless steel*. American Supplier Institute, 5th Symposium
- Peace, Glen Stuart**, 1993, *Taguchi Methods: A Hands-On Approach*, Addison-Wesley Publishing, Reading Massachusetts
- Petzer, D.**, Nov-96, *Optimisation of Carburettor Adapters and Air Cleaners*. Mechanical Engineering, University of Stellenbosch
- Plakett, R.L., Burmann, J. P.**, 1946, *The design of optimum multifactorial experiments*. Biometrika, 33, 305-25
- Plakett, R.L.**, 1930, *Some generalisations in the multifactorial design*. Biometrika, 33, 328

- Quinlan, J**, 1985, *Product Improvement by Application of Taguchi Methods*. ASI News, Winter 1985
- Rosiaux, C.M.J**, 1987, *An Example of Applying a Taguchi-Type Experimental Design*. Revue de le Societe des Ingenieurs de l'Automobile, March 1987
- Roslund, J, Samaniero, C**, 1987, *Changing the product to improve a headlamp aim process*. American Supplier Institute, 5th Symposium, 8-9 October
- Ross, P.J**, Jun-05, *Taguchi Techniques for Quality Engineering, Loss Function, Orthogonal Experiments, Parameter and Tolerance Design*, McGraw-Hill, New York
- Ryan, T.P**, 1989, *Statistical Methods For Quality Improvement*. Wiley, New York
- Shainin, D, Shainin, P**, 1998, *Better than Taguchi Orthogonal Tables*. Quality and Reliability Engineering International, 4, 143-9
- Shetty, R.R, Kinsella, John**, 1992, *Gear Noise Development Using Dr Taguchi's Tolerance Design of Experiment Approach*. SAE, 920763
- Taguchi, Genichi**, 1993, *Taguchi on Robust Technology Development*. American Society of Engineers, New York
- Taylor, A.B**, 1998, *Binnebrand Engines, Mechanical Engineering*, University of Stellenbosch
- Vizard, D**, Dec '93, *Silent but Violent. Fast Car*, Centre for Automotive Engineering, 34
- Yan, R.J.R., Kramer T.**, 1993, *Diesel Combustion and Transien Emissions Optimisation using Taguchi Methods*. SAE, 930600

Appendix A. Channel Listing for ETA Channels (Chapter 3)

Number	Name	function	Units	Modual	High	HighHigh	Low	LowLow	Off-set	Gain
0	Ignition	turn Ignition on	-	AICP-OACJA 220V AC	N/A	N/A	N/A	N/A	N/A	N/A
1	Speed	Frequency	rpm	Frequency 200-20000 Hz	6000	6500	-11	-11	-209	1
2	Torque		Nm	DC Unipolar 0-10 V	1000	1000	-10000	-10000	-77.34	60.7
3	Oil Pressure		kPa	DC current 4 - 20 mA	1000	1000	150	100	-1055	245
4	Water Temperature		°C	J Thermocouple 0-700 °C	95	100	0	0	0	1
5	Oil Temperature		°C	J Thermocouple 0-700 °C	120	125	0	0	0	1
6	Dynomometer Water Temperature			J Thermocouple 0-700 °C	100	130	0	0	0	1
7	Exhaust one Temperature		°C	k Thermocouple 0-1250 °C	850	900	0	0	0	1
8	Exhaust Two Temperature		°C	k Thermocouple -100-950 °C	850	900	0	0	0	1
9	Exhaust Three Temperature		°C	k Thermocouple -100-950 °C	850	900	0	0	0	1
10	Exhaust Four Temperature		°C	k Thermocouple 0-1250 °C	850	900	0	0	0	1
11	Manifold Pressure	0-1 bar absolute		DC current 4 - 20 mA	1000	1000	-1000	-1000	-84.798	17.108
12 to 16	Not Used									
17	Smooth Speed	Average Value over time		Calculated						
18	Smooth Torque	Average Value over time		Calculated						
19	Power			Calculated						
21	Ignition Timing			operator entered						
22	CO1			operator entered						
23	CO2			operator entered						
24	CO3			operator entered						
25	CO4			operator entered						
26	Betzmanometer			operator entered						
27	inclined Manometer			operator entered						
28	Mass Flow	measure fuel flow	kg/s	comm port						
29	Exhaust Average 1,2	Average value	°C	Calculated						
30	Exhaust Average 3,4	Average value	°C	Calculated						
31	Exhaust Average 1,2,3,4	Average Value	°C	Calculated						
32	oil pressure alarm	cut engine on low oil press		operator defined						

Description of each Channel

There are two types of channels in the ETA software. Channels 0-16 are measured channels that measure characteristics from the engine directly and channels 17 upwards are calculated channels.

Measured Channels**Channel 0: Ignition.**

ETA controlled the ignition circuit signal so that the engine could not be started without all the systems first being checked and ready. In the same circuit there were two emergency safety stop buttons, that would cut all power to the system and stop the engine, one in the test cell and one in the control room.

Channel 1: Engine Speed

An inductive speed pick-up was used to measure the engine speed. A toothed gear was attached to the crankshaft behind the fan belt pulley. The pick-up consisted of a powerful permanent magnet and a coil winding. The pickup was mounted close to the teeth on the rotating dish. As each tooth passed through the magnetic field, a voltage was generated in the coil. The frequency of this voltage generation was proportional to the engine speed. The gear that was used in this testing had 59 (60-1) teeth. I.e. that the teeth were machined as though there were 60 teeth but two of them were joined to form a single large tooth. It was the detection of the large induced voltage resulting from the large tooth that determined the TDC position of cylinder one, for both DUPEC and ETA. The engine speed was determined by counting all the teeth and determining the time taken to count 59 teeth (equal to one revolution). The error due to possibly missing a tooth was thus much lower if the probe is counting 59 teeth per revolution instead of counting one tooth per revolution. Engine speed could be calibrated using a tachometer to determine the true engine speed and then validating the reading on ETA. By adjusting the offset and gain in ETA's set-up, the accuracy of the speed-reading was tuned to agree with the tachometer. (See the general calibration procedure at the end of this section)

Channel 2: Dynamometer Torque

As discussed in Chapter 3, the torque was measured using a load cell mounted on the casing of the dynamometer. This load cell was connected via a DC uni-polar 0 to 10 V module in the IO PAK to ETA where the data was recorded. Torque calibration was done by imposing a known torque on the dynamometer casing using a torque arm of known length that was connected to the dynamometer casing, and a suspending a known mass on the end of the arm. The offset and gain was then set in ETA to ensure accurate data. Gain and offset were calculated from a zero and maximum value (240.3 Nm) point with linear interpolation being used within those range values.

Channel 3: Oil Pressure

A 0-10 bar pressure transducer was connected into the oil line and to a 4 to 20 mA module that was used in the IO PAK. Calibration was done with the aid of a pressure gauge and a hand pump to generate a known pressure. The gain and offset in ETA were then determined to give corresponding pressure readings in ETA. The calibration calculation is shown at the end of this section.

Channel 4: Engine Water Temperature

The engine water temperature was monitored in the external water piping for the water using a type J thermocouple. This was monitored with a high and high-high alarm with values as shown in the table above to guard against overheating of the engine. The temperature was controlled using the standard thermostat for the engine and an external heat exchanger.

Channel 5: Engine Oil Temperature

The oil temperature was measured using a type J thermocouple that was mounted in the modified sump plug of the engine. The oil temperature was monitored to guard against engine and oil overheating. The oil would fail at high temperatures and no longer provide the cooling and lubrication needed for correct engine operation conditions. The High-High alarm settings for ETA was coupled with an alarm that would cut the ignition signal and stop the engine, thereby preventing drastic engine damage

Channel 6: Dynamometer Water Temperature

The dynamometer water temperature was monitored to guard against the overheating of the casing that might occur under choked or blocked cooling water flow as well as guarding against torque overload on the dynamometer. A type J thermocouple was mounted in the casing of the dynamometer for this purpose.

Channels 7 through 10: Exhaust Temperature (1,2,3,4)

Four exhaust temperatures were measured (one on each cylinder) to monitor the cylinder to cylinder variation in temperature. Care was taken to ensure that the temperature that was being measured was indeed the temperature representative of the actual gas temperature in the exhaust manifold. Due to the fact that the walls of the manifold are not the same temperatures as the gases that flow in the pipes, the thermocouple probe tips needed to be positioned very accurately. They all needed to be in the middle of the pipe to give an indication of the gas temperature and not be effected by any heat transfer from the manifold walls, and thus show the comparison of the gas temperature unaltered (this proved to be very difficult). Heat transfer to the gas from the walls is also a factor that was taken into consideration so all the thermocouples were positioned the same distance from the exhaust ports. The thermocouples were calibrated using a signal generator to check the thermocouple modules.

Channel 11: Manifold Absolute Pressure (MAP)

MAP was measure using a MAP sensor that measured the absolute pressure in the manifold. It was mounted securely to the instrument panel to avoid detrimental vibration and connected to the manifold by a flexible pipe. This signal was fed into a DC current 4 to 20 mA module in the I/O PAKPLUS before being recorded by ETA.

Channels 12 through 16:

These channels were not needed for this test work

Calculated Channels**Channels 17 and 18: Calculated Smooth torque and speed.**

The values for speed and torque were very variable. In order to obtain a damped reading representative of a time average for test data comparison, ETA calculated channels were used to calculate smooth torque and smooth speed. The user could configure both of these channels to provide an average reading over a specified number of seconds or an average over a specified number of readings.

Channel 19: Calculated Power

Power was calculated from torque and speed measurements as a calculated channel in ETA by the relationship in the equation below.

$$P = (2 \times \pi \times T \times S) / (60 \times 1000) \quad [A-1]$$

Where P is Power [kW], T is Torque [Nm] and S is engine speed [rpm]

Channels 20 through 27: Operator Entered Channels.

There is a provision in ETA where the operator can enter in a number or value, and this will be saved with all the other data relevant to that test point. This is information that ETA does not or cannot monitor remotely, either through the type of data or the lack of available measured channels in the IO PAK. Channels such as CO% for the four exhaust pipes and other emissions data are saved in this way, as well as wet and dry bulb temperatures and airflow data.

Channel 28: Fuel Mass Flow

Mass flow was used to measure the fuel consumption in kg/s. Fuel flow was measured using a mass balance and an intermediate beaker positioned freely on the mass balance. The rate at which the fuel mass was removed from the beaker was measured to give fuel consumption data. The mass was read every ½ second and after 30 seconds the average fuel consumption was calculated and stored as the fuel consumption data. This meant that only equilibrium engine operating conditions had meaningful fuel consumption data. This suited the type of testing that was done. A 4-litre intermediate beaker was used on the mass balance that had a 3-litre capacity for fuelling. Thereafter the beaker would be filled and fuelling data could not be gathered during the filling process. While the intermediate beaker was being filled, ETA would register a 'filling' value in the data log so that the data would not become confusing and create the illusion that the engine was indeed producing fuel.

Fuel was supplied to the intermediate beaker on the mass balance from a 50 litre bulk drum through a standard filter using a standard low-pressure 12-volt fuel pump. This pump, and thus the filling process, was manually operated from the control room for testing undertaken and documented in this document.

Channels 29 through 31: Average Exhaust Temperature.

To give an indication of overall fuelling an average exhaust temperature was used in the calculated channels in ETA. The average calculated channel in ETA however could only calculate the average of two channels at a time and therefore three channels were needed in order to get the average exhaust temperature in °C.

Alarm Channels.

ETA provided for channels that can monitor two or more channels and depending on their values, give an alarm to stop the engine by cutting the ignition channel. For example, when the engine speed is greater than 3000 rpm, the oil pressure must be greater than 3 bar to ensure sufficient lubrication. If this is not the case, then there is a malfunction in the oil supply system, and the ignition signal is cut off before the engine is damaged.

General Calibration Calculation.

All the channels that relied on a gain and offset determination for their calibration require the same process, which is described below.

Set the gain to 1 and the offset to zero. Using two known values (y) record the ETA measured values (x) that correspond to the signal received by ETA. These two readings result in two linear equations both of the form:

$$y = mx + c \text{ with } y_1 \approx x_1 \text{ and } y_2 \approx x_2 \quad [\text{A-2}]$$

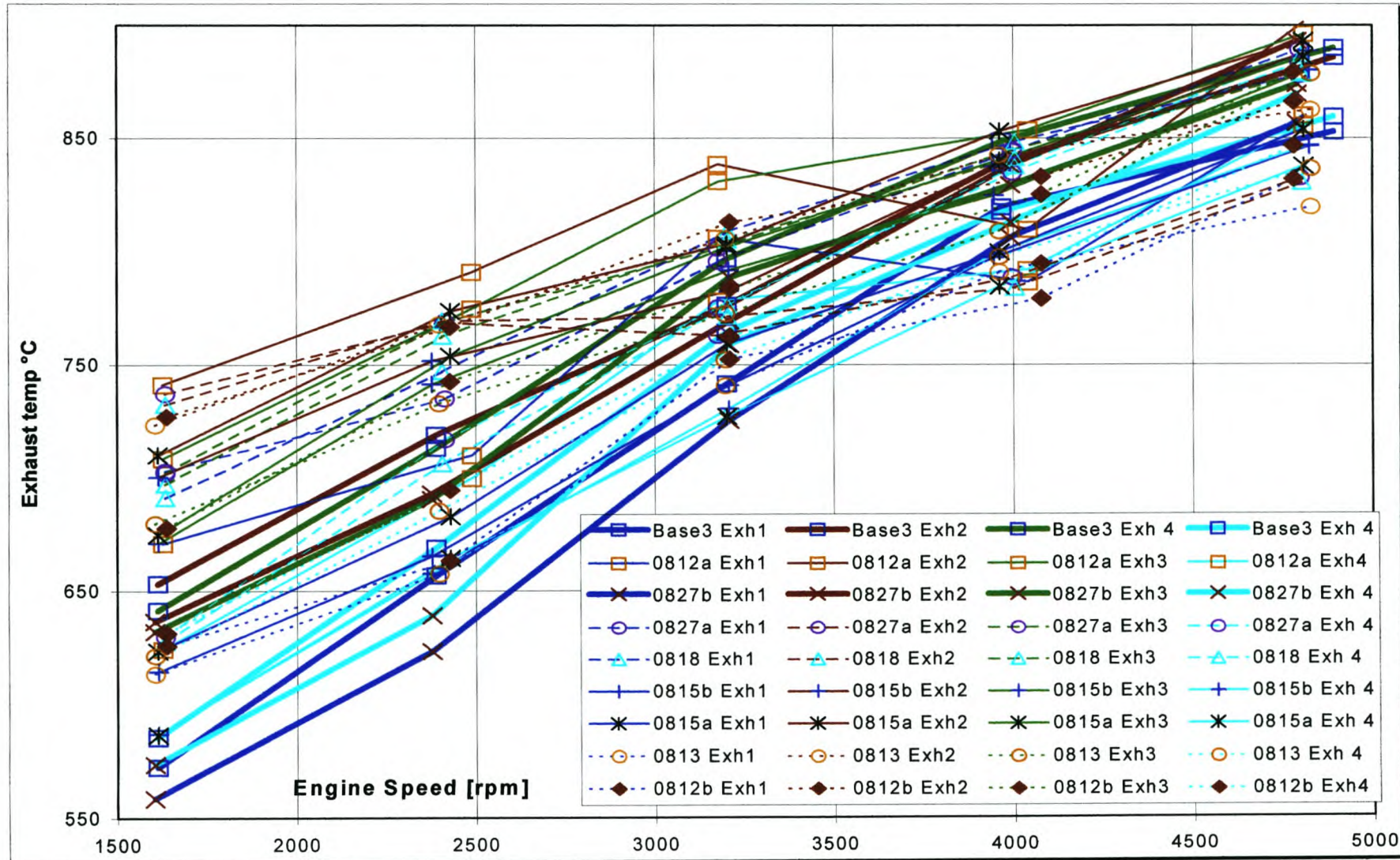
y_1 and y_2 will be the actual variable values (i.e. speed at 1000 rpm and 5000 rpm). x_1 and x_2 will be the I/O module input into ETA (i.e. 4 mA and 20 mA for a 4 to 20 mA module). Solving for the two variables, m (gain) and c (offset) can complete the calibration. The calibration can be refined to be more accurate by setting the offset at a zero set point and the gain at a maximum point. I.e. y_1 and x_1 are at the zero and y_2 and x_2 are at the maximum point to be measured. If the calibration is seen to be incorrect with the offset and gain not equal to 0 and 1 respectively. The offset can be recalibrate at the zero point and the gain at the maximum known point using a ratio or the calibrated reading over the ETA reading vs. the needed gain over the present gain. Solving for the needed gain will recalibrate the channel.

$$\frac{\text{Required Gain}}{\text{Present Gain}} = \frac{\text{Calibrated Reading}}{\text{ETA reading}} \quad [\text{A-3}]$$

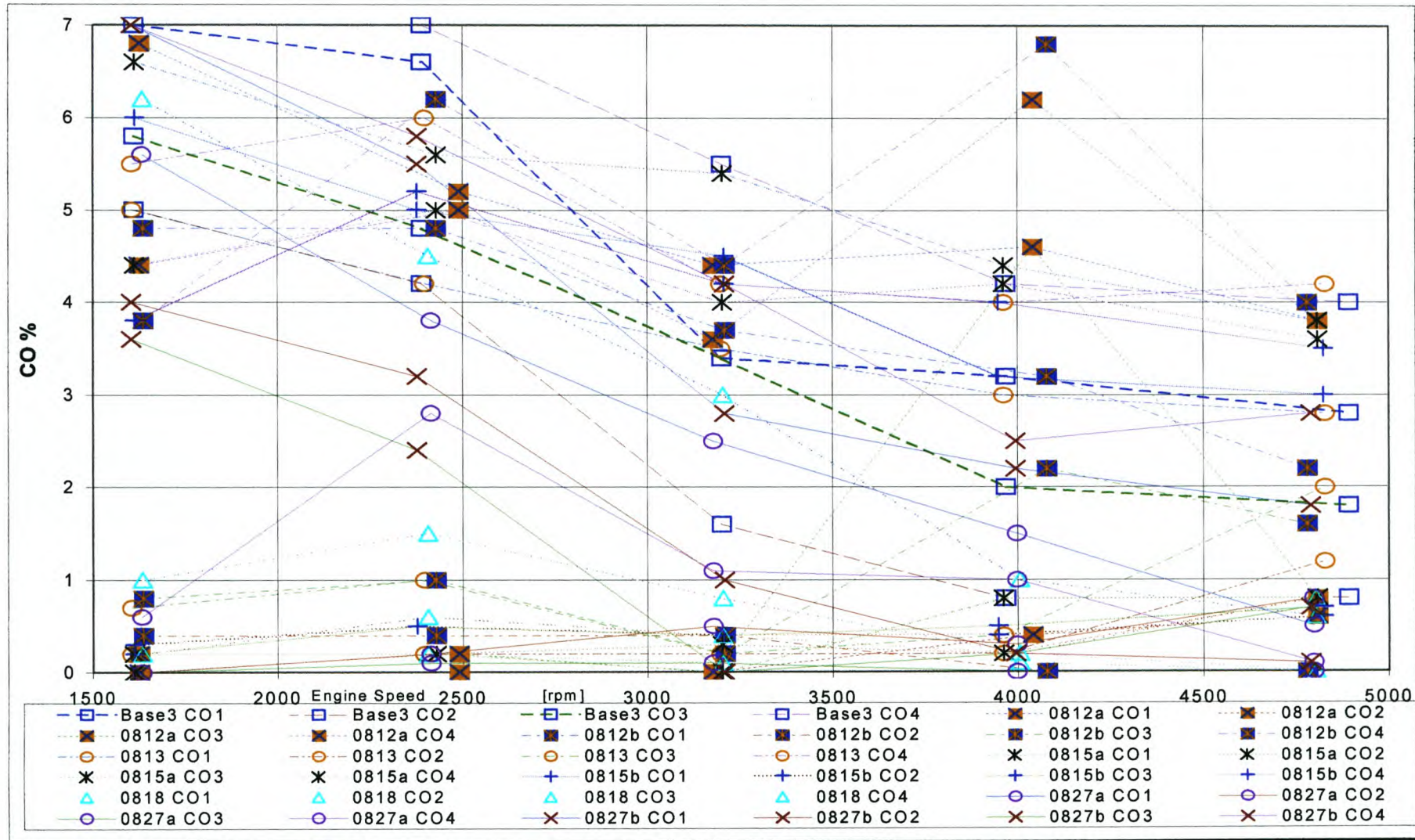
Appendix B. Case Study One Test Summary

Test	Configuration					Plates		comment	Exhaust Temperature						Distribution		CO				CO comment	MRT	TEP			
	Name	Jets	Exhaust	Carb	Inlet piping	COMMENT	Baffle plate		Anti-Swirl Plate	1 [°C]	2 [°C]	3 [°C]	4 [°C]	Average [°C]	Range [°C]	Comparison Exh Temp vs Open Carb (test 2)	Comparison Exh Temp vs Baseline (Test 3)	Exh Temp Comment	Comparison Dist vs open Carburettor (test 2)	Comparison Dist vs Baseline (Test 3)				1	2	3
Test 1	0721	Large	Test	Open	None	Fuelling check	●	●	463-734	556-793	476-721	477-757	631	330	Lowest	Lowest	highest fuelling	-	-	7-3-4 tick shape trend	4.2-2.5 trend	3-0.2 downward trend	6.2-2.5 range	consistant downward trends for all cylinders	171	68.8
Test 2	base3	Small	Std	Open	None	Fuelling check	●	●	572-852	683-885	641-889	585-859	755	318	-	lower	Lower fuelling than test 1	Improved on test 1	Improved on test 1	7-2.8 downward trend	4.7-0.7 downward trend Leanest	5.6-1.8 downward trend	7-4 downward trend Richest	consistant trends for all cylinders, generally richer	166.3	67
Test 3	0812a	Small	Std	Std + filter	Std	Base line	●	●	670-859	741-901	708-896	625-855	786	277	Highest	-	-	Not good	Not good	richest	leanest <0.5%	leaner, spike at 4200rpm	richer, spike at 4200 rpm	very big diff between cyl 1,4 and 2,3	157.6	65
Test 4	0812b	Small	Std	Proto	Std	Run 2	↙	✗	625-831	727-866	688-879	631-879	765	254	same average with flatter trend	lower with flatter trend	Lower than std config (test 3)	Worse	Better	good trend	leanest <0.5%	low, erratic, no trend	rich, erratic, no trend	marked diff between cyl 2,3 and 1,4	155.6	65.4
Test 5	0813	Small	Std	Proto	Std	Run 2	↙	✗	670-818	720-912	680-930	620-830	759	266	same average with flatter trend	lower with similar range	-	similar to Test 4	similar to Test 4	3-5 % good trend	very lean <1%	Very lean <2%	richest, uneven trend.	Different to test 4 on cyl 4	155.9	64.6
Test 6	0815a	Small	Std	Proto	Std	Run 1	↙	↙	620-905	710-890	675-940	580-830	765	307	higher	lower with same trend	Same as test 4	Worse	worse than open carb	3.5-6.5 richest	very lean <1%	very lean <1%	3.5-4.5 stable but erratic	Shows worse distribution	157.7	66.9
Test 7	0815b	Small	Std	Proto	Std	Run 3	✗	↙	665-895	690-940	670-930	580-895	758	302	Higher with flatter trend	flatter and more stable	-	bad	Improved	3-6 downward trend	very lean <0.7%	very lean <0.7%	3.5-5 erratic downward trend	Very bad distribution	159.5	66.7
Test 8	0818	Small	Std	Proto	Std	Run 4	✗	✗	690-928	730-820	690-928	625-938	784	259	higher	comprable values with lower range	Leaner Engine	better, leaner	better, leaner	6-0.5 downward trend	very lean <0.7%	very lean <0.7%	very lean <1.4%	very lean on all cylinders but 1 at low rpm	142.5	58.7
Test 9	0827a	Small	Std	Proto	Std	Run 4	✗	✗	700-940	735-820	700-940	625-935	784	259	higher	comprable values with lower range	-	identicle to test 8	identicle to test 8	5.5-0.4 downward trend	very lean <0.8%	very lean <0.2%	3-0.2 very lean and erratic	lean on all cylinders but 1 at low rpm	145.8	60.9
Test 10	0827b	Small	Std	Open	None	Repeatability	●	●	557-860	635-890	630-925	575-920	743	335	higher	lower	lowest	-	-	7 - 1.8 downward trend	4-0.1 downward trend	3.5 - 0 downward trend	7-2.5 downward trend	consistant trends for all cylinders	166.4	67.1

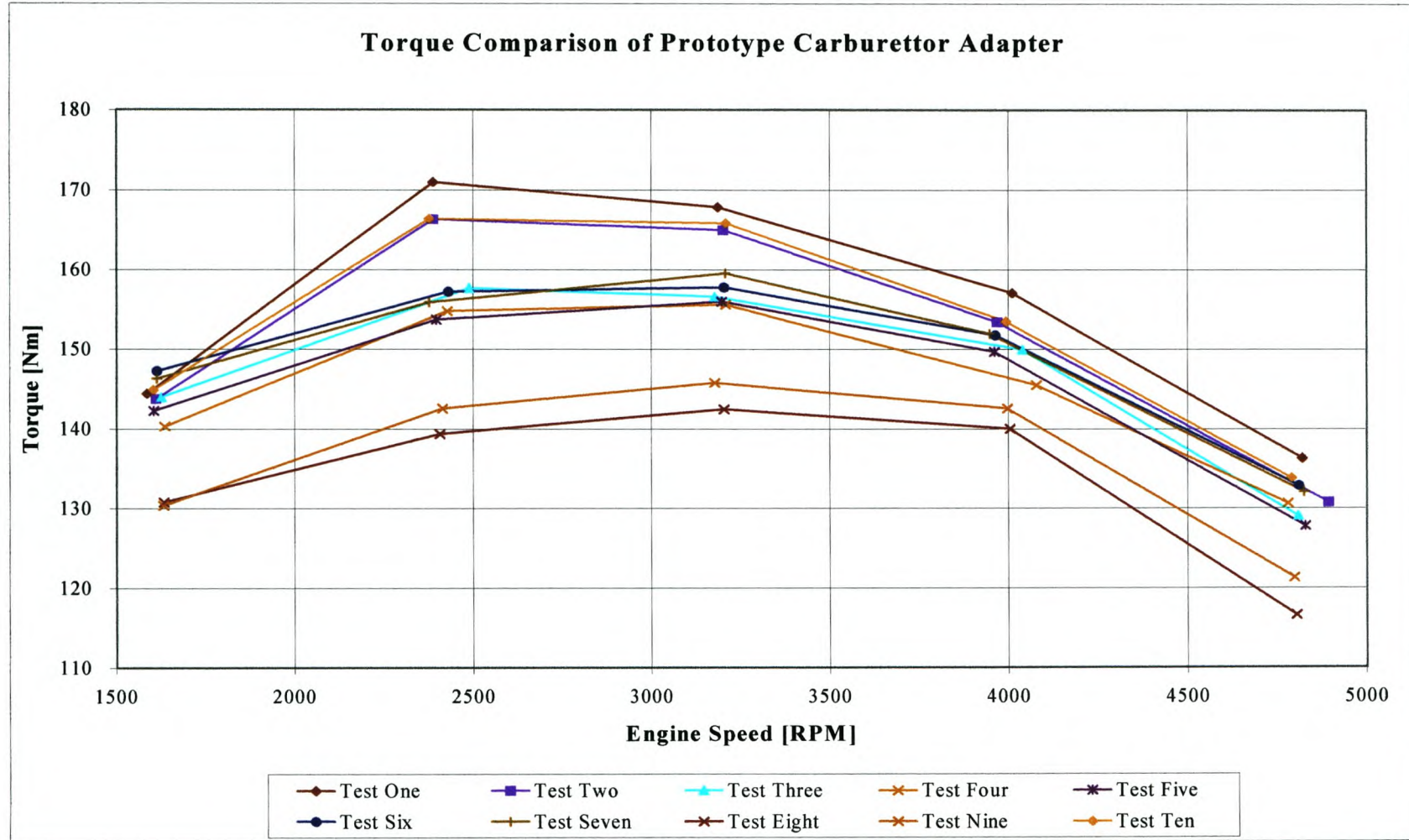
Appendix C. Case Study One Exhaust Temperatures



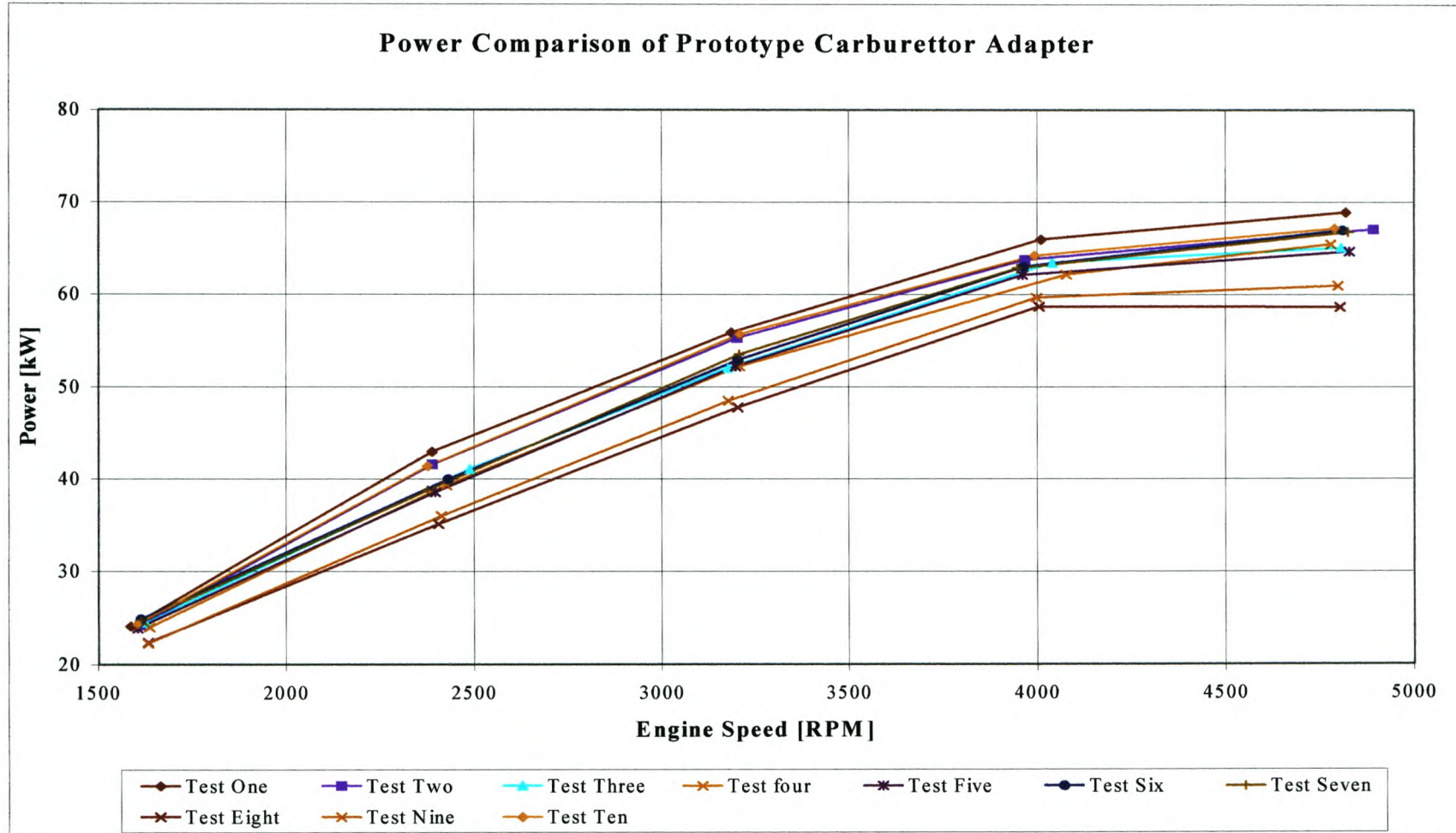
Appendix D. Case Study One CO % Levels



Appendix E. Case Study One Torque Comparison



Appendix F. Case Study One Power Comparison



Appendix G. Case Study One: Carburettor Adapter Results

Exhaust and CO average at 3200

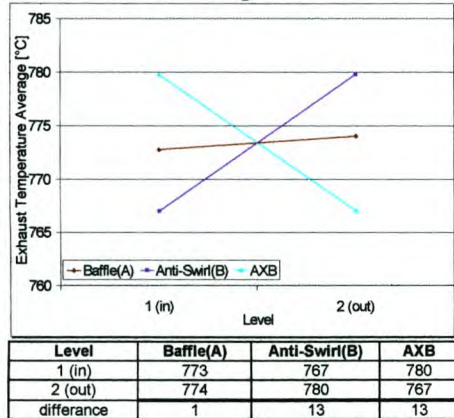


Figure 11-1. Exhaust Average Temperature @ 3200 rpm

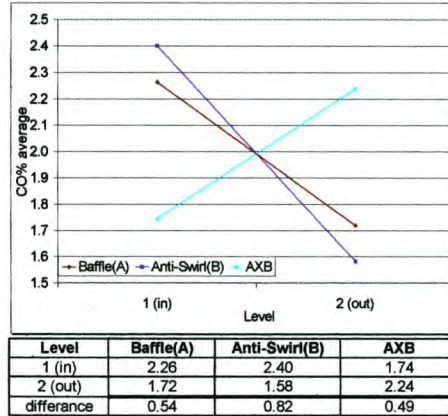


Figure 11-2. CO% Average @ 3200

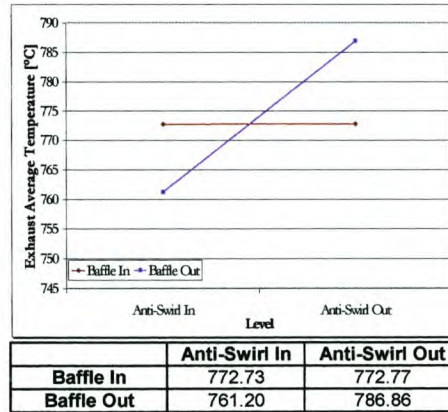


Figure 11-3. Average Exhaust Temp interaction @ 3200rpm

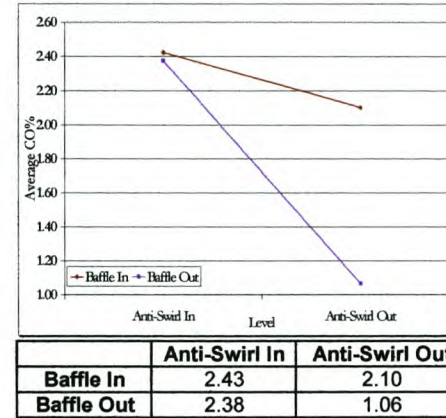


Figure 11-4. Average CO % Interaction @ 3200 rpm.

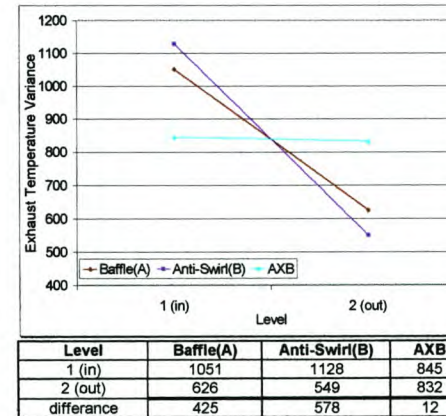


Figure 11-5. Exhaust Temperature Variance @ 3200 rpm.

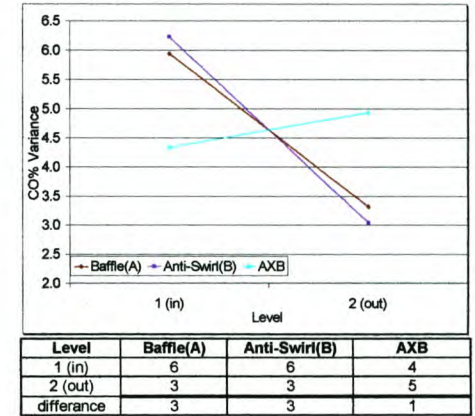


Figure 11-6. CO% Variance @ 3200 rpm.

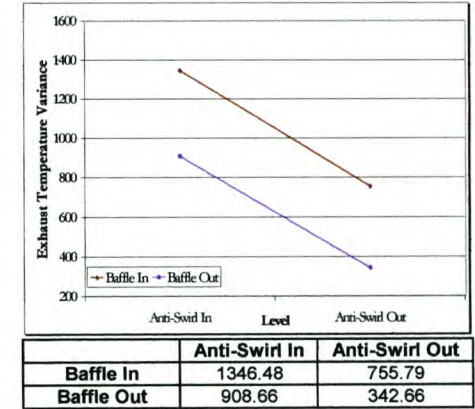


Figure 11-7. Exhaust Temperature Variance @ 3200 rpm.

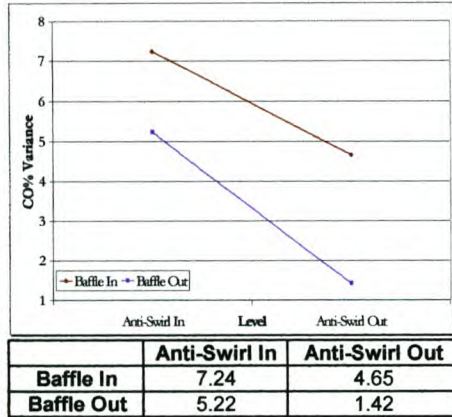


Figure 11-8. CO% Variance @ 3200 rpm.

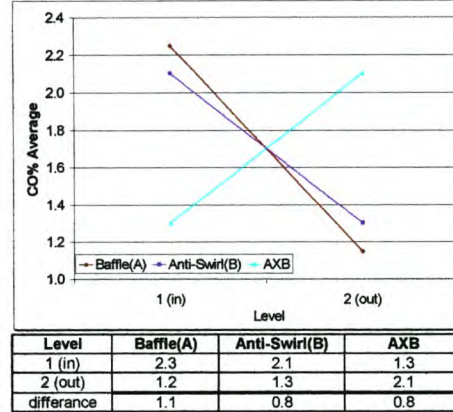


Figure 11-10. Average CO% @ 4800 rpm.

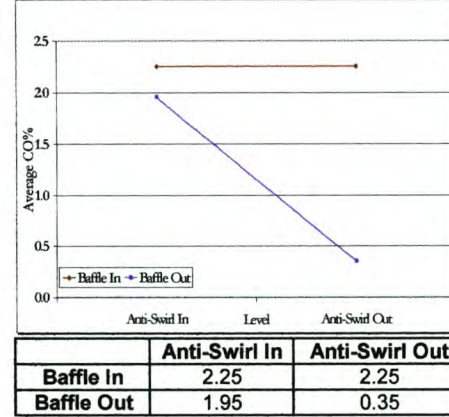


Figure 11-12. Average CO% interaction @ 4800 rpm.

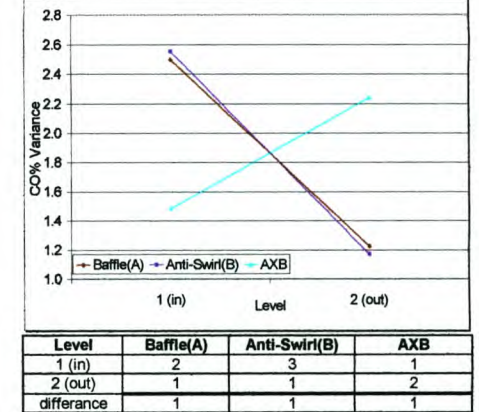


Figure 11-14. CO% Variance @ 4800 rpm.

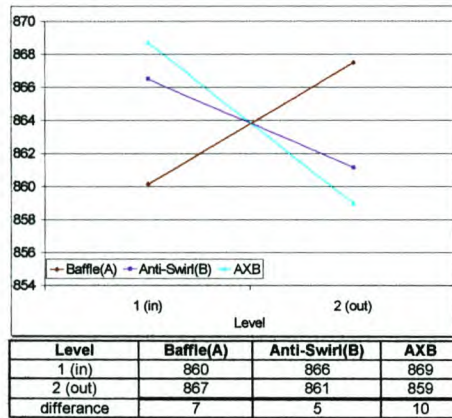


Figure 11-9. Exhaust Average Temperature @ 4800 rpm.

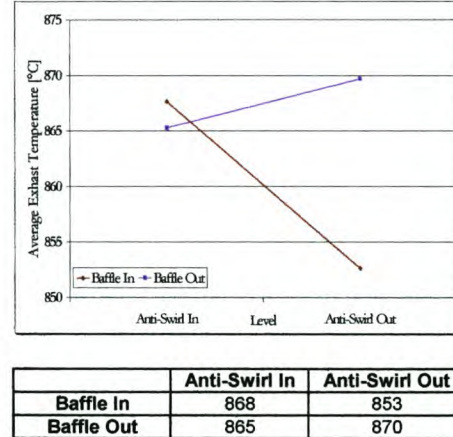


Figure 11-11. Average Exhaust Temperature interaction @ 4800 rpm.

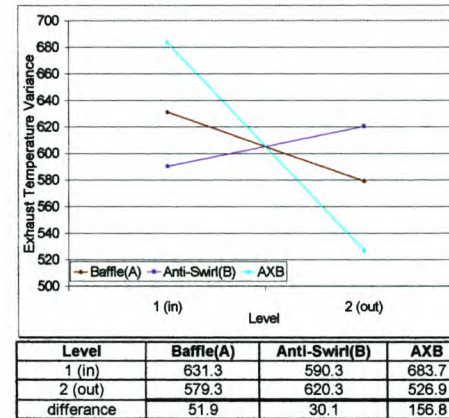


Figure 11-13. Exhaust Temperature Variance @ 4800 rpm.

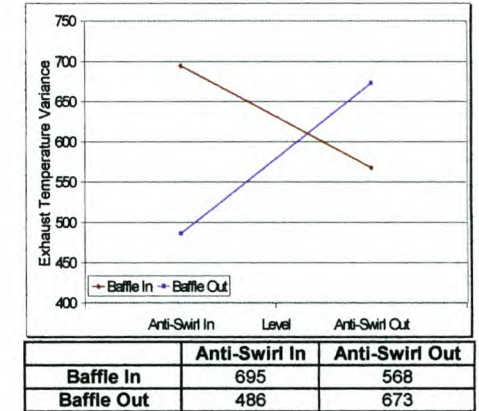
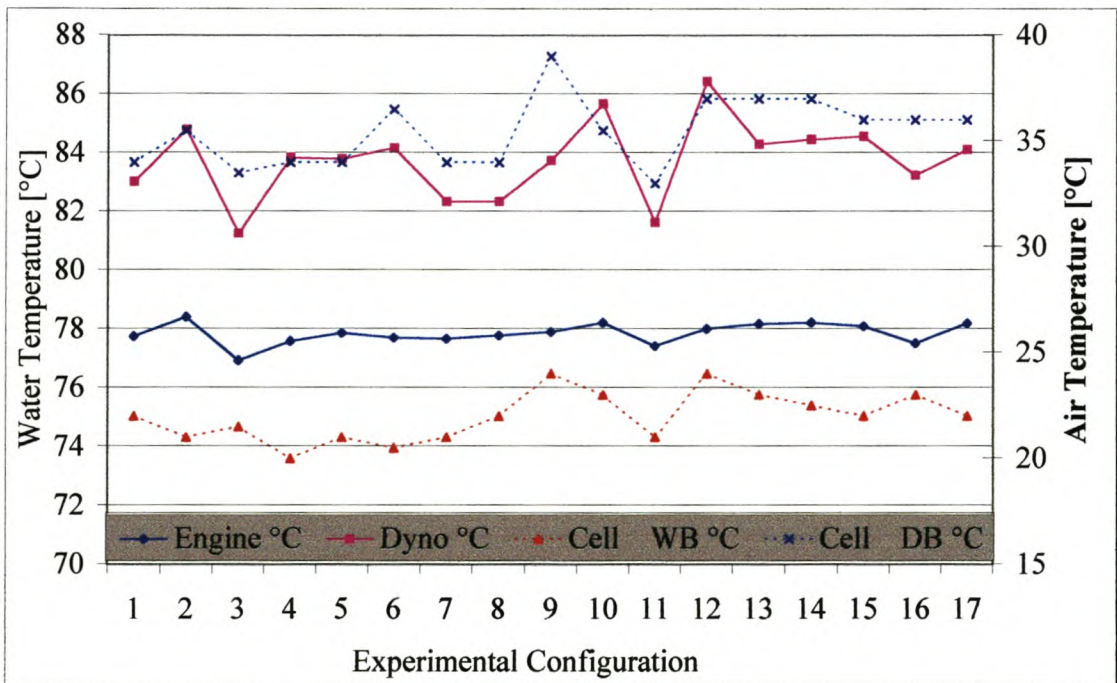
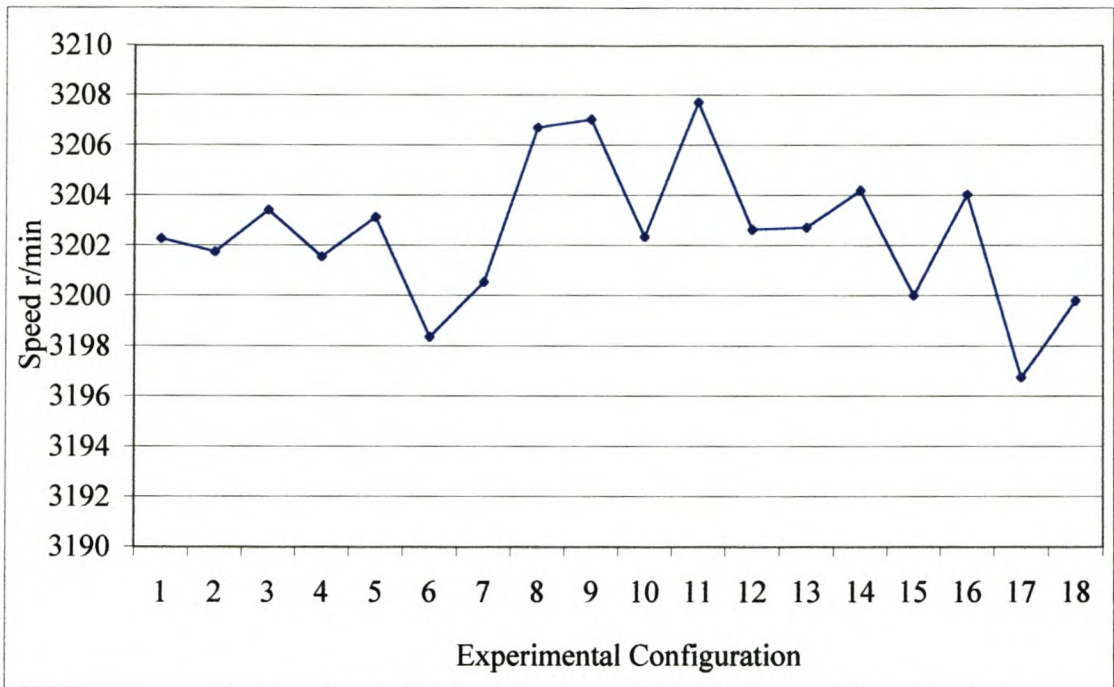


Figure 11-15. Exhaust Temperature Variance @ 4800 rpm.

Appendix H. Case Study Two Data Verification



Appendix I. Case Study Two: Birdcage Application Tabular Results Summary

4800 rpm							Engine		Fuel System			ECU		Oil		Water System Temperature		Air Induction System					Exhaust System Emmissions								
Config	Feed Pipe F	Length	height	Plenum F	Block	Plenum	diffuser	Corr. Power	Corr. Torque	Flow	S.F.C.	Pres	Injet Duration	Spark Adv	Press	Temp.	Engine	Dyno	Cell WB	Cell DB	Air in	Betz	Inclined	Manif Abs Press	CO1	CO2	CO3	CO4	CO average1	CO average2	
No	mm	mm	mm	mm	No	No	No	kW	Nm	kg/hr	g/kWhr	kPa	ms	°CA	kPa	°C	°C	°C	°C	°C	°C	°C	mm H2O	mm H2O	kPa	%VOL	%VOL	%VOL	%VOL	%VOL	%VOL
1	50	530	40	161	1	1	7	67.0	133.3	21.0	313	2.90	4.37	-	359	116.5	79.9	92.3	20	31	31	93.2	166	94.1	5.0	4.5	4.9	5.3	4.7	4.7	
6	60	670	60	161	1	6	6	68.2	135.5	20.1	295	2.95	4.03	-	349	117.4	81.0	94.5	21	35	35	95.4	170	93.0	3.7	3.4	3.4	4.2	4.0	3.8	
8	70	600	60	180	1	8	3	67.8	134.9	20.3	300	2.95	4.37	-	362	116.3	79.3	90.8	22	35	35	94.0	171	95.5	4.1	3.5	3.9	4.7	3.8	3.8	
12	50	670	50	180	1	2	8	67.1	133.2	10.7	159	2.90	4.22	-	358	111.8	79.2	93.0	19	30	30	92.4	165	92.6	4.7	4.9	4.9	4.3	4.7	4.8	
13	60	530	50	200	1	5	5	67.9	134.6	16.6	244	3.00	4.42	-	354	114.1	79.5	93.5	20	32	32	95.0	169	94.7	4.1	4.4	4.5	5.2	4.6	4.0	
17	70	600	40	200	1	9	1	67.9	135.1	13.9	205	2.95	4.13	-	350	117.9	80.7	93.8	20	34	34	93.6	167	93.1	4.7	4.0	4.9	5.3	4.9	4.3	
2	50	600	50	180	2	2	8	66.9	133.1	17.6	264	3.00	4.42	-	356	116.0	80.5	91.3	20	30	30	94.4	168	94.3	3.6	3.1	3.0	3.7	3.4	3.4	
4	60	530	40	180	2	4	4	64.1	127.3	11.9	186	3.00	4.32	-	355	117.4	81.0	90.3	23	36	36	90.5	163	91.0	3.9	3.6	4.0	4.1	3.8	3.9	
9	70	670	40	200	2	9	1	66.9	133.0	15.3	228	3.00	4.51	-	350	119.9	81.3	92.6	21	34	34	94.0	163	94.7	4.2	3.8	4.0	4.2	4.5	4.0	
10	50	530	60	200	2	3	9	66.8	132.7	12.9	194	3.00	4.46	-	344	119.9	81.3	94.2	22	34	34	95.4	169	94.1	3.5	3.4	3.2	3.4	3.5	3.6	
14	60	600	60	161	2	6	6	66.9	133.1	20.4	305	3.00	4.42	-	358	119.4	80.1	90.8	19	29	29	93.4	167	94.9	4.6	3.4	3.5	3.3	3.3	3.9	
18	70	670	50	161	2	7	2	67.5	134.5	10.0	148	3.00	4.51	-	344	120.9	81.3	95.7	22	34	34	88.6	160	94.7	4.2	3.7	4.0	4.5	4.0	4.0	
3	50	670	60	200	3	3	9	67.5	134.4	12.2	180	3.00	4.32	-	356	110.9	79.0	93.0	23	37	37	94.4	170	94.2	4.2	3.4	4.2	5.1	4.5	3.5	
5	60	600	50	200	3	5	5	68.1	135.2	23.4	343	3.00	4.46	-	354	116.3	80.8	94.1	23	37	37	88.0	160	94.8	4.8	4.5	4.8	5.0	5.0	4.0	
7	70	530	50	161	3	7	2	68.3	135.6	20.9	306	3.00	4.37	-	350	122.3	81.3	94.8	23	37	37	91.0	164	94.9	4.2	2.9	4.6	3.6	4.0	4.0	
11	50	600	40	161	3	1	7	67.4	134.1	19.4	288	3.00	4.22	-	357	118.0	80.3	92.4	23	36	36	95.2	173	94.5	3.4	3.0	2.9	3.5	3.5	3.0	
15	60	670	40	180	3	4	4	67.7	134.6	20.6	304	2.90	4.42	-	353	115.0	80.9	93.8	23	36	36	97.0	173	94.3	4.2	4.3	4.7	5.2	4.0	5.1	
16	70	530	60	180	3	8	3	67.9	135.1	20.9	307	2.90	4.42	-	349	116.1	81.1	94.3	22	37	37	94.6	169	94.7	4.6	4.7	4.5	4.6	3.3	5.1	

Exhaust System Emmissions						Exhaust System Emmissions						Exhaust System Emmissions						Exhaust System Emmissions						Exhaust System Emmissions				
CO21	CO22	CO23	CO24	CO2 average1	CO2 average2	Lambda1	Lambda2	Lambda3	Lambda4	Lambda average1	Lambda average2	O21	O22	O23	O24	O2 average1	O2 average2	HC1	HC2	HC3	HC4	HC average1	HC average2	Ex1	Ex2	Ex3	Ex4	Exrange
%VOL	%VOL	%VOL	%VOL	%VOL	%VOL	%VOL	%VOL	%VOL	%VOL	%VOL	%VOL	%VOL	%VOL	%VOL	%VOL	%VOL	%VOL	ppm	ppm	ppm	ppm	ppm	ppm	°C	°C	°C	°C	°C
12.04	13.00	11.97	12.14	12.16	12.16	0.86	0.89	0.87	0.87	0.88	0.88	0.40	0.40	0.39	0.31	0.40	0.40	252	236	257	215	230	230	825	826	817	810	17
12.58	13.20	13.24	12.90	12.74	12.70	0.91	0.91	0.91	0.91	0.90	0.90	0.42	0.43	0.43	0.34	0.37	0.43	255	266	247	210	245	260	835	841	831	820	21
12.40	12.85	12.81	12.71	12.55	12.53	0.89	0.91	0.89	0.88	0.89	0.90	0.40	0.40	0.41	0.30	0.38	0.43	198	202	227	187	195	200	843	848	832	821	27
12.47	12.44	12.76	12.29	12.00	11.84	0.89	0.88	0.87	0.89	0.87	0.86	0.42	0.40	0.41	0.32	0.42	0.38	257	266	273	220	253	233	821	824	815	804	21
12.68	12.36	12.28	12.19	12.04	12.67	0.90	0.99	0.88	0.86	0.88	0.89	0.47	0.39	0.40	0.29	0.38	0.46	282	262	263	221	258	259	822	823	816	808	16
12.19	12.66	12.09	11.79	12.01	12.25	0.88	0.89	0.87	0.85	0.86	0.88	0.41	0.39	0.38	0.28	0.37	0.46	274	283	279	225	270	259	824	829	820	808	22
12.98	13.19	13.15	13.20	13.00	12.78	0.91	0.91	0.92	0.91	0.92	0.91	0.44	0.44	0.47	0.35	0.45	0.44	236	227	239	222	229	223	838	844	832	821	23
12.89	12.89	12.69	12.70	12.56	12.72	0.91	0.91	0.90	0.89	0.91	0.90	0.45	0.43	0.41	0.33	0.41	0.45	253	244	251	215	227	253	836	838	827	818	20
12.55	12.72	12.51	12.40	12.22	12.58	0.89	0.88	0.89	0.88	0.88	0.90	0.40	0.41	0.39	0.39	0.40	0.41	297	291	282	213	256	292	833	842	826	814	28
12.94	12.80	13.99	12.90	12.80	12.71	0.92	0.93	0.91	0.91	0.91	0.91	0.45	0.46	0.47	0.36	0.44	0.45	258	268	256	206	246	252	842	848	834	824	24
12.27	12.23	12.92	13.00	12.88	12.69	0.88	0.91	0.91	0.91	0.91	0.90	0.39	0.41	0.45	0.37	0.42	0.45	232	227	250	260	216	233	834	842	830	819	23
12.50	12.92	12.77	12.50	12.52	12.66	0.89	0.91	0.90	0.89	0.89	0.90	0.47	0.44	0.43	0.31	0.42	0.42	248	254	240	230	234	246	842	849	834	824	25
12.72	12.92	12.00	12.77	12.08	12.76	0.89	0.91	0.89	0.89	0.88	0.90	0.43	0.43	0.42	0.33	0.39	0.47	298	277	292	245	262	281	831	840	825	815	25
12.37	12.30	12.37	12.26	12.30	12.49	0.88	0.88	0.87	0.87	0.89	0.89	0.40	0.40	0.41	0.30	0.41	0.46	289	283	298	230	261	283	826	836	821	811	25
12.58	13.04	12.09	12.91	12.28	12.57	0.89	0.90	0.87	0.90	0.89	0.90	0.42	0.43	0.42	0.35	0.45	0.43	242	250	250	240	229	228	843	853	839	827	26
12.90	13.25	13.30	13.13	13.01	13.06	0.91	0.93	0.93	0.90	0.91	0.92	0.46	0.42	0.48	0.34	0.45	0.43	225	221	248	210	220	220	847	855	841	831	24
12.63	12.60	12.19	12.01	12.84	11.75	0.90	0.88	0.88	0.86	0.86	0.91	0.44	0.42	0.41	0.31	0.37	0.45	245	273	278	221	253	249	828	833	822	812	22
12.97	12.60	12.50	12.65	12.94	11.95	0.87	0.87	0.89	0.88	0.92	0.87	0.37	0.37	0.41	0.33	0.52	0.36	255	255	266	218	249	243	830	836	822	812	25

3200 rpm									Engine		Fuel System			ECU		Oil		Water System		Air Induction System					Exhaust System						
test	Config	Feed Pipe F	Length	height	Plenum F	Block	Plenum	diffuser	Corr. Power	Corr. Torque	Flow	S.F.C.	Pres	Injet Duration	Spark Adv	Press	Temp.	Temperature		Cell WB	Cell DB	Air in	Betz	Inclined	Manif Abs Press	Emmissions					
																		Engine	Dyno							CO1	CO2	CO3	CO4	CO average1	CO average2
No	No	mm	mm	mm	mm	No	No	No	kW	Nm	kg/hr	g/kWhr	kPa	ms	°CA	kPa	°C	°C	°C	°C	°C	°C	mm H2O	mm H2O	kPa	%VOL	%VOL	%VOL	%VOL	%VOL	%VOL
1	1	50	530	40	161	1	1	7	54.4	162.1	14.3	263	2.90	4.46	-	335	111.1	77.8	83.0	22	34	34	65.9	120	96.9	3.2	2.7	2.7	3.2	3.3	3.
2	6	60	670	60	161	1	6	6	55.1	164.5	14.8	269	2.95	4.18	-	328	110.0	78.4	84.8	21	36	36	67.4	123	95.3	3.2	3.1	3.0	3.3	3.0	3.
3	8	70	600	60	180	1	8	3	54.6	162.7	14.4	263	2.90	4.42	-	337	108.9	76.9	81.3	22	34	34	66.6	123	97.5	2.9	2.5	2.4	2.7	2.5	2.
4	12	50	670	50	180	1	2	8	54.8	163.4	14.7	268	2.90	4.32	-	333	109.3	77.6	83.8	20	34	34	67.2	121	95.2	3.2	2.5	3.0	3.4	2.9	3.
5	13	60	530	50	200	1	5	5	54.6	162.8	14.1	258	2.90	4.51	-	332	109.8	77.9	83.8	21	34	34	68.0	123	97.1	3.1	2.4	2.6	2.7	2.4	2.
6	17	70	600	40	200	1	9	1	55.0	164.2	14.5	264	2.90	4.27	-	328	111.3	77.7	84.2	21	37	37	67.6	123	95.5	3.7	3.1	2.8	3.3	3.0	3.
7	2	50	600	50	180	2	2	8	54.7	163.2	12.7	233	3.00	4.46	-	329	111.9	77.7	82.3	21	34	34	67.0	122	96.8	2.5	2.7	2.8	2.9	2.9	2.
8	4	60	530	40	180	2	4	4	52.4	156.0	10.0	190	3.00	4.37	-	331	111.2	77.8	82.3	22	34	34	65.1	120	94.9	3.3	2.9	2.9	3.2	3.1	3.
9	9	70	670	40	200	2	9	1	55.0	163.9	11.7	212	3.00	4.46	-	328	112.6	77.9	83.7	24	39	39	68.4	126	96.9	3.2	2.8	3.0	3.2	3.1	3.
10	10	50	530	60	200	2	3	9	54.6	162.9	11.3	207	3.00	4.56	-	323	111.8	78.2	85.7	23	36	36	67.0	124	96.5	3.6	3.2	3.2	3.5	3.3	3.
11	14	60	600	60	161	2	6	6	55.0	163.7	12.2	221	3.00	4.46	-	335	110.6	77.4	81.6	21	33	33	66.4	121	97.2	3.0	2.7	2.9	2.9	3.0	3.
12	18	70	670	50	161	2	7	2	55.0	164.1	14.3	260	3.00	4.56	-	326	113.2	78.0	86.4	24	37	37	64.8	119	96.8	2.9	2.4	2.2	2.1	3.0	2.
13	3	50	670	60	200	3	3	9	55.1	164.3	14.8	269	3.00	4.42	-	331	109.9	78.2	84.3	23	37	37	66.8	123	96.7	3.8	3.3	3.0	3.4	3.3	3.
14	5	60	600	50	200	3	5	5	55.2	164.4	15.3	278	3.00	4.42	-	332	113.0	78.2	84.5	23	37	37	63.8	118	96.9	3.7	3.1	3.0	3.6	3.7	3.
15	7	70	530	50	161	3	7	2	54.6	163.1	14.7	268	3.00	4.42	-	330	110.8	78.1	84.6	22	36	36	65.4	119	97.0	2.9	3.2	3.2	3.5	3.6	3.
16	11	50	600	40	161	3	1	7	54.5	162.5	14.5	267	3.00	4.37	-	335	110.9	77.5	83.2	23	36	36	66.8	124	97.1	3.4	3.1	3.2	3.5	3.5	3.
17	15	60	670	40	180	3	4	4	54.5	162.7	14.7	269	2.90	4.42	-	330	110.0	78.2	84.1	22	36	36	68.4	125	96.7	3.7	3.2	3.0	3.4	3.2	3.
18	16	70	530	60	180	3	8	3	54.5	162.7	14.2	260	2.90	4.42	-	327	110.9	78.0	84.3	22	37	37	69.0	125	96.9	2.9	2.3	2.5	2.7	2.7	2.

Exhaust System Emissions						Exhaust System Emissions						Exhaust System Emissions						Exhaust System Emissions						Exhaust System Emissions				
CO21	CO22	CO23	CO24	CO2 average1	CO2 average2	Lambda1	Lambda2	Lambda3	Lambda4	Lambda average1	Lambda average2	O21	O22	O23	O24	O2 average1	O2 average2	HC1	HC2	HC3	HC4	HC average1	HC average2	Ex1	Ex2	Ex3	Ex4	Exhange
%VOL	%VOL	%VOL	%VOL	%VOL	%VOL	%VOL	%VOL	%VOL	%VOL	%VOL	%VOL	%VOL	%VOL	%VOL	%VOL	%VOL	%VOL	ppm	ppm	ppm	ppm	ppm	ppm	°C	°C	°C	°C	°C
13.06	13.55	13.54	13.26	12.95	13.20	0.91	0.93	0.93	0.92	0.92	0.92	0.33	0.37	0.37	0.29	0.35	0.36	196	188	210	183	193	190	779	785	768	773	16
13.48	13.57	13.53	13.40	13.40	13.42	0.92	0.92	0.93	0.91	0.93	0.92	0.31	0.34	0.35	0.28	0.33	0.36	203	214	215	187	205	205	770	779	765	756	23
13.49	13.60	13.63	13.70	13.48	13.45	0.93	0.94	0.94	0.93	0.94	0.94	0.33	0.39	0.39	0.30	0.38	0.37	165	171	193	167	178	169	784	792	773	779	19
13.39	13.66	13.33	13.34	13.01	13.37	0.92	0.93	0.92	0.91	0.91	0.93	0.33	0.35	0.34	0.28	0.42	0.36	200	196	219	190	195	184	768	775	763	757	18
13.36	13.73	13.79	13.70	13.66	13.40	0.92	0.94	0.94	0.93	0.94	0.93	0.34	0.41	0.39	0.31	0.39	0.39	203	210	195	170	194	190	784	792	773	782	19
12.98	13.32	13.41	13.33	13.19	13.32	0.91	0.92	0.92	0.92	0.92	0.92	0.32	0.35	0.35	0.28	0.35	0.37	227	226	220	184	218	200	772	778	766	758	20
13.52	13.50	13.47	13.52	13.35	13.35	0.92	0.93	0.92	0.92	0.93	0.93	0.34	0.35	0.35	0.30	0.37	0.37	198	198	211	193	220	220	774	781	767	764	17
13.21	13.41	13.42	13.30	13.15	13.22	0.92	0.93	0.93	0.92	0.92	0.92	0.31	0.35	0.39	0.31	0.30	0.37	195	197	225	198	202	207	773	780	766	765	15
13.26	13.45	13.37	13.32	13.27	13.31	0.91	0.93	0.92	0.92	0.92	0.92	0.31	0.35	0.35	0.30	0.38	0.37	225	220	220	202	216	228	778	786	771	765	20
12.94	13.19	13.14	13.02	12.98	12.98	0.90	0.92	0.92	0.90	0.91	0.91	0.30	0.34	0.36	0.31	0.36	0.34	224	219	229	215	226	235	773	780	764	767	17
13.39	13.65	13.45	13.43	13.30	13.30	0.92	0.93	0.93	0.92	0.93	0.93	0.32	0.36	0.40	0.30	0.36	0.36	187	189	205	190	199	199	774	779	766	759	20
13.56	13.77	13.75	13.92	13.61	13.28	0.93	0.94	0.95	0.95	0.93	0.94	0.33	0.38	0.38	0.35	0.37	0.39	202	199	198	182	213	197	785	791	776	779	15
12.71	13.13	13.18	13.00	13.02	12.99	0.89	0.91	0.92	0.91	0.92	0.92	0.33	0.36	0.38	0.31	0.38	0.39	233	244	242	209	229	220	772	777	763	768	14
13.07	13.26	13.30	12.95	13.17	13.25	0.90	0.92	0.92	0.90	0.91	0.92	0.33	0.38	0.37	0.29	0.38	0.38	220	224	216	201	220	220	777	786	769	772	17
13.00	13.24	13.26	12.99	12.88	13.34	0.92	0.92	0.91	0.90	0.91	0.92	0.34	0.34	0.35	0.30	0.34	0.38	191	201	213	190	198	180	779	788	769	773	19
13.05	13.19	13.20	13.05	12.84	13.11	0.91	0.93	0.92	0.91	0.91	0.92	0.32	0.37	0.34	0.30	0.38	0.40	195	208	210	199	209	220	774	780	765	770	16
13.04	13.31	13.38	13.19	13.04	13.10	0.90	0.92	0.91	0.90	0.91	0.92	0.30	0.36	0.35	0.29	0.36	0.38	196	220	216	195	218	204	774	783	764	768	18
13.55	13.76	13.61	13.74	13.50	13.53	0.93	0.94	0.93	0.93	0.94	0.94	0.34	0.38	0.33	0.31	0.39	0.38	190	196	207	180	187	197	785	793	775	779	18

Appendix J. Birdcage Graph Results

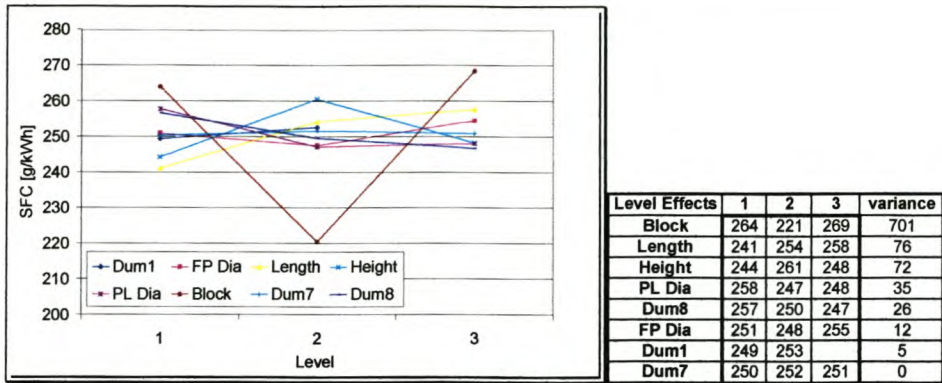


Figure 11-1. SFC @ 3200 rpm.

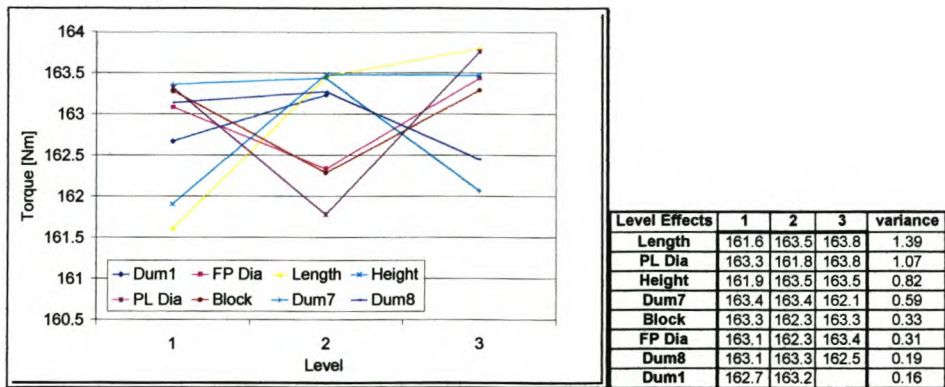


Figure 11-2. Torque @ 3200 rpm.

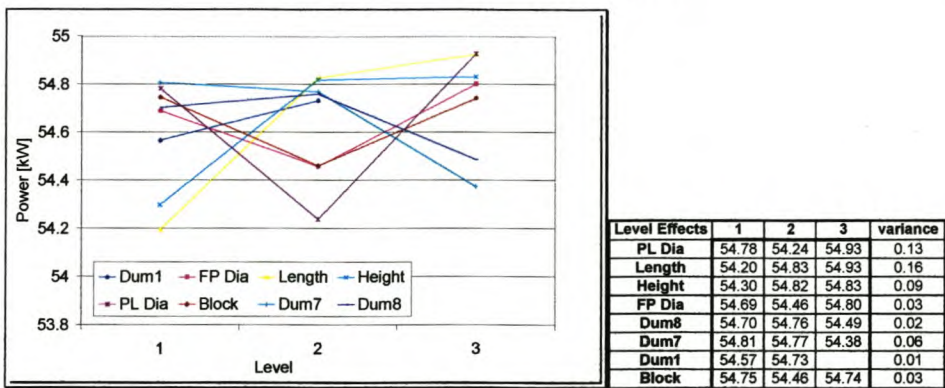


Figure 11-3. Power @ 3200 rpm.

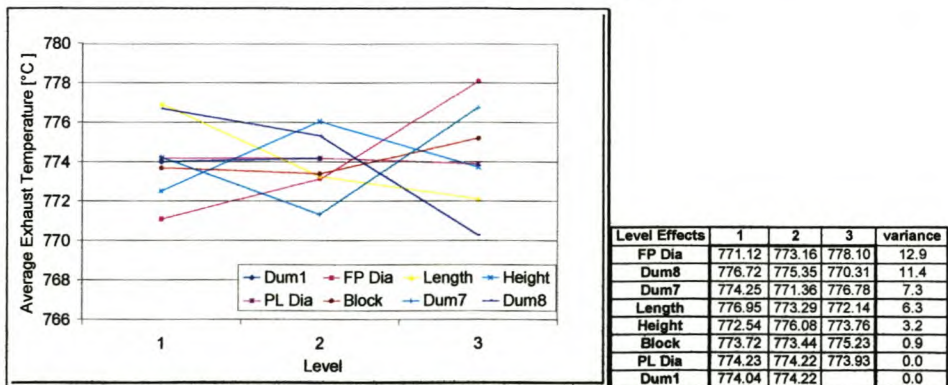


Figure 11-4. Average Exhaust Temp @ 3200 rpm.

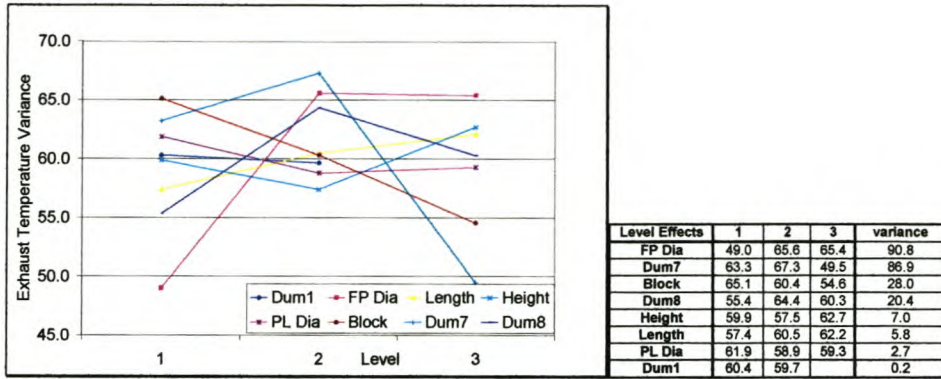


Figure 11-5. Exhaust Temperature Variance @ 3200 rpm.

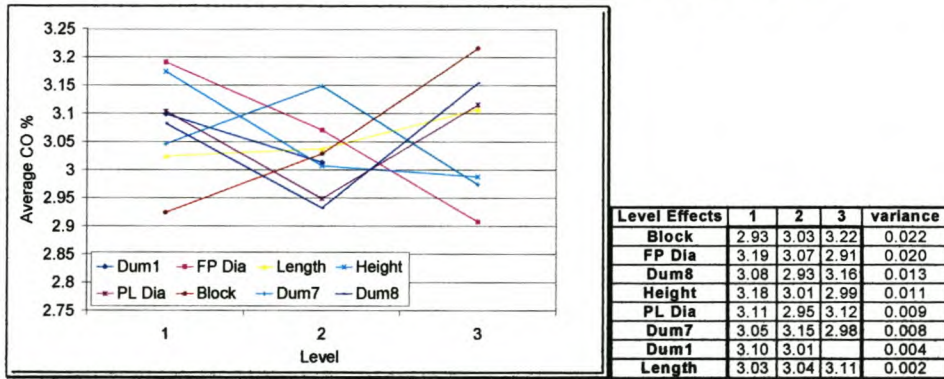


Figure 11-6. Average CO% @ 3200 rpm.

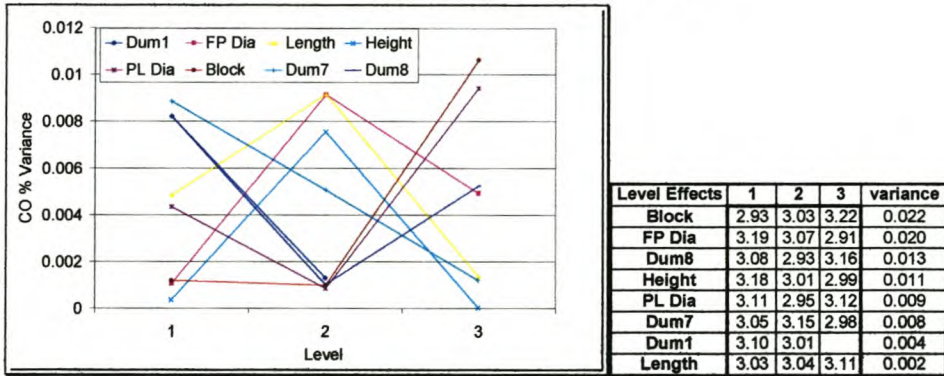


Figure 11-7. CO% Variance @ 3200 rpm.

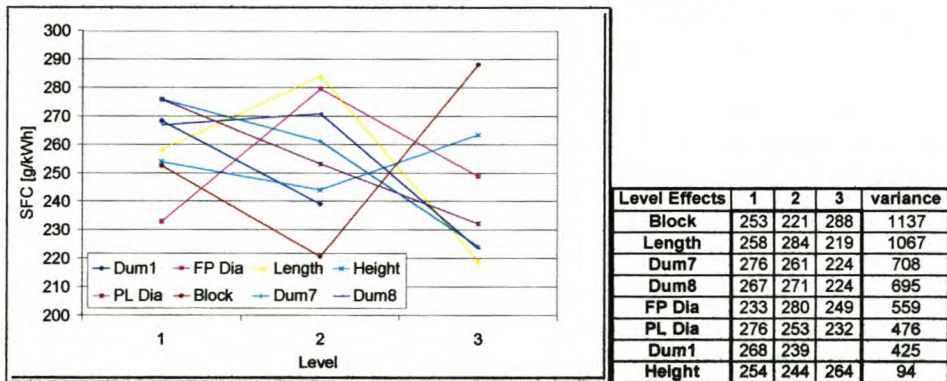


Figure 11-8. SFC @ 4800 rpm.

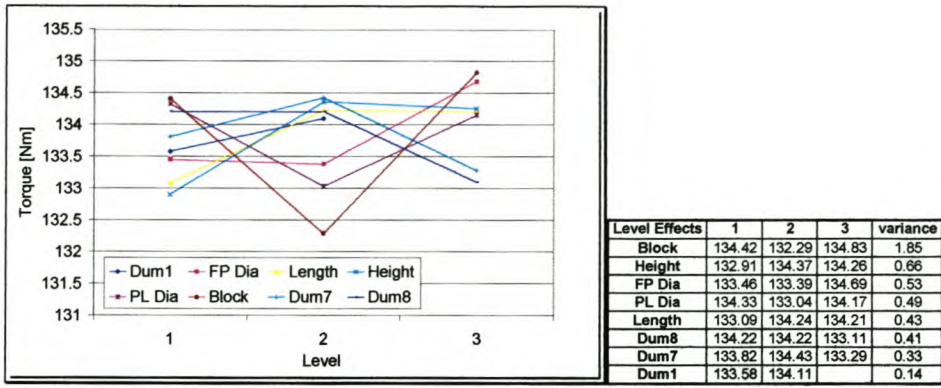


Figure 11-9. Torque @ 4800 rpm.

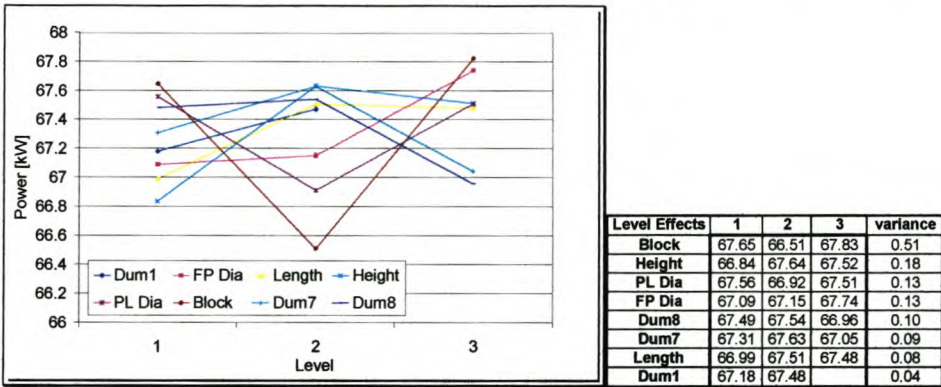


Figure 11-10. Power @ 4800 rpm.

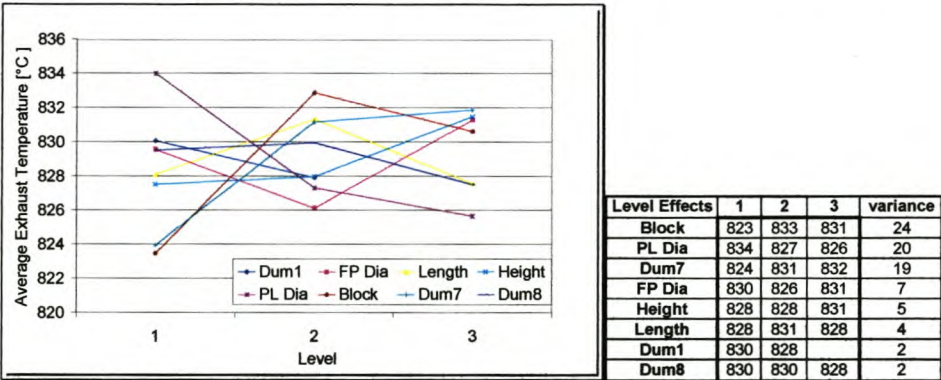


Figure 11-11. Average Exhaust Temperature @ 4800 rpm.

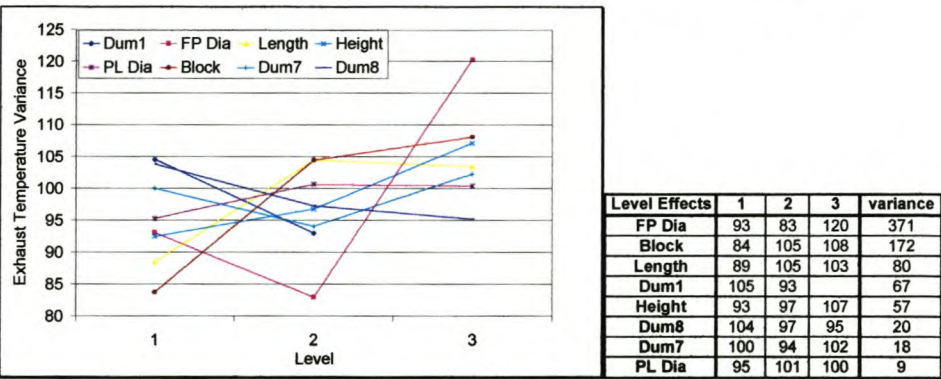


Figure 11-12. Exhaust Temperature Variance @ 4800 rpm.

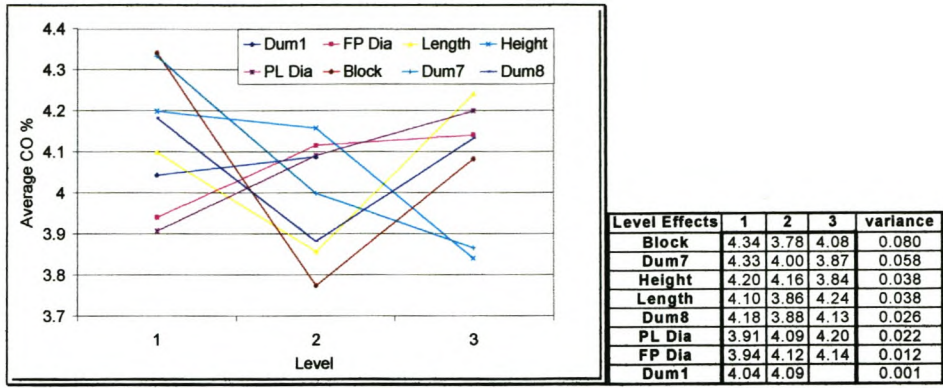


Figure 11-13. Average CO% @ 4800 rpm.

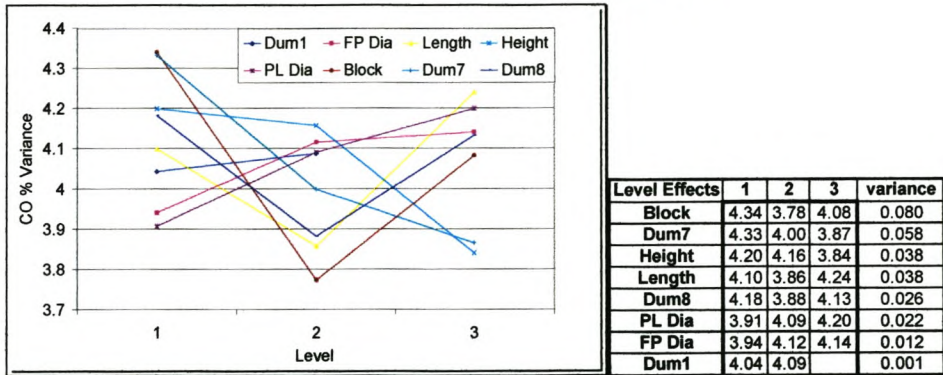


Figure 11-14. CO% Variance @ 4800 rp

Appendix K. Simulation Results for TEP @ 5300 rpm

Test	Speed	IMEP	PMEP	FMEP	BMEP	η_{mech}	η_{vol}	η_{ove}	Torque	Power	FuelCons.	SFC	Tmass	MassIn	MassOut
1	5300	12.924	-0.103	3.17	9.858	76.3	89	32.3	125.15	69.46	19.34	278.4	493.98	471.28	471.3
2	5300	13.198	-0.1	3.17	10.129	76.7	90.4	32.7	128.6	71.373	19.65	275.3	500.66	478.81	478.85
3	5300	12.198	-0.11	3.17	9.139	74.9	84.1	31.7	116.02	64.394	18.29	284.1	469.12	445.82	445.88
4	5300	12.023	-0.113	3.17	8.966	74.6	80.7	32.4	113.83	63.176	17.55	277.8	446.95	427.72	427.85
5	5300	14.215	0.422	3.17	10.624	74.7	97	31.9	134.88	74.858	21.09	281.7	537.59	513.97	513.95
6	5300	12.817	-0.222	3.17	9.869	77	89.1	32.3	125.29	69.54	19.38	278.7	494.26	472.33	472.33
7	5300	14.114	0.362	3.17	10.583	75	94.5	32.7	134.36	74.572	20.55	275.6	521.11	500.87	500.89
8	5300	13.149	-0.567	3.17	10.546	80.2	93.1	33	133.89	74.309	20.25	272.5	516.9	493.51	493.53
9	5300	13.144	0.298	3.17	9.677	73.6	88.3	32	122.85	68.183	19.2	281.5	491.48	467.81	467.81
10	5300	13.123	0.681	3.17	9.272	70.7	86.3	31.3	117.72	65.336	18.77	287.2	479.59	457.34	457.56
11	5300	14.256	-0.514	3.17	11.601	81.4	102.1	33.2	147.28	81.742	22.19	271.4	561.64	540.71	540.71
12	5300	13.124	-0.633	3.17	10.587	80.7	93.6	33	134.41	74.598	20.36	272.9	517.53	496.09	496.12
13	5300	15.155	0.678	3.17	11.307	74.6	100.3	32.9	143.55	79.671	21.82	273.8	553.86	531.67	531.67
14	5300	13.478	0	3.17	10.308	76.5	91.7	32.8	130.86	72.632	19.93	274.4	508.37	485.79	485.8
15	5300	12.528	-0.389	3.17	9.748	77.8	86.9	32.7	123.76	68.687	18.89	275	481.92	460.42	460.48
16	5300	11.63	-0.73	3.17	9.19	79	84.7	31.7	116.67	64.755	18.41	284.2	474.69	448.56	448.62

Appendix L. Simulation results for LET @ 2800 rpm

Test	Speed	IMEP	PMEP	FMEP	BMEP	η_{mech}	η_{vol}	η_{ove}	Torque	Power	FuelCons.	SFC	Tmass	MassIn	MassOut
1	2800	11.461	-0.199	1.782	9.878	86.2	85.3	33.8	125.41	36.772	9.8	266.5	475.14	452.08	452.07
2	2800	12.171	-0.174	1.782	10.563	86.8	90.7	34	134.1	39.32	10.41	264.8	503.62	480.35	480.35
3	2800	12.247	-0.333	1.782	10.797	88.2	92.1	34.2	137.08	40.194	10.58	263.2	511.79	488.09	488.09
4	2800	12.883	-0.223	1.782	11.324	87.9	95.5	34.6	143.77	42.156	10.97	260.1	527.08	505.83	505.83
5	2800	11.411	0.156	1.782	9.473	83	84.1	32.9	120.27	35.265	9.66	273.9	468	445.59	445.86
6	2800	12.101	-0.1	1.782	10.42	86.1	93.2	32.6	132.28	38.788	10.7	275.9	512.76	493.62	493.63
7	2800	11.35	0.099	1.782	9.469	83.4	82	33.7	120.21	35.248	9.41	267.1	455.25	434.29	434.22
8	2800	11.941	-0.438	1.782	10.597	88.7	92.3	33.5	134.54	39.449	10.6	268.7	507.81	489.05	489.05
9	2800	12.326	0.314	1.782	10.23	83	91.8	32.5	129.88	38.082	10.55	277	507.3	486.61	486.6
10	2800	12.499	0.441	1.782	10.276	82.2	91	32.9	130.46	38.254	10.45	273.2	505.55	482.12	482.18
11	2800	10.696	-0.349	1.782	9.262	86.6	81.7	33.1	117.59	34.479	9.39	272.2	451.45	432.97	432.97
12	2800	10.697	-0.533	1.782	9.447	88.3	81.9	33.6	119.94	35.168	9.41	267.6	451.48	434.12	434.12
13	2800	11.476	0.349	1.782	9.346	81.4	81.5	33.4	118.65	34.789	9.36	269.2	455.43	432	432.02
14	2800	10.802	-0.09	1.782	9.11	84.3	78.9	33.7	115.65	33.911	9.06	267.2	436.18	418.02	418
15	2800	12.28	-0.234	1.782	10.733	87.4	93.8	33.4	136.26	39.954	10.77	269.6	517.76	496.94	496.99
16	2800	11.733	-0.792	1.782	10.743	91.6	93.4	33.6	136.39	39.993	10.72	268.2	518.31	494.74	494.74